NATIONAL TRANSPORTATION SAFETY BOARD

Office of Research and Engineering
Washington, D.C. 20594

February 8, 2001

Aircraft Performance

Group Chairman's Aircraft Performance Study
by John O'Callaghan

A. ACCIDENT

Location:	Little Rock National Airport, Little Rock, Arkansas
Date:	June 1, 1999
Time:	11:51 PM Central Daylight Time (CDT)
Flight:	American Airlines Flight 1420
Aircraft:	Boeing (McDonnell Douglas) MD-82, registration: N215AA
NTSB#:	DCA99MA060

B. GROUP

Chairman: John O'Callaghan[1]
Senior Aerospace Engineer
NTSB, RE-60
490 L'Enfant Plaza E, SW
Washington, DC 20594

Members: Derek Troy
Aerodynamics Engineer
Boeing Commercial Airplane Group
Douglas Products Division
3855 Lakewood Blvd. MC D800-0033
Long Beach, CA 90846

John DeWald
Fuel Conservation & Performance Specialist
American Airlines
PO Box 619617, MD 843
DFW Airport, TX 75261-9617

[1] John O'Callaghan assumed the duties of Airplane Performance Group Chairman for this accident from Charles Pereira on September 8, 2000.

Thomas D. Schulte, Jr.
First Officer
Allied Pilots Association
O'Connell Building
14600 Trinity Blvd., Suite 500
Ft. Worth, TX 76155-2512

Bob Drake
Aerospace Engineer
US DOT, Office of Inspector General
JA-10, Room 9217
400 Seventh Street, SW
Washington, DC 20590

Tom Yager
Senior Research Engineer
NASA Langley Research Center
Mail Stop 497
2 West Bush Road
Hampton, VA 23681-2199

C. SUMMARY

On June 1, 1999, at approximately 11:51 PM Central Daylight Time (CDT), a McDonnell Douglas (now Boeing) MD-82, N215AA, operated by American Airlines as flight 1420 (AA1420), regularly scheduled passenger service from Dallas, Texas, overran the end of runway 4R and collided with the Runway 22L approach light stanchion after landing at the Little Rock National Airport, in Little Rock, Arkansas (LIT). The captain and 10 passengers sustained fatal injuries; the remaining 134 passengers and crewmembers sustained various non-life threatening injuries. The airplane was being operated in accordance with 14 CFR 121, and an instrument flight rules (IFR) flight plan had been filed.

The purpose of the Aircraft Performance Group (ACPG) is to determine and analyze the motion of the aircraft and the physical forces that produce that motion. In particular, the Group attempts to define the aircraft position and orientation throughout the flight, and determine its response to control inputs, system failures, external disturbances, or other factors that could affect its trajectory. The data the ACPG uses to obtain this information includes but is not limited to the following:

- Wreckage location and condition.
- Runway and ground impact markings and scars.
- Air Route Surveillance Radar (ARSR) and Airport Surveillance Radar (ASR) data.
- Digital Flight Data Recorder (DFDR) data.
- Cockpit Voice Recorder (CVR) information.
- Weather information.

- Output from computer programs that calculate aircraft performance.
- Ground and flight tests.

This aircraft performance study describes the results of using the data listed above in defining, as far as possible, the motion of American Airlines Flight 1420. The study introduces the aircraft motion data collected during the investigation, describes the methods used to extract additional aircraft motion information from DFDR, radar, CVR, and weather data, and presents the results of these calculations. The study also explores the effects of variations in spoiler position, touchdown ground speed, reverse thrust operation, and braking technique on the airplane's stopping distance and ground handling characteristics.

D. DETAILS OF THE INVESTIGATION

I. Wreckage Location and Runway Scars and Markings

The wreckage of AA1420 was located about 650 feet from the end of LIT Runway 4R. The airplane left tire scrub marks starting about 2000 ft. from the runway threshold and continuing about 400 ft. beyond the departure end of the runway. These tire scrub marks, and a detailed diagram of the wreckage of the airplane, is provided in the Airplane Group Chairman's Factual Report.

II. Radar Data

Description of ASR Data

Little Rock National Airport is serviced by an Airport Surveillance Radar (ASR) that assists tower controllers in maintaining traffic separation in the vicinity of the airport. Targets tracked by the ASR are recorded by a Continuous Data Recording (CDR) system. Returns from AA1420 were tracked and recorded by the LIT ASR8 radar and are tabulated in Table 1. The information presented in this table includes:

- Universal Coordinated Time (UTC) of the radar return, in hours, minutes, and seconds. A radar return is received every 4.6 seconds. The time accuracy is ± 0.16 sec.

- Transponder beacon code associated with the return. The code for AA1420 is 3635.

- Transponder reported altitude in hundreds of feet associated with the return. The transponder reports pressure altitude. The altitude recorded in the CDR file depends on the site recording the data; some sites record both pressure altitude, and pressure altitude adjusted for altimeter setting. Others record the adjusted altitude only. The LIT CDR file includes both altitudes. The resolution of this data is ± 50 ft. The altimeter setting for LIT at the time of the accident was 29.86 inches of mercury (in. Hg)[2].

[2] 29.86 in. Hg is the altimeter setting reported by ATC during AA1420's descent, and is consistent with the pressure altitude and corrected altitude reported in the LIT ASR8 CDR file. However, as described in later sections, the pressure at LIT appeared to be changing rapidly, and during final approach an altimeter setting

- Slant Range from the radar antenna to the return, in nautical miles (NM). The accuracy of this data is ± 1/16 NM or about ± 380 ft.

- Azimuth relative to Magnetic North from the radar antenna to the return, in Azimuth Change Pulses (ACPs). ACP values range from 0 to 4096, where 0 = 0° magnetic and 4096 = 360° magnetic. Thus, the azimuth to the target in degrees would be:

  (Azimuth in degrees) = (360/4096) x (Azimuth in ACPs) = (0.08789) x (Azimuth in ACPs)

  The accuracy of this data is ± 2 ACP or ± 0.176 degrees. The LIT ASR8 uses a nominal magnetic variation of 3° E to compute magnetic azimuth. However, a magnetic variation of 2.6° E results in a better match of the airplane position on the final approach course as derived from the Instrument Landing System (ILS) localizer deviations recorded on the DFDR, and is therefore used in this study instead of the nominal 3° E value.

The above information is the raw data recorded by the CDR system. Knowing the latitude/longitude coordinates of the radar antenna and of the runway 4R threshold, the elevation of the radar antenna, and the magnetic variation used by the radar software to compute magnetic bearings, the following information (also presented in Table 1) can be calculated:

- CDT = Central Daylight Time in hours, minutes, and seconds. Local Air Traffic Control (ATC) time in CDT is the reference time used throughout this performance study, and all CDT times are PM unless otherwise indicated. Section D-III of this study describes how ATC CDT time is related to the LIT radar UTC time.

- Distance North (true) of Runway 4R threshold in NM.

- Distance East (true) of Runway 4R threshold in NM.

The location of the LIT ASR8 antenna is: 34° 43' 55.03" N Latitude
92° 12' 46.73" W Longitude
Antenna Elevation: 297 ft.

---

of 29.92 in. Hg would have been more accurate (resulting in an indicated altitude about 55 ft. higher than that obtained with the 29.86 in. Hg setting).

Presentation of the ASR Data

Figures 1a-f show the radar data presented in Table 1 plotted relative to the Runway 4R threshold. Also shown in these Figures are symbols indicating the occurrence of selected events on the CVR, and, near the runway, the location of the ILS localizer centerline and "1 and 2 dot" deviation beams, and the path of the aircraft as determined from an integration of the DFDR accelerometer data (see below). The background of these Figures is a topographical map of the terrain beneath the AA1420 flight path, over which a colored image representing reflectivity from the North Little Rock Weather Surveillance Radar 1988 Doppler (WSR-88D) has been superimposed. Figure 2 contains a legend for converting the weather Doppler radar color codes into precipitation levels.

Next to the CVR event symbols in Figures 1a-f are numbers enclosed within angled brackets: e.g., <51>. These numbers are codes identifying the CVR event associated with each symbol. Table 2 lists the CVR events corresponding to each code, together with the ATC time and airplane altitude at which they occur. The altitudes in Table 2 are based on the DFDR recorded pressure altitude, corrected for atmospheric conditions (more on these corrections below). Table 2 does not constitute a comprehensive transcript of the CVR; many CVR events deemed to be of minor relevance are not included in Table 2 or in the various Figures in this study that include callouts of selected CVR events. For a complete transcript of the CVR, see the Cockpit Voice Recorder Group Chairman's Factual Report.

The Doppler weather radar reflectivity images shown in Figures 1a-f must be interpreted with care. The reflectivity seen by the radar changes with time as storms move and the precipitation intensity over different areas vary. In addition, the radar may detect different reflectivity levels at different radar beam scan angles, corresponding to the different levels of precipitation at various altitudes. Consequently, the radar reflectivity images presented in Figures 1a - 1f are snapshots corresponding to both a specific time period, and to a specific method for handling the different reflectivity levels at different beam scan angles.

Showing a single radar image superimposed on a long flight path is potentially misleading because the image can display information valid only for a specific time period, and so might reflect properly the conditions at one point in the flight path, but not at another. Each of Figures 1a-f indicate the time interval for which the weather radar image is valid; for Figures 1b-f, the interval is selected to be consistent with the time the airplane actually was in the area covered by the image, and the flight path lengths in these Figures are short enough to make this possible. However, Figure 1a shows a large scale view of the flight path, covering about 55 miles and about twenty minutes of flight. For this Figure, it is not possible to select one weather radar image that will be valid for the whole flight path, so the image chosen corresponds to a time of 11:51:41-11:57:23, or the six minutes immediately following the accident. This means that the image is more valid for portions of the flight path near the airport, and becomes increasingly invalid for portions of the flight path far (in distance and time) from the airport. This can be seen by comparing Figures 1a and 1b in the area about 37 NM South and 3 NM West of the runway; Figure 1a shows red and yellow coded reflectivity in this area, whereas Figure 1b, which corresponds more closely to the time at which the airplane was in that area, shows only green coded reflectivity.

All the weather radar images in Figures 1a-f correspond to a "composite reflectivity," meaning that the returns from various radar beam scans (altitudes) are used together to provide a view of the reflectivity at multiple levels of the atmosphere over the area in question. Consequently, even though Figures 1a-f may show the airplane flight path crossing an area of red reflectivity, it does not necessarily follow that the immediate environment of the airplane corresponded to such reflectivity; the precipitation causing that reflectivity could well be above or below the airplane.

In summary, the weather radar reflectivity images in Figures 1a-f provide a general indication of the precipitation environment surrounding AA1420, but do not necessarily indicate the precipitation conditions at any specific location along the airplane's flight path. For more information on the weather Doppler radar data and the meteorological conditions of the flight, see the Meteorology Group Chairman's Factual Report.

The position data for AA1420 recorded by the LIT ASR8 radar is also presented in Figures 4a-b, 5, and 6a-b, which show the radar altitude and position as a function of time and as a function of distance along the extended runway centerline from the runway 4R threshold. These plots also present information from other sources, which are described in later sections of this study.

III. Digital Flight Data Recorder (DFDR) and Cockpit Voice Recorder (CVR) Data

DFDR and CVR Data Description

The aircraft cockpit voice recorder (CVR) and digital flight data recorder (DFDR) were recovered from the accident wreckage and sent to Washington, DC for readout.

Descriptions of the DFDR and CVR and the recorder readout processes can be found in the Factual Reports of the Flight Data Recorder and Cockpit Voice Recorder Groups, respectively. The DFDR readout results in tabulated and plotted values of the recorded flight parameters versus time. The CVR readout results in a transcript of the CVR events, a partial list of which is shown in Table 2. Selected CVR events listed in Table 2 are also presented along with other information in various Figures throughout this study.

Coordination of ATC, Radar, DFDR, and CVR Times

The LIT ASR8 radar, the DFDR, and the CVR record their information with respect to time, but these recorded times are not synchronized. To use these data sources together, their times must be synchronized to a single reference time. This reference time is the local ATC CDT time introduced in Section D-II and used throughout this study.

Time on the DFDR is measured in terms of the Subframe Reference Number (SRN), with one SRN equivalent to one second of time. The ATC CDT time is related to the DFDR SRN by noting that, according to the transcript of the communications between AA1420 and ATC, the last transmission from AA1420 occurred at about 11:48:42. The last microphone keying event recorded on the DFDR occurs at a SRN of approximately 18742.8, and so the following relationship is established:

11:48:42 (CDT) Local ATC Time = 18742.8 DFDR SRN [1]

The relationship between the UTC time recorded by the LIT ASR radar and the DFDR SRN is established by comparing the DFDR pressure altitude to the radar recorded pressure altitude data, and adjusting the time conversion so that the two coincide as closely as possible (see Figure 3). This process gives the result

04:30:00 (UTC) LIT Radar Time = 17622.3 DFDR SRN [2]

Using Equations [1] and [2] gives

04:30:00 (UTC) LIT Radar Time = 11:30:01.5 PM (CDT) Local ATC Time [3]

The relationship between the times of events recorded on the CVR and the ATC reference time is established by first establishing the conversion from CVR to DFDR time, and then using the DFDR to ATC time conversion described by Equation [1].

The mapping of CVR event times to DFDR Subframe Reference Numbers is accomplished by comparing the times of events recorded on both the DFDR and CVR. These common events include the start and end of radio transmissions (both recorders detect microphone keying activity[3]), the activation of the "Sink Rate" warning (a discrete changes value on the DFDR, and the aural alarm is heard on the CVR), and the contact of the airplane with the runway (a normal load factor "spike" is observed on the DFDR, and the sound of touchdown in heard on the CVR). Assuming that the CVR and DFDR stopped recording at the same instant, the end of both recordings will also be a common event. However, this assumption is not necessarily valid, and so the end of recording events are best used as a check on the CVR and DFDR time alignment, rather than as data points used to derive that alignment.

The time alignment of these common DFDR and CVR events is complicated by two factors:

- The DFDR Microphone Keying and Sink Rate Warning discretes are only sampled once every second, and so the times of these events have an uncertainty of -1 to +0 seconds.

- The CVR tape does not record a time parameter, and so the timing of CVR events must be determined at the time the tape is replayed. If the tape is not replayed at the same speed at which it was recorded, the CVR times established during the process will be in error. Furthermore, the speed of the CVR tape during recording can vary, so the appropriate playback speed may depend on the portion of tape being read.

The correct playback speed of the CVR tape can be approximated by adjusting it so that, upon playback, the AC electrical noise signal that bleeds into the CVR system and is recorded on the CVR produces a signal whose frequency matches that of the AC generator that produced the noise. The frequency of this generator is assumed to be

[3] Twelve microphone keying events throughout the 31 minute CVR recording were used in this study to define the relationship between the CVR times and DFDR Subframe Reference Numbers.

exactly 400 Hz. If the CVR tape is played too quickly, the AC noise signal frequency will be greater than 400 Hz, and if it is played too slowly, the frequency will be less than 400 Hz. The actual AC generator on the airplane may not have been operating at exactly 400 Hz, and the tape speed itself can vary during recording, so this method only gives a first approximation of the timing of CVR events.

The approximate CVR times of the common CVR/DFDR events, together with the precise DFDR SRNs defining the intervals in which those events occur on the DFDR, provide a series of constraints that help define the relationship between CVR times and DFDR SRNs. Any mathematical mapping between CVR time and DFDR SRN that satisfies these constraints may be used to define the time alignment between the two recorders. In practice, the preferred mapping is a straight line. If no single line will satisfy all the constraints, multiple lines will need to be used. For the AA1420 CVR, a single linear relationship between the CVR times and DFDR SRNs that satisfied the constraints imposed by the common events was found; this relationship indicates that the CVR was played back at a speed that was only 0.35% slower than the recording speed.

Once the mapping from CVR time to DFDR SRN is established, the times of all CVR events (even those that do not have corresponding events on the DFDR) can be converted to their equivalent DFDR SRN. Equation [1] can then be used to convert from DFDR SRN to the ATC CDT reference time.

In Table 2, the time of CVR events is expressed in the reference ATC time.

IV. Processing of Radar and DFDR Data

Overview

The airplane performance parameters of primary interest in this accident are those that define the motion of the airplane on the runway, including the airplane's position, ground speed, air speed, heading, track and drift angles, and deceleration. The motion of the airplane on approach prior to touchdown is also of interest, since the approach sets up the initial conditions for the motion of the airplane on the runway. Approach parameters of interest include the position of the airplane relative to the ILS localizer and glide slope beams, airspeed and ground speed, heading, bank, pitch, drift, and flight path angles, and rate of climb or descent. The control inputs, power settings and winds that affected the aircraft during the approach and on the ground are also of interest. This section describes the methods used to calculate these airplane performance parameters based on the available radar, DFDR, and weather data, and presents the results of the calculations.

While the radar data provides aircraft position information directly, it is not precise or frequent enough to define an accurate history of the aircraft position relative to the ILS beams or the dimensions of the runway. For example, the ASR8 altitude data simply repeats the pressure altitude sensed and reported by the aircraft transponder, which is not corrected for non-standard pressure or temperature effects; furthermore, it is reported to the nearest 100 ft, and so there is a ±50 ft. uncertainty in the recorded values. The DFDR records data more accurately and frequently, but does not record position data directly. Fortunately, both DFDR and radar data can be used along with weather information, the runway tire markings, and the wreckage location to calculate a precise flight path that can be compared to the nominal approach path defined by the ILS, the deviation from that path recorded by the DFDR localizer and glideslope deviation data, and the nominal runway touchdown point and stopping distance.

In this study, the motion of AA1420 is examined rigorously from about 440 ft. above the ground on approach, until the end of the recorded DFDR data at about 650 ft. from the end of runway 4R (the bulk of the airplane wreckage was spread out between 650 and 850 ft. from the end of the runway). The position of the airplane during this time is determined by integrating the longitudinal, lateral, and vertical[4] load factor DFDR data. The load factor data suffer from inherent biases that if not accounted for can introduce significant error into the position calculations. These biases drift with time and can be changed by sudden impacts (such as touchdown loads); these effects limit the usefulness of the integrations to a period of about 40 to 60 seconds, depending on the noisiness of the data (turbulent air generally limits the usefulness of the integration to about 40 seconds, while in smooth air good results can be obtained up to about 60 seconds). For these reasons, the AA1420 flight path is integrated in two steps: from about 440 ft. above the ground to 20 ft. above the ground (the “in air” trajectory), and from 20 ft. above the ground through the end of the DFDR data (the “on ground” trajectory). The details of the load factor integrations and other airplane performance calculations that follow from the integrated data are presented below for each of these two trajectory segments.

In Air Trajectory Segment

Position Calculation. The biases in the longitudinal, lateral, and vertical load factor data can be estimated and accounted for in the integration if the approximate airplane position throughout the integration period is known from a separate, “calibration” source. The biases are selected so that the integrated airplane trajectory matches the calibration trajectory as closely as possible. When the differences between the integrated and calibration trajectories are minimized, the details of the motion are in general given more accurately by the integration than by the calibration trajectory. This is because the DFDR accelerometer data, upon which the integrated trajectory is based, is usually sampled at a higher rate and with more precise sensors than the data used to determine the calibration trajectory. The integration relies on the calibration trajectory, however, to serve as a basis and check of the estimate of the accelerometer biases; if the integrated trajectory deviates significantly from the calibration trajectory, then the incorrect biases have been used and the integrated trajectory is erroneous.

For the in air trajectory segment of AA1420, the calibration trajectory is given by a curve fit through the LIT ASR8 radar data (for the horizontal components of the trajectory) and by the DFDR pressure altitude data, corrected for atmospheric conditions (for the vertical component of the trajectory). The curve fit of the radar data also provides an initial ground speed and ground track angle for the accelerometer integration. Once the integrated trajectory has been calculated, the deviations from the ILS localizer and glide slope that follow from that trajectory can be compared to the ILS deviations recorded on the DFDR, providing another check of the integrated trajectory.

---

[4] The vertical load factor n_z is equal and opposite to the normal load factor recorded on the DFDR: n_z = -nlf.

DFDR pressure altitude is recorded from the Air Data Computer (ADC) and provides the basis for the vertical component of the calibration trajectory used in determining the accelerometer biases. An altimeter interprets static pressure as altitude based on the sea level static pressure set in the Kollsman window, and on the equations of the standard atmosphere. These equations are solutions of the hydrostatic equation[5] that assume an adiabatic atmosphere and standard sea level temperature and temperature lapse rate. For the pressure altitude recorded on the DFDR, the Kollsman window setting is standard sea level static pressure (29.92 in. Hg). In reality, the temperature, pressure, and temperature lapse rate are not standard, and so the pressure altitude is not the true altitude of the airplane above sea level. Most, but not all, of the difference between pressure altitude and actual altitude can be removed by adjusting the Kollsman window setting to the actual sea level static pressure in the area of interest. The remaining error is due to non-standard temperature effects and is of little concern when altimeters are used to maintain the vertical separation of aircraft, but it must be taken into account when a more accurate estimate of actual altitude is needed.

The remaining error can be reduced by solving the hydrostatic equation using the actual temperature and pressure along the flight path. The solution will give the *change* of altitude along the path; adjusting the solution to match the known altitude of the touchdown point gives the actual altitude along the path.

The pressure along the flight path can be computed from the DFDR recorded pressure altitude. The static temperature can be computed from the DFDR recorded total temperature and calibrated airspeed.

Abrupt maneuvers and large angles of attack or sideslip can cause significant changes in the local airflow over the static pressure ports. These airflow changes result in erroneous pressure measurements at the ports. Consequently, the altitude calculations based on pressure measurements during abrupt maneuvers or large angles of attack and sideslip may be unreliable. In the case of AA1420, when the crew transitioned from a crab to a sideslip maneuver (i.e., wing down/top rudder method) before touchdown, the sideslip angle may have increased to 10 degrees, which would possibly have an effect on the static ports and introduce some error into the DFDR altitude and calibrated airspeed parameters. Details on the calculation of the angles of attack and sideslip during the approach are presented below.

Figure 4b shows the result of the DFDR altitude corrections, and the altitude that results from integrating the accelerometers using the corrected DFDR altitude as the calibration altitude. Immediately following the accident, the altimeter setting for the field (local sea level static pressure) was recorded as 29.98 in. Hg; using this altimeter setting and the DFDR recorded temperature as described above to correct the DFDR pressure altitude results in the curve in Figure 4b labeled "Corrected Altitude (based on 29.98 in. Hg and DFDR Total Temp.)" The integrated altitude that results from using this altitude as a calibration has the airplane touching down about 75 feet above the runway. Since this is

---

[5] The hydrostatic equation describes the pressure increment across a differential element of air required to balance the weight of the element: $dP = -(\rho)(g)(dh)$, where dP is the pressure increment, ρ is the density of the air element, g is gravitational acceleration, and dh is the altitude increment.

impossible, the integrated altitude is shifted down in Figure 4b so that the airplane Center of Gravity (CG) is about 6 feet above the runway, which is more reasonable. To get the "Corrected" DFDR altitude to match this shifted integrated altitude, it too must be shifted down, and the result is shown in Figure 4b as the curve labeled "Corrected Altitude with Shift." Note that this shifted, corrected altitude matches the original, uncorrected DFDR pressure altitude rather well. This result indicates that at the time the DFDR was recording altitude, the actual altimeter setting was very close to 29.92 in. Hg, or standard pressure.

Interestingly, the official altimeter setting given by ATC during the approach was 29.86 in. Hg; the curves in Figures 4a-b labeled "Mode C Adjusted Altitude (based on 29.86 in. Hg)" show that when the transponder reported altitude is adjusted based on this setting, the resulting altitude is about 100 feet low.

The altimeter setting given to the crew during the descent was 29.86 in. Hg, during final approach the correct setting appears to be about 29.92 in. Hg., and immediately after the accident the recorded setting was 29.98" Hg. These numbers indicate that the atmospheric pressure was rising rapidly during the descent and landing. The "noisiness" in the DFDR altitude data compared to the integrated data also suggests that there were small, erratic disturbances in pressure at the static ports, as would be expected during a turbulent approach.

The integrated altitude, DFDR corrected altitude, and DFDR corrected altitude with the 75 ft. shift are also plotted in Figure 5 as a function of distance along the extended runway centerline. Figure 5 also shows the location of the ILS glide slope centerline and 1 and 2 dot deviation beams. The ILS geometry shown in Figure 5 is based on an inspection of the ILS conducted on November 20, 1998; the data from this inspection used to calculate the ILS geometry is presented in Table 3.

The horizontal position of the airplane resulting from the accelerometer integration is shown in Figures 1f and 6b, for both the in air and ground trajectory segments (the ground trajectory segment is discussed further below). Figure 1f presents the results overlaid on a topographical map of the airport environment, and 6b presents the results as a function of time. Both Figures show good agreement between the integrated accelerometer data and the recorded radar data. The accelerometer biases used in the in air portion of the integration are as follows:

Longitudinal Load Factor Bias (Δn_x)	=	-0.005 g's
Lateral Load Factor Bias (Δn_y)	=	-0.00529 g's
Vertical Load Factor Bias (Δn_z)	=	-0.0185 g's

The corrected load factors are plotted together with the original DFDR data in Figure 12.

<u>True Airspeed Calculation.</u> True airspeed can be calculated from calibrated airspeed, static pressure, and static temperature. Calibrated airspeed is recorded directly from the ADC, and the static pressure can be determined from the DFDR pressure altitude and total temperature data. True airspeed is plotted in Figure 7 along with the DFDR recorded calibrated airspeed and the ground speed computed from the integrated position data.

Also shown in Figure 7 are the ILS localizer and glide slope deviations that follow from the position data obtained by integrating the accelerometers. Note that these calculated ILS deviations do not agree perfectly with the ILS deviations recorded on the DFDR, though they show the same trends and direction of deviations. This is not surprising, because even though the position obtained by integrating the accelerometer integrations is very accurate, it still has some degree of uncertainty in it. The disagreement between the calculated and recorded ILS deviations provides a measure of this uncertainty. For example, at 11:50:00 the recorded localizer deviation is about 0.3 dots greater than the calculated localizer deviation, and the recorded glide slope deviation is about 0.8 dots greater than the calculated deviation. At this time, the airplane is about 0.5 NM from the runway threshold, and these localizer and glide slope deviation differences equate to about 67 ft. horizontally and 19 feet vertically. Given the use of relatively imprecise radar data as the initial condition source and calibration trajectory for the accelerometer bias calculation, the integrated trajectory result, as measured by the recorded ILS deviations, is very good. The airplane itself is about 30 feet high, 147 feet long and 107 feet wide, so half a nautical mile from the threshold the error in the integrated position data is within the dimensions of the airplane. At the threshold, these same errors (0.3 dots on the localizer and 0.8 dots on the glide slope) equate to 50 feet horizontally and 5 feet vertically. However, at this point (at time 11:50:13), the calculated and recorded ILS deviations are in excellent agreement.

Wind Calculations. The wind encountered by AA1420 on the approach is of interest because the magnitude of the wind speed and the direction the wind is blowing from affect important items such as crew workload, the magnitude of the crab angle that must be maintained and removed during the flare, the touchdown ground speed and drift angle of the airplane, and the directional control of the airplane on the ground.

Velocity (of an airplane, of the wind, etc.) is a vector quantity, i.e., it has components in different directions. These components can be described in terms of a Cartesian coordinate system, such as North and East components, or components aligned with the airplane body axes, or components aligned with the runway, and so on. The components can also be described in polar coordinates, defining a radius (magnitude of the velocity) and angle (direction in which the velocity vector points). The velocity of the airplane over the ground is the vector sum of the velocity of the airplane through the air and the velocity of the air itself over the ground (the wind). The wind can therefore be computed by subtracting (vectorially) the velocity through the air from the velocity over the ground. In this study, the wind is computed by first calculating the components of the ground and air velocity vectors in the airplane body axis system, and then calculating the difference between these components, giving the components of the wind vector in the airplane body axis system. Finally, the wind components are transformed back into the Earth axis system, where the wind can be expressed in terms of North and East wind or in terms of velocity and direction.

The velocity over the ground can be derived from the position data obtained from the accelerometer integrations. Since the orientation of the airplane body axes relative to the Earth Cartesian axis system is known through the pitch, roll, and heading angles recorded on the DFDR, the components of the ground velocity in the airplane axis system can be computed.

The airplane body axis components of the airplane's velocity through the air can be computed if the true airspeed and angles of attack and sideslip are known. True airspeed can be found from recorded DFDR data as described above. Angle of attack and sideslip angle are not recorded on the DFDR and so must be derived from other parameters.

Angle of Attack Calculation. The angle of attack can be determined from the known aerodynamic characteristics of the airplane once the Lift Coefficient (C_L) is calculated:

$$C_L = \frac{-n_z W}{\frac{1}{2}\rho V^2 S} \qquad [4]$$

n_z is the vertical load factor (equal to the normal load factor recorded by the DFDR multiplied by –1), W is the airplane weight (127,749 lb., based on the estimated landing weight), ρ is the air density, V is true airspeed, and S is the wing reference area (1,209.3 ft^2). The MD-82 Flaps 40 lift curve was used to determine the angle of attack corresponding to a given C_L.

Another estimate of angle of attack can be obtained by subtracting the airplane flight path angle from the pitch angle when the wings are relatively level. The flight path angle is the angle the velocity vector of the airplane makes with the horizon. In a wind, the flight path angle computed using the ground velocity vector will be different from that computed using the air velocity vector; the latter is the flight path angle relative to the air and the correct angle to be used for computing angle of attack. Using the velocity relative to the ground results in an "inertial flight path angle" that is not the proper angle for computing angle of attack, but which is in general less noisy than the angle computed using the air velocity vector. The inertial flight path angle is plotted along with rate of climb in Figure 9.

The angle of attack resulting from the C_L calculation, and an angle of attack estimate made using the inertial flight path angle, are shown in Figure 8. The noisiness of the C_L based calculation is evidence of turbulence during the approach.

Sideslip Angle (β) Calculation. An estimate of β can be made if the side force (Y) characteristics of the airplane are known and if the side force generated during the flight can be calculated. The most significant contributors to the side force are β and rudder deflection (δr):

$$C_Y = \frac{Y}{\frac{1}{2}\rho V^2 S} = \frac{\partial C_Y}{\partial \beta}\beta + \frac{\partial C_Y}{\partial \delta r}\delta r + \{\textit{smaller terms}\} \qquad [5]$$

Ignoring the smaller terms, [5] can be solved for an estimate of β:

$$\beta \cong \frac{C_Y - \left(\frac{\partial C_Y}{\partial \delta r}\right)\delta r}{\frac{\partial C_Y}{\partial \beta}} \qquad [6]$$

The derivatives $\partial C_Y / \partial\beta$ and $\partial C_Y / \partial\delta r$ are aerodynamic characteristics of the airplane that are known from wind tunnel and flight tests.

The side force Y can be calculated using

$$Y = Wn_y \qquad [7]$$

Where n_y is the lateral load factor, corrected for the accelerometer bias calculated above.

The results of the β calculation are presented in Figure 8 and show a buildup of negative β during the final part of the approach. This is consistent with a de-crab maneuver in a left crosswind.

With the angle of attack and sideslip angle calculations complete, the winds can be calculated as outlined above. The results of the wind calculation are shown in Figure 10, and are presented in terms of both magnitude and direction, and headwind and crosswind components. The headwind and crosswind axes are tied to the airplane body axes, not to the runway axes, however; the headwind component in Figure 10 is equivalent to the component of the wind along the airplane's longitudinal axis, and the crosswind component is equivalent to the component of the wind along the airplane's lateral axis. Because the airplane is generally aligned with the runway, the wind headwind and crosswind components in runway coordinates would be similar to those shown in Figure 10.

The wind speed and direction presented in Figure 10 are generally consistent with the wind reports issued by ATC during the approach, though the wind direction calculation appears to be about 10° to 20° more Westerly than what ATC was reporting. Note that Figure 10 indicates that the wind was almost entirely a crosswind, or may even have had a small tailwind component. This means that the wind did not reduce the ground speed in any way, and that the 20 knot airspeed additive made for the wind conditions resulted in at least a 20 kt. increase in the ground speed component parallel to the runway. This increase in ground speed would have increased the energy needed to be dissipated during the landing roll, and the landing distance required to do so.

The wind calculations presented above depend on resolving the components of the ground and air velocity vectors into the airplane body axis system, which requires an estimate of the angles of attack and sideslip. The sideslip angle is estimated based on the side force acting on the airplane, as determined from the recorded lateral load factor, and by assuming that the side force is entirely due to the aerodynamic influence of the sideslip angle and the airplane's rudder. While in the air, this assumption is a good approximation. However, on the ground, the landing gear can impose lateral forces on the airplane, and there is no way to separate the lateral load factor caused by gear forces from those caused by rudder deflection and/or sideslip angle. Hence, on the ground the sideslip angle can not be calculated, the components of the air velocity vector can not be resolved into their airplane axis system components, and it is not possible to solve for the wind vector. Thus the wind calculations presented in Figure 10 end just before touchdown, and no wind estimate is made for period when the airplane is on the ground.

Other approach parameters of interest, including angular rates, control surface positions, and Engine Pressure Ratio (EPR) settings, are presented in Figures 11 and 13.

On Ground Trajectory Segment

Position Calculation. The position calculation for the on ground trajectory segment is done in much the same way as that for the in air trajectory segment: a set of biases that makes the trajectory resulting from an integration of the accelerometer data match an independent "calibration" trajectory is sought, and then the integrated trajectory is taken as the more complete and precise definition of the airplane's position. The calibration trajectory for the on ground segment is defined by the constant altitude of the CG while on the runway (assumed to be 266 ft.), and by the tire scrub markings left by AA1420 on the runway.

While the tire scrub markings provide a precise definition of the points on the runway through which the airplane passed, they do not provide any information about *when* the airplane passed through the points, and so do not comprise a complete trajectory definition. However, the time of touchdown can be determined from the normal load factor trace on the DFDR, and if the touchdown point on the runway is assumed to be the point at which the tire markings begin, both the time and place of touchdown are known, adding a little more definition to the calibration trajectory. On the other end of the runway, the wreckage location is known, as well as the time the DFDR ends. Thus we have two points at which the time and position of the airplane are known, and in between these points we have the runway tire marks that indicate the trajectory of the airplane in space (but not in time). Solving for the entire trajectory consists of selecting initial conditions and accelerometer biases that, when the accelerometers are integrated, satisfy the constraints imposed by the touchdown and DFDR end points and the runway tire marks.

As mentioned above, the ground trajectory segment starts at a point about 20 feet above the runway and continues until the end of the DFDR data. The initial conditions for the integration include the ground speed, track angle, and flight path angle at the 20 foot point. These values are defined by the trajectory solution for the in-air segment; however, very small changes in the initial conditions - less than two knots of airspeed, and fractions of a degree of track and flight path angle - can have a significant effect on the results of the integrated ground trajectory. Since the solution of the in air segment is not known to this degree of certainty, there is some flexibility in adjusting the initial conditions within these small margins in order to achieve the best ground solution. To avoid discontinuities in the overall solution at the point where the in air segment ends and the on ground segment starts, the data is smoothed over a two second period where the two solutions overlap.

Accelerometer biases that result in a ground trajectory that satisfies the constraints described above are as follows[6]:

Longitudinal Load Factor Bias (Δn_x)	=	0.01921 g's
Lateral Load Factor Bias (Δn_y)	=	-0.01727 g's

[6] These biases are also described in Figures 14 and 15a-f as "corrections" to be applied to the recorded DFDR load factors.

Vertical Load Factor Bias (Δn_z) = -0.00626 g's

The results of the ground trajectory integration are presented in Figures 14a-b and 15a-f, which show the measured runway tire mark locations along with the calculated CG position as a function of distance from the runway 4R threshold. Also shown on these plots as a function of distance down the runway are various calculated and recorded airplane performance parameters that describe the motion of the airplane on the ground, and the behavior of the airplane's control surfaces, thrust levels, reverse thrust activity, and brake pedal positions.

Figure 14a is an overview plot that shows the entire ground trajectory on one page, together with the other airplane performance parameters of interest. Because of space constraints, the runway diagram at the top of the plot is not to scale. Figure 14b is a to-scale overview plot of just the airplane position and trajectory on the runway, overlaid with diagrams showing the position, orientation and velocity vector of the airplane at one second intervals.

Figures 15a-f plot the data presented in Figure 14a with the runway scaled properly; hence the requirement for six pages to show the entire trajectory. Because Figures 15a-f are to scale, the diagrams showing the orientation and velocity vector of the airplane at one second intervals can be shown.

The airplane diagrams in Figures 14b and 15a-f also indicate how well the calculated trajectory and recorded DFDR heading coincide with the left and right main gear and nose gear tire markings left on the runway. In general, the calculated trajectory correctly shows the drift over the runway that makes the tire marks line up with the corresponding gear locations on the airplane. However, there are points in the trajectory where it appears that the drift angle needs to be a little larger in order to place the nose gear over the measured nose gear tracks; for example, at 3,600 ft. from the threshold, the airplane looks like it needs to be yawed a little more to the left, and at 7,300 ft. from the threshold, the airplane looks like it needs to be yawed a little more to the right. However, these small discrepancies probably have more to do with inaccuracies in the heading measurement than errors in the trajectory itself, given the excellent match the calculated CG trajectory makes with the runway marks, and the proper correspondence the calculated trajectory has with the time and place of touchdown, and the time and place of the end of the DFDR data.

V. Ground Deceleration Study

The previous sections of this Airplane Performance Study present data and calculations that describe the motion of AA1420; i.e., they define the position and orientation of the airplane in the air and on the ground as a function of time. This information describes *what* the airplane did, but does not reveal *why*; in other words, the physical forces acting on the airplane that drive its motion are not considered. This section of the study explores the aerodynamic, propulsive, and ground reaction forces that govern the motion of the airplane on the runway, and identifies the most significant factors affecting the deceleration and stopping distance of the airplane.

While it is relatively straightforward to determine the total force in each axis acting on an airplane once its mass properties and trajectory are defined, it is extremely difficult to resolve these forces into their aerodynamic, propulsive, and ground reaction components, particularly when the airplane is landing in a crosswind. The biggest problem in determining the aerodynamic forces on the airplane is that, as described in Section D-IV, the sideslip angle on the ground is unknown. Even if the winds on the ground were known with certainty and the sideslip angle could be estimated, any meaningful estimate of the aerodynamic forces would require a very detailed aerodynamic model of the airplane that accounts for the effects of ground proximity, large sideslip angles, and asymmetric reverse thrust, all in different combinations. Furthermore, it is unlikely that there is any flight test data with which to validate such a model at the extreme conditions that are of interest in this accident.

Fortunately, a detailed definition of the aerodynamic, propulsive, and ground reaction forces acting on AA1420 is not required in order to explore the influence each of these had on the motion of the airplane, and how changes in each of these forces affect the airplane deceleration and stopping distance. The approach used here is to simplify the AA1420 stopping distance problem by eliminating secondary effects, and then to evaluate the influence of various deceleration devices on the simplified problem. This approach brackets the range of possible outcomes and provides perspective on the limited role that the secondary effects that complicate the AA1420 scenario have on the airplane's stopping distance.

The simplifying assumptions are as follows:

- Only the airplane motion along its longitudinal axis is considered; i.e., the problem is limited to slowing the airplane to a stop from an initial ground speed, and no consideration will be given in this section to directional control while on the ground (directional control is discussed in Section D-VI).

- The wind component parallel to the runway will be assumed to be zero. This assumption is consistent with the wind calculation during the approach, which showed that at least during that time, the wind was almost entirely a crosswind.

- Reverse thrust will be assumed to be always symmetrical, applied at a nominal 1.3 engine EPR value, and to remain engaged until the airplane has come to rest.

- Brakes are applied in a manner consistent with what is seen on the AA1420 DFDR, with the exception that once the brakes are on, they remain on until the airplane comes to rest and neither brake pedal is relaxed (Figure 14 indicates that on AA1420 the left brake was relaxed briefly about 5,500 ft. from the runway threshold).

The effects various deceleration devices have on the airplane stopping distance are evaluated using The Boeing Company's Operational Landing Program for the MD-80. This computer program is primarily used to calculate operational landing performance on wet or icy runways and includes the effects of aerodynamics, thrust changes, and contaminated runways. The program calculates airplane deceleration in quarter-second time intervals and integrates the results to provide a time history of speed and distance.

The Operational Landing Program computer runs for this investigation were performed by Boeing's representative on the Airplane Performance Group at the request of the Airplane Performance Group Chairman. The conditions tested in the program were as follows:

Airplane Weight:	127,000 lb.
CG Position:	16.7% MAC
Temperature:	25°C (77°F)
Rolling friction coefficient:	0.02
Wet runway friction coefficient:	See Table 4
Touchdown speed:	152 and 162 knots
Reverse Thrust:	None, and Constant Symmetric Reverse @ 1.3 EPR[7]
Braking:	None, AA1420 Braking, and Normal Braking
Spoiler Deployment:	Spoilers Up and Spoilers Down

The "Normal" braking profile differs from the AA1420 braking profile in that the brakes are applied 0.25 seconds after touchdown and full braking is achieved 1.25 seconds thereafter, whereas in the AA1420 profile, which is based on the brake pedal position recorded by the DFDR, the brakes are applied 5 seconds after touchdown and full braking is achieved 6 seconds thereafter (11 seconds after touchdown).

The results of a selection of the computer runs are presented in Figures 16-18. The top plot in Figure 16 shows the ground speed of the airplane as a function of distance from the runway 4R threshold for several combinations of spoiler deployment, reverse thrust, and braking scenarios. In all cases, the initial ground speed is 162 knots, which is close to the 160 kt. touchdown ground speed determined from the on ground trajectory calculation described in Section D-IV. Also, the initial position on the runway in each case has been set equal to the AA1420 touchdown point, about 2,000 ft. from the threshold. The AA1420 ground speed vs. distance profile, as derived from the integrated accelerations, is shown in Figure 16 as curve "A," labeled "***AA1420 Data***."

With no deceleration devices of any kind - brakes, spoilers, or reverse thrust - all deceleration is due to rolling friction and aerodynamic drag. This case corresponds to curve "B" in Figure 16. In this case, the airplane would depart the end of the runway (7,200 ft. from the threshold) with a ground speed of about 142 knots According to curve "A" in Figure 16, AA1420 crossed the runway end with a ground speed of about 97 knots, so more than just rolling friction and aerodynamic drag forces were acting on the airplane.

Curve "D" in Figure 16 shows the ground speed profile if the spoilers remain down and no brakes are used but a constant, symmetrical reverse thrust at 1.3 EPR is used. In this case, the airplane leaves the runway going about 117 knots, or still 20 knots faster than the actual accident airplane. Consequently, AA1420 experienced more deceleration than what the thrust reversers alone can provide at 1.3 EPR (this is particularly true given that the reversers on AA1420 were not applied consistently throughout the ground roll). Since the DFDR indicates that the spoilers did not deploy on AA1420 (except in response to

---

[7] A constant 1.3 EPR is used because the Operational Landing Program can not modulate the reverse thrust during the run; i.e., once reverse thrust is engaged, it must remain constant until the end of the run. 1.3 EPR is the maximum recommended reverse thrust engine setting for operations on wet or slippery runways.

normal wheel inputs), the additional deceleration required to slow the airplane to 97 knots at the end of the runway must have come from the airplane's brakes.

In fact, curve "C" in Figure 16, corresponding to no spoilers but with reverse thrust and the AA1420 braking profile applied, matches the AA1420 data best and has the airplane departing the end of the runway at 95 knots. This indicates that the braking performance of AA1420 is consistent with what would be expected given the status of the spoilers and the wet runway friction coefficients given by Table 4. Indeed, Figure 16 indicates that the initial deceleration of AA1420 exceeded what would have been expected given the airplane configuration and touchdown conditions (this is perhaps due to the use of reverse thrust at greater than 1.3 EPR immediately after touchdown). The loss of deceleration around 5,600 ft. from the threshold coincides with a stowing of the reversers and a relaxation of the left brake pedal.

The curves in Figure 16 discussed so far indicate that AA1420 must have experienced a braking friction coefficient at least as high as those indicated in Table 4, i.e., about 0.23 at 140 knots and 0.21 at 160 knots. Since the maximum achievable friction coefficient is about 0.04 when the tire is hydroplaning[8], or about 6 times smaller than what AA1420 actually experienced, the data indicate that hydroplaning did not occur. This conclusion is consistent with the post-accident condition of the aircraft tires, as documented in Addendum 2 to the Systems Group Chairman's Factual report.

Curves "E" and "F" in Figure 16 illustrate the effect of spoiler deflection on the ground speed profile. Curve "F" includes the effect of reverse thrust, while curve "E" does not. It is clear from these curves that the effectiveness of the brakes, and the resulting deceleration and stopping distance, is critically dependent on spoiler deflection. Without reverse thrust but with the spoilers deployed and using the AA1420 braking profile, the airplane departs the runway at 20 knots, as opposed to the 95 knots that results from braking and reverse thrust with the spoilers stowed. If the spoilers are deployed and reverse thrust is used as well, the airplane can be stopped about 500 feet before the end of the runway.

The bottom plot in Figure 16 indicates why the braking performance is so dependent on the spoiler position. The retarding force provided by a braked tire is

$$F_t = W\, r_t\, \mu \qquad [6]$$

where W is the airplane weight, r_t is the fraction of the airplane weight supported by the tire, and μ is the braking friction coefficient. This equation shows that the share of the airplane weight supported by the tire is just as important a factor in the retarding force as is the friction coefficient. The bottom plot in Figure 16 shows that without spoiler deflection, at high speeds most of the airplane weight is still supported by the wings, and very little by the gear; consequently, the retarding force will be small, even with the highest possible μ.

---

[8] When hydroplaning, the tire is supported by a layer of water and the resistance to forward motion is due to rolling friction and the displacement of water ahead of the tire. Typical friction coefficients for this condition range from 0.02 to 0.04.

The importance of having weight on the gear in order to brake the airplane is further illustrated by Figure 17. This Figure plots an "effective μ" as a function of ground speed; the effective μ is the μ required to make the retarding force with the spoilers up equivalent to the retarding force with the spoilers down; i.e., it is the μ that would have to exist on the runway to make the airplane braking performance with the spoilers up match the braking performance with the spoilers down on a runway with a nominal μ. The effective μ can be determined from Equation [6]:

$$F_t|_{SU} = F_t|_{SD} \quad [7]$$

$$W\, r_t|_{SU}\, \mu_{eff} = W\, r_t|_{SD}\, \mu_{nom} \quad [8]$$

$$\mu_{eff} = (r_t|_{SD} / r_t|_{SU})\, \mu_{nom} \quad [9]$$

The subscripts SU and SD refer to Spoilers Up and Spoilers Down, respectively. The nominal μ_{nom} used to calculate μ_{eff} is 0.25.

Figure 17 shows that μ_{eff} does not climb above 0.04 until the airplane has decelerated to 140 knots. In other words, with the spoilers down the braking performance above 140 knots is no better than that achieved when hydroplaning; not because the runway surface conditions are lowering the friction coefficient, but because the lift from the wings is preventing the gear from putting much force on the runway. The effective braking friction coefficient only reaches the nominal values for a wet runway (0.20 - 0.25) after the airplane has slowed below 85 knots. Figures 16 and 17 make it clear that spoiler deployment is crucial in slowing the airplane effectively.

The stopping distance is very dependent on the touchdown ground speed. The reference airspeed for the approach is about 131 knots; adding 20 knots for the wind conditions, the appropriate approach airspeed is 151 knots. The DFDR data indicates that the airspeed during the approach was approximately 156 knots (though varying about ±5 knots because of the gusty conditions). The approximately 5 knot tailwind component shown in Figure 10 brought the ground speed up to about 160 knots. In zero wind conditions, the approach airspeed would be the reference speed plus about 10 knots, or about 140 knots. This would also be the touchdown ground speed of the airplane. Hence, at 160 knots AA1420 touched down at a ground speed 20 knots higher than that which would have been expected in zero wind conditions.

The top plot in Figure 18 illustrates the effect a 10 knot reduction in touchdown ground speed has on the stopping distance. Curves "B" and "C" in Figure 18 compare the ground speed profiles for the airplane with no spoiler deployment and using reverse thrust and the AA1420 braking profile, starting at touchdown ground speeds of 162 and 152 knots, respectively. On curve "C," the airplane departs the runway at 60 knots (as opposed to 95 knots for curve "B") and, at the point where the DFDR data ends, the ground speed has decreased to 20 knots, compared to 75 knots for curve "B," and 85 knots for the actual AA1420 data. Assuming that the DFDR data ends where the airplane impacted the light stanchion, curves "A" and "C" in Figure 18 indicate that a 10 knot reduction in the touchdown ground speed may have reduced the impact speed from 85 knots to 20 knots. This represents a 94% reduction in the kinetic energy at impact. Even if, after the airplane departs the runway and is no longer on a hard surface, the deceleration decreases from the level shown in curve "C" to that shown in curve "A," the impact speed would still be reduced from 85 knots to about 45 knots. This represents a 72% reduction in the kinetic energy at impact.

The top of Figure 18 also shows that without using reverse thrust but with the spoilers deployed, a 10 knot reduction in the touchdown ground speed would have allowed the airplane to stop about 400 feet short of the end of the runway.

These results indicate that the extra ground speed carried on touchdown (compared to the expected touchdown ground speed in zero wind or headwind conditions) exacerbated the stopping distance problem and the consequences of impacting the light stanchion. Had the wind been more of a headwind than a crosswind, then given the same airspeed the touchdown ground speed would have been lower.

The bottom plot in Figure 18 shows the effect of using a "Normal" braking profile, as opposed to the "AA1420" braking profile, on stopping distance when the touchdown ground speed is 152 knots (because of a limitation in the Operational Landing Program, this comparison could not be done for a touchdown ground speed of 162 knots). As mentioned above, in the "Normal" braking profile the brakes are applied 0.25 seconds after touchdown and full braking is achieved 1.25 seconds thereafter. In the AA1420 profile, the brakes are applied 5 seconds after touchdown and full braking is achieved 6 seconds thereafter. Curves "B" and "C" in the bottom plot of Figure 18 show that when the spoilers are not deployed, the different braking techniques produce only about a 200 foot difference in stopping distance. However, when the spoilers are deployed, curves "D" and "E" indicate that the more aggressive "Normal" braking profile stops the airplane 800 feet sooner than does the "AA1420" braking profile.

VI. Directional Control on the Ground

Figures 14 and 15a-f indicate that AA1420 developed a substantial drift angle while on the runway, i.e., the airplane's heading was not aligned with the velocity vector of the center of gravity. The airplane drifted both to the right and to the left of the direction it was pointed by as much 16 degrees, and just before the DFDR data ended the airplane heading was 20 degrees to the right of the direction of travel. These circumstances point to directional control difficulties while on the runway.

As mentioned above, the forces acting on the airplane on the ground are aerodynamic, propulsive, and gear reaction forces. These forces have components along the longitudinal, lateral, and vertical axes of the airplane. For the airplane to track straight down the runway without any drift, aerodynamic forces in the airplane's lateral axis (side force) must be balanced by ground reactions at the landing gear, while the heading angle is controlled with the rudder and differential braking. Aerodynamic side forces are produced by sideslip angles arising from crosswinds over the runway. The sideslip angles also introduce a yawing moment that must be countered with the rudder and/or differential braking[9].

Successful control of the airplane on the ground in crosswinds depends on the ability of the landing gear tires to produce cornering, or side forces, that balance the aerodynamic side forces generated by both sideslip and rudder deflections required to control heading. However, Equation [6], which describes the braking force acting on a tire, also describes the side force acting on a tire (if μ is the cornering friction coefficient), and indicates that the tire must bear some weight before it can produce any side force. Because AA1420's spoilers did not deploy on touchdown and the wing continued to bear most of the weight at high speeds, very little reaction force was available at the gear to counter the aerodynamic side forces produced by the left crosswind, and consequently the airplane drifted to the right. Thus the same physics that diminished the braking performance of the airplane also created a directional control problem.

Another aspect of directional control on the ground is control of the airplane's heading. The heading can be controlled both with the rudder and by differential braking of the left and right landing gear; however, the latter method depends on the effectiveness of the brakes, and so any reduction in braking performance will also reduce the effectiveness of differential braking. Since for the reasons discussed above the effectiveness of the brakes on AA1420 was reduced substantially at high speeds, differential braking at these speeds would not have been effective at controlling the airplane heading. Thus the heading could only have been controlled by the rudder; however, the DFDR data indicates that the rudder performance may have been impaired by the effects of reverse thrust, further exacerbating the directional control problem.

The difficulty in controlling the heading can be seen in Figure 14a, most notably starting about 3,000 feet from the threshold. From 3,000 feet to 5,800 feet, the rudder is consistently in the trailing edge right (nose right) direction, yet the heading of the airplane between these points is continuously decreasing (moving nose left) at between 1 and 3 degrees/second. The heading stops decreasing briefly between 4,000 and 4,600 feet, which appears to coincide with a brief stowing of the reversers. At 5,200 feet, with full right rudder, the heading continues to decrease at about -1.5 degrees/second until 5,800 feet, at which point the reversers are stowed once again and the airplane appears to react dramatically to the rudder, with the yaw rate reversing and the heading starting to increase at up to 7 degrees/second. By 6,600 feet, the right reverser remains stowed but the left reverser is deployed again, but the engine EPRs are at idle, and the airplane continues to yaw nose right at about 4 degrees/second.

The observations just outlined appear to indicate that the airplane response to the rudder is reduced when the thrust reversers are deployed and the engine EPRs are above 1.3. In fact, a McDonnell Douglas (now Boeing) All Operators Letter (AOL) dated February 15, 1996 notes that

> as reverse thrust increases above approximately 1.3 EPR, rudder and vertical stabilizer effectiveness continue to decrease until at reverse thrust greater than approximately 1.6 EPR the rudder and vertical stabilizer provide little or no directional control.

---

[9] While differential braking can be used for directional control, Boeing does not recommended the technique as it reduces the braking force available to slow the airplane.

> While this may not be as relevant on a dry runway, rudder effectiveness is of extreme importance when surface friction is low. This is especially applicable when crosswind or tail wind conditions are also present. Specifically, if the airplane is inadvertently landed in a crab on a slippery runway, when the thrust reverser buckets are deployed, the forces acting on the airplane will move it toward the downwind side of the runway. Directional control to compensate for this drift may only be available from the rudder.
>
> The current Douglas MD-80 FCOM procedures recommend reverse thrust settings no greater than 1.6 EPR. If landing on wet or slippery runways the procedures recommend application of reverse thrust to idle reverse, gradually increasing as required, and reducing thrust if any difficulty in maintaining directional control is experienced during reverse thrust operations.
>
> To further reduce the possibility of runway excursions during heavy weather operations, Douglas will revise its recommended procedures to limit reverse thrust to 1.3 EPR when landing on wet or slippery runways. Limiting reverse thrust to 1.3 EPR during heavy weather landings will avoid operations in the regime where reverse thrust decreases rudder effectivity.

Further on the AOL advises,

> If difficulty in maintaining directional control is experienced during reverse thrust operation, reduce thrust as required and select forward idle if necessary to maintain or regain control. Do not attempt to maintain directional control by using asymmetric reverse thrust.

The right engine EPR on AA1420 is greater than 1.3 almost continuously between 3,200 and 5,800 feet from the threshold, and climbs to at least 1.8 during a couple of points while the reversers are out. The left engine EPR is consistently less than that of the right engine, but apparently reaches levels above 1.6 a couple of times during the reverser deployment (the sample rate of the reverser position parameter on the DFDR makes correlating the exact reverser position with an EPR value somewhat difficult).

The directional control problems experienced by AA1420 on the runway appear to confirm the observations in the AOL about the effects of reverse thrust on rudder effectiveness. The complete text of the AOL is included as an attachment to the Operations Group Chairman's Factual Report.

While runway 4R was certainly wet, the effective "slipperiness" of the runway arises not so much from the condition of the runway surface as from the lack of loading on the gear due to the failure of the spoilers to deploy. This lack of loading on the gear may also have been exacerbated by the position of the elevator surfaces during the landing roll; according to Figure 14a, between 2,800 and 5,000 feet from the threshold, both the left and right elevator surfaces were deflected full nose down (15 degrees). The Douglas AOL quoted above says that

> When operating on wet or slippery runways, apply sufficient down elevator after nose gear contact to increase weight on the nose wheel for improved steering effectiveness but not an excessive amount which will unload the main gear and reduce braking efficiency.

The AOL also advises "Observe the 10 knot tail wind component limitation." According to Figure 10, the winds experienced by AA1420 may have had about a 5 knot tailwind component, which is within the limitation. Just prior to touchdown, the control tower reported the winds to be from 320° at 23 knots, which would provide a 4 knot headwind.

It appears that AA1420 experienced many of the difficulties discussed in the All Operators Letter: greatly reduced reaction forces on the gear (due to the spoiler position), unloading of the main gear due to large nose down elevator inputs, strong crosswinds, loss of vertical stabilizer and rudder effectiveness due to reverse thrust greater than 1.3 EPR, and a slight tailwind (though the tailwind was within limitations). In addition, the airplane touched down 2,000 feet down the 7,200 foot runway going about 20 knots faster than the zero-wind touchdown ground speed. The resulting ground trajectory of the airplane presented in this study is consistent with the expected airplane performance as determined from Boeing's Operational Landing Program, and with the operational experience outlined in the All Operators Letter.

E. CONCLUSIONS

This study presents the radar and DFDR data available for AA1420, and describes additional airplane performance information derived from these sources. Using this information to calculate the trajectory of AA1420 on final approach and on the runway produces the results presented in detail in the Figures discussed throughout this study. Some important aspects of the performance of the airplane that can be gleaned from these results are described here.

On final approach, the airspeed averaged about 156 knots, about 25 knots faster than the reference airspeed, and jumped about erratically within about a ±5 knot band. These airspeed jumps, along with the noisiness of the lateral and vertical load factor data, are consistent with gusty and turbulent winds on approach. The wind calculations indicate that the wind direction varied mostly between 300° and 320° and the wind speed varied mostly between 14 and 34 knots, with occasional excursions in direction and speed beyond these values. In airplane body axes, the wind was mostly along the lateral axis, blowing from the left side of the airplane to the right (a left crosswind), though there was an approximately 5 knot tailwind component. This tailwind component brought the ground speed up to about 160 knots, or about 20 knots faster than the ground speed that would have been expected in zero wind conditions.

According to the recorded DFDR ILS glide slope deviation, at about 0.5 NM from the threshold, the airplane was about 0.5 dots high on the glide slope and continued to deviate above the glide slope centerline until passing above the 2 dot (full scale) fly down deviation beam about 1,200 feet from the runway threshold. The airplane touched down 2,000 feet beyond the runway threshold (1,000 feet beyond the glide slope antenna) drifting about 5° to the right. On touchdown, the spoilers did not deploy, and so the wings continued to support most of the airplane's weight, transferring very little weight to the landing gear. The light loading of the landing gear reduced substantially both the effectiveness of the brakes, and the ability of the gear to develop cornering loads to counter the aerodynamic side loads produced by the crosswind. Consequently, the deceleration was greatly diminished and the airplane started to drift towards the right edge of the runway.

Concurrently, the thrust reversers were deployed and reverse thrust was applied at EPR levels up to 1.9 on the left engine and 1.6 on the right engine. As is documented in a Boeing All Operators Letter, reverse thrust at these EPR levels virtually eliminates the effectiveness of the vertical stabilizer and rudder. This reduction in rudder effectiveness on AA1420 is evident in that despite substantial right rudder inputs, the airplane started to yaw into the wind (the vertical stabilizer apparently retained some effectiveness). The airplane eventually started to move back towards the left side of the runway, though it remained in about a 10° - 16° right drift (skid). During this period, the reverse thrust was momentarily removed, with an associated increase in rudder response. However, when reverse thrust was again applied, the airplane started to yaw left once more in spite of right rudder input. When the reverse thrust was removed a second time, the airplane immediately started to yaw to the right in a manner consistent with the rudder inputs. However, the airplane departed the left side of the runway, though it continued to yaw to the right. Eventually, the airplane crossed the departure end of the runway, with the nose gear on the left edge and the main gear off the left edge of the runway. The ground speed at this point was about 97 knots. The airplane started to return towards the extended centerline of the runway, until it impacted the approach light stanchion at about 83 knots and broke apart.

The directional control problems evident in the airplane's trajectory are not unexpected given the known deterioration of rudder effectiveness in reverse thrust at EPR levels above 1.3, and the lack of gear cornering and differential braking effectiveness resulting from the light loads on the gear.

The deceleration of the airplane is also consistent with the expected performance of the airplane given the high touchdown ground speed and airspeed and the lack of spoiler deployment. Specifically, the braking performance of the airplane is consistent with the vertical loads on the landing gear and nominal wet runway friction coefficients, and does not exhibit any evidence of hydroplaning.

This study indicates that the lack of spoiler deployment on touchdown is the most significant factor in both the handling problems on the runway and the airplane's poor braking performance. However, the study does not discuss any possible explanations for this lack of spoiler deployment.

John O'Callaghan
Senior Aerospace Engineer
Office of Research and Engineering

This page intentionally left blank

This page intentionally left blank

LIT ASR UTC Time, HH:MM:SS	LIT ATC CDT Time, HH:MM:SS	Pressure Altitude, ft.	Corrected Altitude, ft.	Range, nmi	Azimuth, ACP	Distance N of 4R, nmi	Distance E of 4R, nmi
04:31:30.68	11:31:32.18	16600	16500	54.31	2123	-52.87	-8.76
04:31:35.42	11:31:36.92	16500	16400	53.81	2122	-52.40	-8.59
04:31:40.13	11:31:41.63	16300	16200	53.31	2120	-51.93	-8.35
04:31:44.75	11:31:46.25	16200	16100	52.88	2120	-51.51	-8.28
04:31:49.49	11:31:50.99	16000	15900	52.38	2117	-51.05	-7.96
04:31:53.99	11:31:55.49	15800	15700	51.88	2111	-50.63	-7.41
04:31:58.85	11:32:00.35	15700	15600	51.38	2111	-50.14	-7.34
04:32:03.68	11:32:05.18	15500	15400	50.88	2111	-49.64	-7.26
04:32:08.09	11:32:09.59	15300	15200	50.38	2108	-49.18	-6.96
04:32:12.80	11:32:14.30	15200	15100	49.88	2108	-48.69	-6.89
04:32:17.54	11:32:19.04	15000	14900	49.38	2106	-48.21	-6.67
04:32:22.16	11:32:23.66	14800	14700	48.88	2106	-47.72	-6.59
04:32:26.90	11:32:28.40	14700	14600	48.38	2105	-47.24	-6.45
04:32:31.72	11:32:33.22	14500	14400	47.88	2103	-46.76	-6.24
04:32:36.35	11:32:37.85	14400	14300	47.38	2102	-46.28	-6.10
04:32:41.09	11:32:42.59	14200	14100	46.88	2100	-45.80	-5.89
04:32:45.71	11:32:47.21	14000	13900	46.38	2101	-45.30	-5.89
04:32:50.42	11:32:51.92	13900	13800	45.94	2098	-44.89	-5.62
04:32:55.16	11:32:56.66	13700	13600	45.44	2097	-44.40	-5.49
04:32:59.90	11:33:01.40	13500	13400	44.94	2095	-43.92	-5.29
04:33:04.61	11:33:06.11	13400	13300	44.44	2093	-43.44	-5.09
04:33:09.35	11:33:10.85	13200	13100	43.94	2093	-42.95	-5.03
04:33:14.09	11:33:15.59	13000	12900	43.50	2094	-42.50	-5.04
04:33:18.71	11:33:20.21	12900	12800	43.00	2090	-42.04	-4.72
04:33:23.53	11:33:25.03	12700	12600	42.50	2089	-41.55	-4.60
04:33:28.16	11:33:29.66	12500	12400	42.00	2088	-41.06	-4.48
04:33:32.78	11:33:34.28	12400	12300	41.50	2085	-40.59	-4.23
04:33:37.52	11:33:39.02	12200	12100	41.00	2086	-40.08	-4.24
04:33:42.23	11:33:43.73	12000	11900	40.50	2085	-39.59	-4.12
04:33:46.97	11:33:48.47	11900	11800	40.00	2083	-39.11	-3.95
04:33:51.71	11:33:53.21	11700	11600	39.56	2083	-38.67	-3.90
04:33:56.42	11:33:57.92	11600	11500	39.06	2083	-38.18	-3.85
04:34:01.16	11:34:02.66	11500	11400	38.56	2082	-37.68	-3.74
04:34:05.90	11:34:07.40	11400	11300	38.06	2082	-37.19	-3.68
04:34:10.52	11:34:12.02	11400	11300	37.56	2082	-36.69	-3.63
04:34:15.23	11:34:16.73	11300	11200	37.13	2081	-36.27	-3.53
04:34:19.85	11:34:21.35	11200	11100	36.63	2081	-35.77	-3.48
04:34:24.59	11:34:26.09	11200	11100	36.13	2081	-35.27	-3.43
04:34:29.33	11:34:30.83	11100	11000	35.69	2080	-34.84	-3.33
04:34:34.04	11:34:35.54	11000	10900	35.19	2080	-34.34	-3.28
04:34:38.85	11:34:40.35	10900	10800	34.69	2080	-33.84	-3.23
04:34:43.52	11:34:45.02	10900	10800	34.25	2079	-33.41	-3.13

Table 1. LIT ASR8 Radar Data (page 1 of 6). Corrected Altitude is based on an altimeter setting of 29.86 in. Hg. The transponder beacon code for all returns is 3635.

LIT ASR UTC Time, HH:MM:SS	LIT ATC CDT Time, HH:MM:SS	Pressure Altitude, ft.	Corrected Altitude, ft.	Range, nmi	Azimuth, ACP	Distance N of 4R, nmi	Distance E of 4R, nmi
04:34:48.23	11:34:49.73	10800	10700	33.75	2079	-32.91	-3.08
04:34:52.97	11:34:54.47	10700	10600	33.31	2080	-32.47	-3.09
04:34:57.59	11:34:59.09	10600	10500	32.81	2078	-31.98	-2.94
04:35:02.41	11:35:03.91	10600	10500	32.31	2078	-31.49	-2.89
04:35:07.04	11:35:08.54	10500	10400	31.88	2078	-31.06	-2.84
04:35:11.85	11:35:13.35	10400	10300	31.38	2079	-30.56	-2.84
04:35:16.52	11:35:18.02	10400	10300	30.88	2077	-30.07	-2.70
04:35:21.23	11:35:22.73	10300	10200	30.44	2076	-29.63	-2.61
04:35:25.97	11:35:27.47	10300	10200	29.94	2072	-29.15	-2.38
04:35:30.71	11:35:32.21	10200	10100	29.50	2074	-28.70	-2.43
04:35:35.41	11:35:36.91	10200	10100	29.00	2074	-28.21	-2.38
04:35:40.04	11:35:41.54	10200	10100	28.50	2072	-27.71	-2.25
04:35:44.78	11:35:46.28	10100	10000	28.06	2072	-27.28	-2.21
04:35:49.52	11:35:51.02	10100	10000	27.56	2072	-26.78	-2.17
04:35:54.14	11:35:55.64	10100	10000	27.13	2070	-26.36	-2.05
04:35:58.97	11:36:00.47	10000	9900	26.63	2069	-25.86	-1.96
04:36:03.59	11:36:05.09	10000	9900	26.19	2068	-25.43	-1.89
04:36:08.33	11:36:09.83	10000	9900	25.75	2066	-24.99	-1.77
04:36:12.95	11:36:14.45	10000	9900	25.31	2065	-24.56	-1.70
04:36:17.78	11:36:19.28	10000	9900	24.88	2062	-24.13	-1.55
04:36:22.40	11:36:23.90	10000	9900	24.44	2063	-23.69	-1.55
04:36:27.23	11:36:28.73	10000	9900	24.00	2063	-23.25	-1.52
04:36:31.85	11:36:33.35	9800	9700	23.63	2059	-22.89	-1.35
04:36:36.59	11:36:38.09	9700	9600	23.19	2062	-22.45	-1.42
04:36:41.33	11:36:42.83	9600	9500	22.75	2062	-22.01	-1.39
04:36:45.95	11:36:47.45	9400	9300	22.38	2062	-21.64	-1.36
04:36:50.78	11:36:52.28	9300	9200	21.94	2059	-21.21	-1.23
04:36:55.40	11:36:56.90	9100	9000	21.50	2058	-20.77	-1.17
04:37:00.23	11:37:01.73	8900	8800	21.13	2056	-20.41	-1.08
04:37:04.85	11:37:06.35	8800	8700	20.69	2056	-19.97	-1.05
04:37:09.59	11:37:11.09	8600	8500	20.25	2057	-19.53	-1.05
04:37:14.33	11:37:15.83	8500	8400	19.81	2053	-19.10	-0.90
04:37:18.95	11:37:20.45	8300	8200	19.44	2054	-18.73	-0.91
04:37:23.66	11:37:25.16	8200	8100	19.00	2052	-18.29	-0.83
04:37:28.28	11:37:29.78	8000	7900	18.63	2052	-17.93	-0.80
04:37:33.14	11:37:34.64	7900	7800	18.19	2051	-17.49	-0.75
04:37:37.76	11:37:39.26	7700	7600	17.81	2049	-17.11	-0.67
04:37:42.47	11:37:43.97	7600	7500	17.44	2050	-16.74	-0.68
04:37:47.09	11:37:48.59	7500	7400	17.00	2049	-16.30	-0.63
04:37:51.95	11:37:53.45	7400	7300	16.63	2050	-15.93	-0.64
04:37:56.57	11:37:58.07	7300	7200	16.19	2049	-15.50	-0.59
04:38:01.28	11:38:02.78	7300	7200	15.81	2049	-15.12	-0.57

Table 1. LIT ASR8 Radar Data (page 2 of 6). Corrected Altitude is based on an altimeter setting of 29.86 in. Hg. The transponder beacon code for all returns is 3635.

LIT ASR UTC Time, HH:MM:SS	LIT ATC CDT Time, HH:MM:SS	Pressure Altitude, ft.	Corrected Altitude, ft.	Range, nmi	Azimuth, ACP	Distance N of 4R, nmi	Distance E of 4R, nmi
04:38:06.02	11:38:07.52	7200	7100	15.44	2047	-14.75	-0.50
04:38:10.64	11:38:12.14	7100	7000	15.00	2049	-14.31	-0.52
04:38:15.38	11:38:16.88	7000	6900	14.63	2048	-13.94	-0.48
04:38:20.09	11:38:21.59	6900	6800	14.25	2046	-13.56	-0.42
04:38:24.83	11:38:26.33	6800	6700	13.88	2045	-13.19	-0.38
04:38:29.45	11:38:30.95	6600	6500	13.50	2042	-12.82	-0.30
04:38:34.19	11:38:35.69	6500	6400	13.06	2040	-12.38	-0.24
04:38:38.90	11:38:40.40	6400	6300	12.69	2037	-12.01	-0.17
04:38:43.64	11:38:45.14	6200	6100	12.31	2034	-11.64	-0.10
04:38:48.26	11:38:49.76	6100	6000	11.94	2031	-11.27	-0.03
04:38:53.00	11:38:54.50	6000	5900	11.56	2026	-10.89	0.07
04:38:57.71	11:38:59.21	5800	5700	11.19	2019	-10.52	0.19
04:39:02.45	11:39:03.95	5700	5600	10.75	2012	-10.08	0.31
04:39:06.95	11:39:08.45	5500	5400	10.38	2005	-9.71	0.42
04:39:11.69	11:39:13.19	5400	5300	10.00	1994	-9.33	0.59
04:39:16.64	11:39:18.14	5200	5100	9.63	1987	-8.96	0.68
04:39:21.14	11:39:22.64	5100	5000	9.31	1977	-8.63	0.81
04:39:25.88	11:39:27.38	5100	5000	8.94	1963	-8.25	0.98
04:39:30.38	11:39:31.88	5000	4900	8.56	1953	-7.86	1.08
04:39:35.24	11:39:36.74	4900	4800	8.19	1941	-7.47	1.19
04:39:39.86	11:39:41.36	4800	4700	7.88	1929	-7.15	1.30
04:39:44.57	11:39:46.07	4700	4600	7.50	1914	-6.75	1.42
04:39:49.31	11:39:50.81	4600	4500	7.19	1898	-6.41	1.55
04:39:54.05	11:39:55.55	4500	4400	6.81	1881	-6.00	1.65
04:39:58.67	11:40:00.17	4400	4300	6.50	1863	-5.66	1.77
04:40:03.38	11:40:04.88	4300	4200	6.13	1844	-5.26	1.85
04:40:08.00	11:40:09.50	4300	4200	5.81	1823	-4.90	1.95
04:40:12.74	11:40:14.24	4200	4100	5.50	1799	-4.54	2.05
04:40:17.48	11:40:18.98	4100	4000	5.19	1774	-4.18	2.14
04:40:22.06	11:40:23.56	4000	3900	4.88	1744	-3.80	2.23
04:40:26.72	11:40:28.22	4000	3900	4.63	1714	-3.48	2.32
04:40:31.43	11:40:32.93	3900	3800	4.38	1676	-3.14	2.43
04:40:36.17	11:40:37.67	3900	3800	4.13	1628	-2.76	2.56
04:40:40.91	11:40:42.41	3900	3800	4.00	1577	-2.47	2.74
04:40:45.53	11:40:47.03	3900	3800	3.94	1516	-2.18	2.98
04:40:50.03	11:40:51.53	3900	3800	3.94	1459	-1.94	3.21
04:40:54.53	11:40:56.03	3900	3800	4.06	1402	-1.74	3.52
04:40:59.27	11:41:00.77	3900	3800	4.25	1353	-1.59	3.86
04:41:04.01	11:41:05.51	3900	3800	4.50	1313	-1.49	4.21
04:41:08.63	11:41:10.13	3900	3800	4.75	1284	-1.42	4.53
04:41:13.46	11:41:14.96	3800	3700	5.06	1262	-1.41	4.88
04:41:18.20	11:41:19.70	3800	3700	5.38	1255	-1.48	5.20

Table 1. LIT ASR8 Radar Data (page 3 of 6). Corrected Altitude is based on an altimeter setting of 29.86 in. Hg. The transponder beacon code for all returns is 3635.

LIT ASR UTC Time, HH:MM:SS	LIT ATC CDT Time, HH:MM:SS	Pressure Altitude, ft.	Corrected Altitude, ft.	Range, nmi	Azimuth, ACP	Distance N of 4R, nmi	Distance E of 4R, nmi
04:41:22.82	11:41:24.32	3800	3700	5.69	1250	-1.57	5.50
04:41:27.44	11:41:28.94	3700	3600	6.06	1253	-1.74	5.83
04:41:32.06	11:41:33.56	3700	3600	6.31	1260	-1.90	6.04
04:41:36.77	11:41:38.27	3700	3600	6.63	1273	-2.15	6.28
04:41:41.51	11:41:43.01	3600	3500	6.88	1288	-2.40	6.44
04:41:46.25	11:41:47.75	3600	3500	7.06	1306	-2.65	6.51
04:41:50.96	11:41:52.46	3500	3400	7.25	1325	-2.92	6.58
04:41:55.58	11:41:57.08	3500	3400	7.38	1345	-3.18	6.58
04:42:00.32	11:42:01.82	3500	3400	7.44	1368	-3.43	6.49
04:42:05.27	11:42:06.77	3400	3300	7.50	1389	-3.67	6.41
04:42:09.89	11:42:11.39	3400	3300	7.50	1411	-3.87	6.26
04:42:14.72	11:42:16.22	3400	3300	7.44	1433	-4.03	6.06
04:42:19.34	11:42:20.84	3400	3300	7.31	1454	-4.13	5.80
04:42:24.20	11:42:25.70	3400	3300	7.31	1478	-4.33	5.63
04:42:28.91	11:42:30.41	3400	3300	7.25	1499	-4.46	5.42
04:42:33.53	11:42:35.03	3400	3300	7.19	1521	-4.59	5.20
04:42:38.39	11:42:39.89	3400	3300	7.13	1545	-4.72	4.97
04:42:43.01	11:42:44.51	3400	3300	7.13	1572	-4.91	4.74
04:42:47.72	11:42:49.22	3400	3300	7.13	1594	-5.05	4.55
04:42:52.34	11:42:53.84	3400	3300	7.06	1618	-5.15	4.30
04:42:57.41	11:42:58.91	3400	3300	7.06	1640	-5.28	4.10
04:43:02.03	11:43:03.53	3400	3300	7.06	1665	-5.42	3.87
04:43:06.77	11:43:08.27	3400	3300	7.06	1683	-5.52	3.71
04:43:11.47	11:43:12.97	3400	3300	7.13	1711	-5.73	3.47
04:43:16.22	11:43:17.72	3400	3300	7.13	1732	-5.82	3.26
04:43:20.96	11:43:22.46	3300	3200	7.13	1753	-5.92	3.05
04:43:25.79	11:43:27.29	3300	3200	7.06	1774	-5.94	2.82
04:43:30.53	11:43:32.03	3300	3200	7.00	1795	-5.96	2.58
04:43:35.15	11:43:36.65	3300	3200	6.94	1817	-5.98	2.34
04:43:39.86	11:43:41.36	3300	3200	6.88	1836	-5.98	2.13
04:43:44.60	11:43:46.10	3300	3200	6.81	1857	-5.96	1.90
04:43:49.34	11:43:50.84	3300	3200	6.69	1877	-5.89	1.67
04:43:54.17	11:43:55.67	3300	3200	6.63	1896	-5.87	1.47
04:43:58.79	11:44:00.29	3300	3200	6.50	1913	-5.77	1.28
04:44:03.62	11:44:05.12	3400	3300	6.44	1934	-5.74	1.07
04:44:08.36	11:44:09.86	3400	3300	6.38	1958	-5.70	0.83
04:44:13.10	11:44:14.60	3400	3300	6.25	1979	-5.59	0.62
04:44:17.72	11:44:19.22	3400	3300	6.19	2002	-5.54	0.39
04:44:22.43	11:44:23.93	3400	3300	6.13	2023	-5.48	0.20
04:44:27.17	11:44:28.67	3400	3300	6.13	2048	-5.47	-0.04
04:44:31.79	11:44:33.29	3400	3300	6.06	2072	-5.38	-0.26
04:44:36.62	11:44:38.12	3400	3300	6.06	2096	-5.36	-0.48

Table 1. LIT ASR8 Radar Data (page 4 of 6). Corrected Altitude is based on an altimeter setting of 29.86 in. Hg. The transponder beacon code for all returns is 3635.

LIT ASR UTC Time, HH:MM:SS	LIT ATC CDT Time, HH:MM:SS	Pressure Altitude, ft.	Corrected Altitude, ft.	Range, nmi	Azimuth, ACP	Distance N of 4R, nmi	Distance E of 4R, nmi
04:44:41.57	11:44:43.07	3400	3300	6.06	2122	-5.32	-0.72
04:44:46.31	11:44:47.81	3400	3300	6.06	2144	-5.29	-0.92
04:44:50.93	11:44:52.43	3300	3200	6.06	2168	-5.24	-1.13
04:44:55.55	11:44:57.05	3300	3200	6.19	2190	-5.31	-1.37
04:45:00.38	11:45:01.88	3300	3200	6.31	2206	-5.39	-1.55
04:45:05.00	11:45:06.50	3300	3200	6.50	2217	-5.54	-1.71
04:45:09.74	11:45:11.24	3300	3200	6.69	2225	-5.69	-1.84
04:45:14.48	11:45:15.98	3200	3100	6.88	2232	-5.85	-1.97
04:45:19.19	11:45:20.69	3100	3000	7.06	2240	-5.99	-2.11
04:45:23.93	11:45:25.43	3000	2900	7.25	2247	-6.15	-2.25
04:45:28.67	11:45:30.17	2900	2800	7.44	2255	-6.29	-2.40
04:45:33.38	11:45:34.88	2800	2700	7.69	2262	-6.50	-2.57
04:45:38.24	11:45:39.74	2800	2700	7.88	2268	-6.65	-2.71
04:45:42.95	11:45:44.45	2700	2600	8.06	2275	-6.78	-2.86
04:45:47.69	11:45:49.19	2600	2500	8.31	2281	-6.98	-3.03
04:45:52.43	11:45:53.93	2500	2400	8.50	2288	-7.12	-3.18
04:45:57.05	11:45:58.55	2500	2400	8.69	2295	-7.26	-3.35
04:46:01.76	11:46:03.26	2500	2400	8.88	2301	-7.39	-3.50
04:46:06.50	11:46:08.00	2400	2300	9.06	2310	-7.50	-3.69
04:46:11.24	11:46:12.74	2400	2300	9.25	2322	-7.60	-3.93
04:46:15.95	11:46:17.45	2300	2200	9.31	2336	-7.56	-4.13
04:46:20.69	11:46:22.19	2300	2200	9.44	2353	-7.55	-4.41
04:46:25.31	11:46:26.81	2400	2300	9.50	2366	-7.51	-4.60
04:46:30.05	11:46:31.55	2400	2300	9.56	2381	-7.45	-4.82
04:46:34.76	11:46:36.26	2400	2300	9.63	2396	-7.38	-5.04
04:46:39.50	11:46:41.00	2400	2300	9.69	2407	-7.34	-5.21
04:46:44.24	11:46:45.74	2400	2300	9.75	2424	-7.25	-5.45
04:46:48.95	11:46:50.45	2400	2300	9.75	2439	-7.11	-5.63
04:46:53.69	11:46:55.19	2400	2300	9.69	2456	-6.91	-5.79
04:46:58.43	11:46:59.93	2400	2300	9.56	2469	-6.69	-5.86
04:47:03.14	11:47:04.64	2400	2300	9.44	2483	-6.46	-5.94
04:47:07.88	11:47:09.38	2400	2300	9.25	2498	-6.18	-5.97
04:47:12.62	11:47:14.12	2400	2300	9.06	2510	-5.92	-5.96
04:47:17.33	11:47:18.83	2300	2200	8.81	2517	-5.68	-5.86
04:47:22.07	11:47:23.57	2400	2300	8.56	2523	-5.44	-5.74
04:47:26.90	11:47:28.40	2400	2300	8.38	2524	-5.30	-5.62
04:47:31.64	11:47:33.14	2400	2300	8.06	2525	-5.07	-5.41
04:47:36.38	11:47:37.88	2400	2300	7.81	2525	-4.89	-5.23
04:47:41.00	11:47:42.50	2400	2300	7.56	2523	-4.73	-5.04
04:47:45.83	11:47:47.33	2400	2300	7.31	2524	-4.55	-4.87
04:47:50.45	11:47:51.95	2300	2200	7.06	2525	-4.36	-4.70
04:47:55.07	11:47:56.57	2200	2100	6.81	2521	-4.21	-4.49

Table 1. LIT ASR8 Radar Data (page 5 of 6). Corrected Altitude is based on an altimeter setting of 29.86 in. Hg. The transponder beacon code for all returns is 3635.

LIT ASR UTC Time, HH:MM:SS	LIT ATC CDT Time, HH:MM:SS	Pressure Altitude, ft.	Corrected Altitude, ft.	Range, nmi	Azimuth, ACP	Distance N of 4R, nmi	Distance E of 4R, nmi
04:47:59.81	11:48:01.31	2100	2000	6.56	2521	-4.04	-4.32
04:48:04.52	11:48:06.02	2000	1900	6.31	2523	-3.84	-4.16
04:48:09.14	11:48:10.64	1900	1800	6.06	2519	-3.69	-3.95
04:48:13.88	11:48:15.38	1900	1800	5.81	2518	-3.52	-3.77
04:48:18.62	11:48:20.12	1800	1700	5.56	2517	-3.35	-3.59
04:48:23.33	11:48:24.83	1700	1600	5.38	2515	-3.23	-3.46
04:48:28.07	11:48:29.57	1700	1600	5.13	2513	-3.06	-3.27
04:48:32.69	11:48:34.19	1600	1500	4.94	2513	-2.93	-3.14
04:48:37.43	11:48:38.93	1500	1400	4.75	2513	-2.79	-3.01
04:48:42.14	11:48:43.64	1500	1400	4.50	2510	-2.62	-2.82
04:48:46.88	11:48:48.38	1400	1300	4.31	2508	-2.49	-2.68
04:48:51.62	11:48:53.12	1400	1300	4.13	2507	-2.37	-2.55
04:48:56.32	11:48:57.82	1300	1200	3.88	2503	-2.20	-2.36
04:49:00.95	11:49:02.45	1300	1200	3.69	2501	-2.07	-2.22
04:49:05.69	11:49:07.19	1200	1100	3.50	2499	-1.94	-2.09
04:49:10.43	11:49:11.93	1100	1000	3.31	2495	-1.81	-1.94
04:49:15.14	11:49:16.64	1100	1000	3.13	2495	-1.68	-1.82
04:49:19.88	11:49:21.38	1000	900	2.88	2489	-1.51	-1.63
04:49:24.50	11:49:26.00	1000	900	2.69	2486	-1.38	-1.50
04:49:29.24	11:49:30.74	900	800	2.50	2482	-1.25	-1.36
04:49:33.95	11:49:35.45	900	800	2.31	2477	-1.12	-1.22
04:49:38.69	11:49:40.19	800	700	2.13	2468	-1.00	-1.08
04:49:43.42	11:49:44.92	700	600	1.88	2458	-0.83	-0.90
04:49:48.05	11:49:49.55	700	600	1.69	2440	-0.71	-0.75
04:49:52.76	11:49:54.26	600	500	1.50	2419	-0.59	-0.59
04:49:57.38	11:49:58.88	500	400	1.31	2397	-0.46	-0.44
04:50:02.12	11:50:03.62	400	300	1.06	2372	-0.27	-0.27
04:50:06.86	11:50:08.36	400	300	0.88	2342	-0.14	-0.14
04:50:11.57	11:50:13.07	300	200	0.69	2297	0.01	-0.01
04:50:16.10	11:50:17.60	200	100	0.50	2201	0.16	0.14
04:50:20.48	11:50:21.98	200	100	0.31	1994	0.33	0.29

Table 1. LIT ASR8 Radar Data (page 6 of 6). Corrected Altitude is based on an altimeter setting of 29.86 in. Hg. The transponder beacon code for all returns is 3635.

CODE	TIME (PM)	ALT (ft.)	COMMENT
<36>	11:31:42	16192	**CAM-2** breaking out of this (crud). good.... doing good.
<40>	11:32:08	15272	**CAM-1** * just some lightning straight ahead.
<41>	11:32:14	15106	**CAM-2** *** think we're gonna be okay. right there.
<43>	11:32:31	14492	**CAM-1** down the bowling alley.
<49>	11:33:48	11810	**CAM-1** that's 40 miles.
<50>	11:33:49	11778	**CTR** AA1420, contact LIT approach 135.4.
<51>	11:33:50	11735	**CAM-2** yeah.
<54>	11:34:05	11351	**RDO-2** American uh, 1420 at uh, 11 3 for 10000.
<55>	11:34:11	11300	**APR** AA1420, LIT approach roger. ah we have a thunderstorm just northwest of the airport moving uh, through the area now. wind is 280 at 28, gusts 44 and uh, I'll have new weather for you in just a moment I'm sure.
<56>	11:34:23	11100	**RDO-2** yeah we can see the uh, lightning and uh, you wanta repeat those winds again.
<57>	11:34:28	11060	**APR** right now the wind current wind is 290 at 28, gusts 44.
<58>	11:34:34	10933	**CAM-1** all right 280 at 44.
<59>	11:34:36	10890	**CAM-2** gusts to 44 *.
<60>	11:34:38	10849	**CAM-1** right near the limit.
<61>	11:34:39	10828	**CAM-2** yeah, it's uh, 40 degrees off. what's our cross(wind) *.
<62>	11:34:43	10800	**APR** AA1420 expect an ILS runway 22L.
<63>	11:34:46	10779	**CAM-1** thirty.
<64>	11:34:47	10758	**RDO-2** 22L, we've got that, 1420.
<65>	11:34:50	10694	**CAM-2** no that's that's *, you're, not out of the limits because of the angle *, but it's pretty close.
<66>	11:34:56	10567	**CAM-1** yeah.
<67>	11:35:21	10237	**CAM-2** 22L is the right one.... so uh....
<68>	11:35:29	10168	**CAM-2** I uh, I didn't realize that.
<69>	11:35:32	10104	**CAM-?** eerraaw.
<70>	11:35:37	10100	**APR** AA1420, descend at pilot's discretion. maintain 4000.
<71>	11:35:40	10100	**RDO-2** * down to 4000, American uh, 1420.
<72>	11:35:46	10006	**CAM-1** 4000 set.
<73>	11:35:50	10000	**CAM-2** okay, 10000 foot, seatbelt sign no smoking.
<74>	11:35:52	10000	**CAM** [sound of "ding dong" similar to flight at10dant call chime]
<75>	11:35:53	10000	**CAM-1** yeah I'll get down in a second *.
<76>	11:35:55	10000	**CAM-2** okay.
<77>	11:36:02	9900	**CAM-2** yeah it's 10 knots uh...
<78>	11:36:04	9900	**CAM-1** thirty knots is the crosswind limitation but...
<79>	11:36:06	9900	**CAM-1** thirty knots is the.. wet, well.
<80>	11:36:08	9900	**CAM-2** that's the dry.
<81>	11:36:09	9900	**CAM-1** yeah, dry.
<82>	11:36:10	9900	**CAM-2** what about wet?
<83>	11:36:11	9900	**CAM-1** wet.
<84>	11:36:12	9900	**CAM-2** yeah.
<85>	11:36:12	9900	**CAM-1** is twenty.

Table 2. Selected CVR Transcript Information (Page 1 of 7).

CODE	TIME (PM)	ALT (ft.)	COMMENT
<86>	11:36:13	9900	**CAM-2** ah, it's 25. aw, what the #.
<87>	11:36:30	9845	**PA-1** flight attendants prepare for landing please.
<88>	11:36:40	9560	**CAM-2** you got the NOTAMS, with ya?
<89>	11:37:17	8349	**CAM-2** see the airport?
<90>	11:37:18	8306	**CAM-1** see it blinking out there.
<91>	11:37:20	8219	**CAM-2** ** to the north,
<92>	11:37:20	8219	**CAM-1** straight ahead.
<93>	11:37:21	8188	**CAM-2** well there's a couple runways here so, the problem is we're 16 miles south of the VOR and the airport's another 5 miles past that.
<94>	11:37:29	7934	**CAM-1** all right. (doesn't) matter.
<95>	11:37:32	7854	**CAM-2** so we've still got a little ways to go… bad part….. I'll tell you what. I'm gonna stay on the run… the VOR till we get a little closer.
<96>	11:38:22	6791	**CAM-1** oh I think I see, I see where it is.
<97>	11:38:25	6728	**CAM-2** yeah it's on **.
<98>	11:38:26	6707	**CAM-1** it's straight up there, yeah…
<99>	11:38:27	6671	**CAM-2** * (blinking) *.
<100>	11:38:28	6628	**CAM-1** it looks like there's stratus a layer, right over there.
<101>	11:38:36	6393	**CAM-2** *** I definitely got **. (I'll show you this later).
<102>	11:38:54	5911	**CAM-1** he said there was a storm just northwest of the field?
<103>	11:38:56	5836	**CAM-2** he said northwest.
<104>	11:38:57	5794	**CAM-1** yeah.
<105>	11:38:58	5751	**CAM-2** lightning strike he said storm, uh.
<106>	11:39:00	5683	**APR** AA1420, descend and maintain, 3000.
<107>	11:39:03	5620	**RDO-2** out of 4 for 3, American uh, 1420.
<108>	11:39:06	5509	**APR** AA1420 uh, you're equipment's a lot better than uh, what I have. how 's the final for 22L lookin'?
<109>	11:39:12	5325	**CAM-1** what's that?
<110>	11:39:12	5325	**RDO-2** okay, we can uh, see the airport from here. we can barely make it out but uh, we should be able to make 22. uh, that storm is moving this way like your, radar says it is but a little bit farther off than you thought.
<111>	11:39:23	5000	**APR** AA1420 roger, would you just want to shoot a visual approach?
<112>	11:39:27	5000	**CAM-1** naw.
<113>	11:39:28	4986	**RDO-2** uh, at this point we can't really make it out. we're gonna have to stay with you as long as possible.
<114>	11:39:32	4898	**APR** AA1420 roger. and uh, the winds kinda kicked around a little bit right now. it's 330, at uh, 11.
<115>	11:39:38	4773	**CAM-1** whoa.
<116>	11:39:39	4751	**RDO-2** okay, well that's a little bit, better than it was.
<117>	11:39:42	4686	**CAM-1** * thirty is a, tailwind though.
<119>	11:39:45	4623	**APR** and uh, right now I have a uh, windshear alert. the center field wind is 340 at 10 north boundary wind is 330 at 25. northwest boundary wind is 010 at 15.
<121>	11:39:56	4390	**CAM-1** ** be landing on 4?
<122>	11:39:59	4325	**RDO-2** is there a possibility to get runway 4?
<123>	11:40:01	4282	**APR** AA1420 yes sir. we can do runway 4 if * you'd prefer that.

Table 2. Selected CVR Transcript Information (Page 2 of 7).

CODE	TIME (PM)	ALT (ft.)	COMMENT
<124>	11:40:05	4200	**CAM-1** it'd be a headwind.
<125>	11:40:06	4200	**CAM-2** yeah.
<126>	11:40:06	4200	**CAM-2** I think we're gonna need…
<127>	11:40:08	4200	**RDO-2** …we would rather do the headwinds sir.
<128>	11:40:09	4200	**APR** I'm sorry, say again AA1420.
<129>	11:40:12	4147	**RDO-2** yeah, we're gonna want the headwind of course…. runway 4.
<130>	11:40:19	4000	**CAM-1** we're going to 3, right?
<131>	11:40:20	3978	**APR** American uh, 1420 uh, turn right heading of uh, 250 vectors for the ILS runway 4R final approach course.
<132>	11:40:22	3934	**CAM-2** yeah, 3000.
<133>	11:40:26	3900	**RDO-2** okay, a right turn to 250 uh, the long way around?
<134>	11:40:29	3883	**APR** uh, yes sir, you're a little close to the airport.
<135>	11:40:31	3841	**CAM-1** yeah right.
<136>	11:40:32	3820	**RDO-2** 250, that'll work.
<137>	11:40:36	3800	**CAM-2** *, runway 4.
<138>	11:40:46	3800	**CAM-2** 4R. 111.3, 042. I think we were, I think that was the airport right below us.
<139>	11:41:02	3800	**CAM-1** yeah it was. okay, 111.3.
<140>	11:41:07	3800	**CAM-2** 111.3, 042. 460 on decision altitude.
<141>	11:41:14	3720	**CAM-2** 4000 for 3000, is armed.
<142>	11:41:16	3700	**CAM-1** okay.
<143>	11:41:19	3700	**CAM-2** uh, MSA is thirty 300 feet all the way around.
<144>	11:41:22	3700	**APR** AA1420 uh, maintain 3300 for now please.
<145>	11:41:25	3685	**RDO-2** 3300. we just saw it, thanks.
<147>	11:41:31	3600	**CAM-2** okay. and 2217 glide slope intercept all the way down missed approach right turn to 4000…. ***.
<148>	11:41:57	3400	**CAM-2** let's see, you got the airport? tell you what. *.
<149>	11:42:00	3400	**CAM-1** yeah. ** I don't have the airport.
<150>	11:42:03	3376	**CAM-2** **, I'm saying you got the ILS.
<151>	11:42:04	3356	**CAM-1** yeah, I got the ILS
<153>	11:42:13	3300	**CAM-2** yeah, there it is. I got the airport.
<154>	11:42:16	3300	**CAM-1** okay, and decision height is 460.
<156>	11:42:19	3300	**CAM-1** do you have the airport?
<158>	11:42:20	3300	**CAM-1** is that it right there?
<160>	11:42:23	3300	**CAM-2** * see, I can't.
<161>	11:42:24	3300	**CAM-1** I don't see a runway.
<162>	11:42:26	3300	**CAM-2** go out this way.
<163>	11:42:27	3300	**APR** AA1420, it appears we have uh, second part of this storm moving through. the winds now, 340 at 16, gusts 34.
<164>	11:42:34	3300	**CAM-1** okay.
<165>	11:42:35	3300	**RDO-2** roger that.
<166>	11:42:40	3300	**CAM-2** you wanna accept a short approach? want to keep it in tight?
<167>	11:42:42	3300	**CAM-1** yeah, if you see the runway. 'cause I don't quite see it.
<168>	11:42:45	3300	**CAM-2** yeah, it's right here, see it?

Table 2. Selected CVR Transcript Information (Page 3 of 7).

CODE	TIME (PM)	ALT (ft.)	COMMENT
<169>	11:42:48	3300	**CAM-1** [sound of grunt] you just point me in the right direction and I'll start slowing down here. give me flaps 11.
<170>	11:42:54	3300	**RDO-2** and uh....
<171>	11:42:55	3300	**CAM-2** #, it's going right over the... f-field.
<173>	11:42:56	3300	**APR** AA1420, did you call me?
<174>	11:42:59	3300	**RDO-2** well we got the airport. we're going between clouds. I think it's right off my uh, 3 o'clock low, about 4 miles.
<175>	11:43:05	3300	**APR** AA1420, that's it. do you wanna shoot the visual approach or you wanna go out for the ILS?
<176>	11:43:09	3300	**RDO-2** I can, we'll, we'll (start) the visual. if we we can do it.
<177>	11:43:11	3300	**APR** AA1420's cleared visual approach runway 4R. if you lose it, need some help. let me know please.
<178>	11:43:15	3300	**RDO-2** I'll stay with you as long as possible, OK?
<179>	11:43:18	3294	**APR** that's fine, I'm working everything, AA1420.
<180>	11:43:20	3252	**RDO-2** that works for me.
<181>	11:43:21	3231	**APR** all right.
<182>	11:43:23	3200	**CAM-1** well you keep me straight.
<183>	11:43:23	3200	**CAM-2** keep it right here, keep it right here, ** right here.
<184>	11:43:25	3200	**CAM-1** what?
<185>	11:43:26	3200	**CAM-2** okay, did you notice something? there's the airport right there. okay?
<186>	11:43:31	3200	**CAM-1** where?
<187>	11:43:31	3200	**CAM-2** okay, you're set up on a base for it. okay?
<188>	11:43:33	3200	**CAM-1** I'm on a base now?
<189>	11:43:35	3200	**CAM-2** well, you're on a dogleg. you're comin' in. there's the airport.
<190>	11:43:38	3200	**CAM-1** uh, I lost it.
<191>	11:43:39	3200	**CAM-2** right there, you're you're downwind. see it's right there.
<192>	11:43:44	3200	**CAM-1** I still don't see it. [sound of chuckle] well just vector me. I don't know.
<193>	11:43:47	3200	**CAM-2** okay, well just go * right here.
<194>	11:43:49	3200	**CAM-1** okay.
<195>	11:43:59	3200	**APR** AA1420, you can monitor 118.7, runway 4R, cleared to land. the wind right now 330 at 21.
<196>	11:44:05	3298	**RDO-2** 18.7, we'll monitor, AA1420, thanks. cleared to land runway 4.
<198>	11:44:13	3300	**CAM-2** if you look at ....
<199>	11:44:14	3300	**CAM-1** those red lights out there. where, where's that in relation to....
<200>	11:44:18	3300	**CAM-2** there's another, there's two runways here. there's three runways.
<201>	11:44:19	3300	**CAM-1** yeah I know. see we're losing it. I don't think we can maintain visual.
<206>	11:44:28	3300	**RDO-2** and approach AA1420.
<207>	11:44:29	3300	**APR** AA1420, yes sir.
<208>	11:44:30	3300	**RDO-2** and there's a cloud between us and the airport. we just lost the field and I'm uh, on this vector here, I have the uh, basically last vector you gave us, we're on kind of a dog leg it looks like.
<209>	11:44:39	3300	**APR** AA1420, can you fly heading 220? I'll take you out for the ILS.
<211>	11:44:43	3300	**RDO-2** yeah 220's fine.
<212>	11:44:45	3300	**APR** and it will be just 1 probably 1 turn on from uh, downwind to final, for the ILS.

Table 2. Selected CVR Transcript Information (Page 4 of 7).

CODE	TIME (PM)	ALT (ft.)	COMMENT
<213>	11:44:49	3274	**RDO-2** 'K that's how it's gonna have to be, thanks.
<214>	11:44:51	3231	**CAM-2** yeah, I had it but I lost it with the clouds and that's what I was saying.
<215>	11:44:54	3200	**CAM-1** okay.
<216>	11:44:54	3200	**APR** AA1420, descend and maintain 2300.
<217>	11:44:56	3200	**RDO-2** 2300, AA1420.
<218>	11:44:59	3200	**CAM-2** 2300.
<219>	11:45:00	3200	**CAM-1** set and armed. uh, now it is.
<220>	11:45:07	3200	**CAM-2** #, * we had it.
<221>	11:45:09	3200	**CAM-1** yeah. I just, I never saw the runway.
<222>	11:45:11	3200	**CAM-2** no no, it's okay. I **.
<225>	11:45:15	3121	**CAM-1** I hate droning around visual at night in weather without, having some clue where I am.
<226>	11:45:23	2951	**CAM-2** yeah but, the longer we go out here the …
<227>	11:45:24	2930	**CAM-1** yeah, I know.
<230>	11:45:29	2825	**CAM-2** see how we're going right into this crap.
<231>	11:45:31	2782	**CAM-1** right.
<232>	11:45:47	2546	**RDO-2** and approach AA1420, I know you're doing your best sir. we're getting pretty close to this storm. we'll keep it tight if we have to.
<233>	11:45:52	2441	**APR** * AA1420 uh, turn right heading of uh, 270.
<235>	11:45:57	2400	**RDO-2** 270, AA1420.
<236>	11:45:59	2400	**APR** and uh, when you join the final, you're going to be right at just a little bit outside the marker if that's gonna be okay for ya.
<237>	11:46:04	2384	**CAM-1** that's great.
<238>	11:46:05	2363	**RDO-2** that's great with us.
<239>	11:46:06	2342	**APR** AA1420, roger.
<241>	11:46:11	2300	**CAM-2** see we're right on the base of these clouds so …
<242>	11:46:13	2294	**CAM-1** yeah.
<243>	11:46:14	2273	**CAM-2** … it's not worth it.
<245>	11:46:20	2200	**CAM-2** 270, 2300?
<246>	11:46:23	2218	**CAM-1** yes sir. * where I am.
<247>	11:46:25	2261	**APR** AA1420, turn right heading 300.
<248>	11:46:29	2300	**RDO-2** right turn 300 AA1420.
<249>	11:46:39	2300	**APR** AA1420 is uh, 3 miles from the marker. turn right heading 020. maintain 2300 'til established on the localizer. cleared ILS runway 4R approach.
<250>	11:46:43	2300	**CAM** [brief sound of Morse Code identifier]
<251>	11:46:47	2300	**RDO-2** 020 'til established, AA1420, cleared 4L approach.
<252>	11:46:52	2300	**CAM-1** aw, we're goin' right into this.
<253>	11:46:52	2300	**APR** AA1420, right now we have uh, heavy rain on the airport. the uh, current weather on the ATIS is not correct. I don't have new weather for ya, but the uh, visibility is uh, less than a mile. runway 4R RVR is 3000.
<255>	11:47:04	2300	**CAM-1** 3000.
<256>	11:47:04	2300	**RDO-2** roger that, 3000, American uh, 4teen twenty. this is 4R, correct?
<258>	11:47:08	2300	**APR** AA1420, that's correct sir. and runway 4R, cleared to land. the wind 350 at 30, gusts 45.

Table 2. Selected CVR Transcript Information (Page 5 of 7).

CODE	TIME (PM)	ALT (ft.)	COMMENT
<259>	11:47:10	2300	**CAM-1** can we land?
<260>	11:47:16	2260	**RDO-2** 030 at 45, AA1420.
<261>	11:47:19	2204	**CAM-2** ** zero forecast right down the runway.
<262>	11:47:22	2267	**CAM-1** 3000 RVR. we can't land on that.
<263>	11:47:24	2300	**CAM-2** 3000 if you look at uh…
<265>	11:47:27	2300	**CAM-1** what do we need?
<266>	11:47:28	2300	**CAM-2** no it's 2400 RVR.
<267>	11:47:29	2300	**CAM-1** okay, fine.
<268>	11:47:30	2300	**CAM-2** yeah, we're doing fine.
<269>	11:47:31	2300	**CAM-1** all right.
<270>	11:47:34	2300	**CAM-1** uh, fifteen.
<273>	11:47:44	2300	**CAM-1** landing gear down.
<276>	11:47:49	2264	**CAM-1** and lights ** please.
<278>	11:47:52	2199	**CAM-5** stabilizer motion
<279>	11:47:53	2177	**APR** windshear alert, center field wind, 350 at 32, gusts 45. north boundary wind 310 at 29. northeast boundary wind 320 at 32.
<281>	11:48:02	1985	**CAM-5** stabilizer motion.
<282>	11:48:03	1964	**CAM-2** flaps 28?
<283>	11:48:10	1814	**CAM-1** add twenty.
<284>	11:48:12	1800	**CAM-2** right.
<285>	11:48:12	1800	**CAM-1** add twenty knots.
<286>	11:48:12	1800	**APR** AA1420, the runway 4R RVR now is 1600.
<287>	11:48:14	1800	**CAM-2** okay.
<288>	11:48:17	1766	**CAM-2** aw #.
<289>	11:48:18	1745	**CAM-1** well we're established on the final.
<290>	11:48:20	1703	**CAM-2** we're established we're inbound, right.
<291>	11:48:24	1618	**RDO-2** okay, AA1420, we're established inbound.
<292>	11:48:26	1600	**APR** AA1420 roger, runway 4R, cleared to land, and the wind, 340 at 31. north wind, north uh, boundary wind is 300 at 26, northeast boundary wind 320 at 25, and the 4R RVR is 1600.
<294>	11:48:41	1400	**RDO-2** American uh, 1420, thanks.
<295>	11:48:43	1400	**CAM-2** that's a good point.
<297>	11:48:47	1329	**CAM-2** keep the speed.
<298>	11:48:50	1300	**CAM-2** 1000 feet.
<299>	11:48:54	1281	**CAM-1** I don't see anything. lookin' for 460.
<301>	11:49:00	1200	**CAM-2** it's there.
<302>	11:49:02	1200	**CAM-2** want forty flaps?
<303>	11:49:04	1167	**CAM-1** oh yeah, thought I called it.
<304>	11:49:05	1146	**CAM-2** forty now. 1000 feet. twenty, forty forty land.
<306>	11:49:10	1041	**APR** wind is 330 at 28.
<307>	11:49:12	1000	**CAM-1** this is, this is a can of worms.
<310>	11:49:24	900	**CAM-1** (I'm gonna stay above it a little)
<311>	11:49:24	900	**CAM-2** there's the runway off to your right, got it?

Table 2. Selected CVR Transcript Information (Page 6 of 7).

CODE	TIME (PM)	ALT (ft.)	COMMENT
<312>	11:49:26	900	**CAM-1** no.
<313>	11:49:27	879	**CAM-2** I got the right runway in sight.
<314>	11:49:30	816	**CAM-2** you're right on course. stay where you're at.
<315>	11:49:31	800	**CAM-1** I got it, I got it.
<316>	11:49:32	800	**APR** wind 330 at 25.
<317>	11:49:37.73	752	**CAM-?** wipersss.
<319>	11:49:46.40	667	**CAM-2** 500 feet.
<321>	11:49:53.07	602	**APR** wind 320, at 23.
<322>	11:49:53.67	596	**CAM-1** plus twenty.
<323>	11:49:56.56	545	**CAM-?** aw #, we're off course.
<325>	11:50:00.45	477	**CAM-2** we're way off.
<326>	11:50:01.55	466	**CAM-1** I can't see it.
<327>	11:50:04.43	436	**CAM-2** got it?
<328>	11:50:05.13	428	**CAM-1** yeah I got it.
<329>	11:50:07.92	394	**CAM-2** hundred feet.
<330>	11:50:09.42	375	**CAM-?** above.
<331>	11:50:11.11	356	**CAM-2** hundred.
<332>	11:50:12.76	330	**CAM-5** sink rate.
<333>	11:50:13.66	318	**CAM-2** fifty.
<334>	11:50:14.16	312	**CAM-5** sink rate.
<335>	11:50:14.50	307	**CAM-2** forty.
<336>	11:50:15.79	289	**CAM-2** thirty.
<337>	11:50:17.59	276	**CAM-2** twenty.
<338>	11:50:18.29	273	**CAM-2** 10.
<339>	11:50:20.18	266	**CAM** [sound of two thuds similar to aircraft touching down on runway concurrent with unidentified squeak sound]
<340>	11:50:22.17	266	**CAM-2** we're down.
<341>	11:50:24.36	266	**CAM-2** we're sliding.
<342>	11:50:26.06	266	**CAM-1** #... #.
<343>	11:50:31.84	266	**CAM-?** on the brakes.
<344>	11:50:33.13	266	**CAM-?** oh sh ...
<345>	11:50:33.53	266	**CAM** [sound similar to increase in engine RPM]
<346>	11:50:35.13	266	**CAM-?** other one, other one, other one.
<347>	11:50:40.91	266	**CAM-?** aw #.
<348>	11:50:41.60	266	**CAM-?** ##.
<349>	11:50:43.80	266	**CAM** [sound of impact]
<350>	11:50:44.29	266	**CAM-?** ##.
<351>	11:50:46.88	266	**CAM** [sound of several impacts]
<352>	11:50:48.08	266	**END of RECORDING**
			END of TRANSCRIPT

RDO: Radio transmission from aircraft
CAM: Cockpit area microphone voice or sound source
PA: Transmission over aircraft public address system
CTR: Radio transmission from LIT center controller
APR: Transmission from LIT Approach/Tower controller
-1: Voice identified as Pilot-in-Command (PIC)
-2: Voice identified as Co-Pilot (SIC)
-5: Voice identified as aircraft mechanical voice

Table 2. Selected CVR Transcript Information (Page 7 of 7). Altitudes are ASR8 reported altitudes above 700 feet, and integrated accelerometer altitudes below 700 feet. All altitudes are MSL.

Runway Heading (Degrees True)	46.52°
Localizer Heading (Degrees True)	46.55°
Distance of Localizer Antenna from Threshold	1.25245 nmi
Localizer Width (150 μA dot to 150 μA dot)*	5.03°
Localizer Symmetry*	49.9
Elevation of Glide Slope Antenna	252.6 ft.
Glide Slope Angle*	2.93°
Distance of Glide Slope Antenna from Threshold	0.164601 nmi
Glide Slope Width (75 mV to 75mV)*	0.69°
Glide Slope Symmetry*	49.2

* These items are taken from the report of an ILS inspection conducted on 11/20/98.

Table 3. ILS data used to calculate glide slope and localizer beam geometry.

Ground Speed (knots)	Wet Runway Braking Friction Coefficient
0	0.1900
40	0.2593
65	0.2800
90	0.2800
200	0.1625

Table 4. Wet runway braking friction coefficients used in Boeing's Operational Landing Program for the MD-80.

This page intentionally left blank

This page intentionally left blank

American Airlines Flight 1420 - Little Rock, AR, 6/22/99
Plan View of Flight Path for Final 20 minutes of Radar Data
with Selected Transmissions from ATC

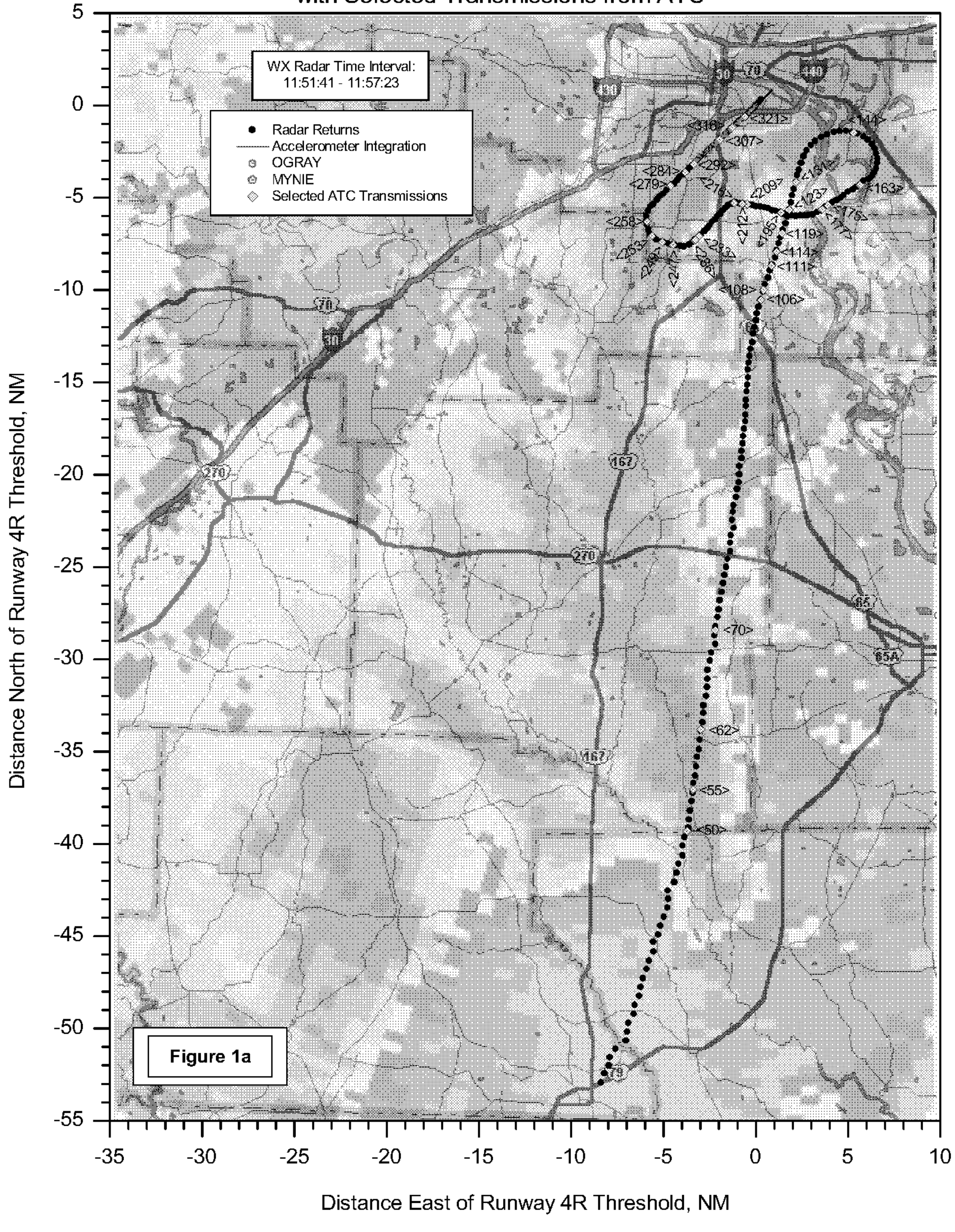

American Airlines Flight 1420 - Little Rock, AR, 6/22/99
Plan View of Flight Path for Final 20 minutes of Radar Data
with Selected CVR and ATC Information - Page 1 of 5

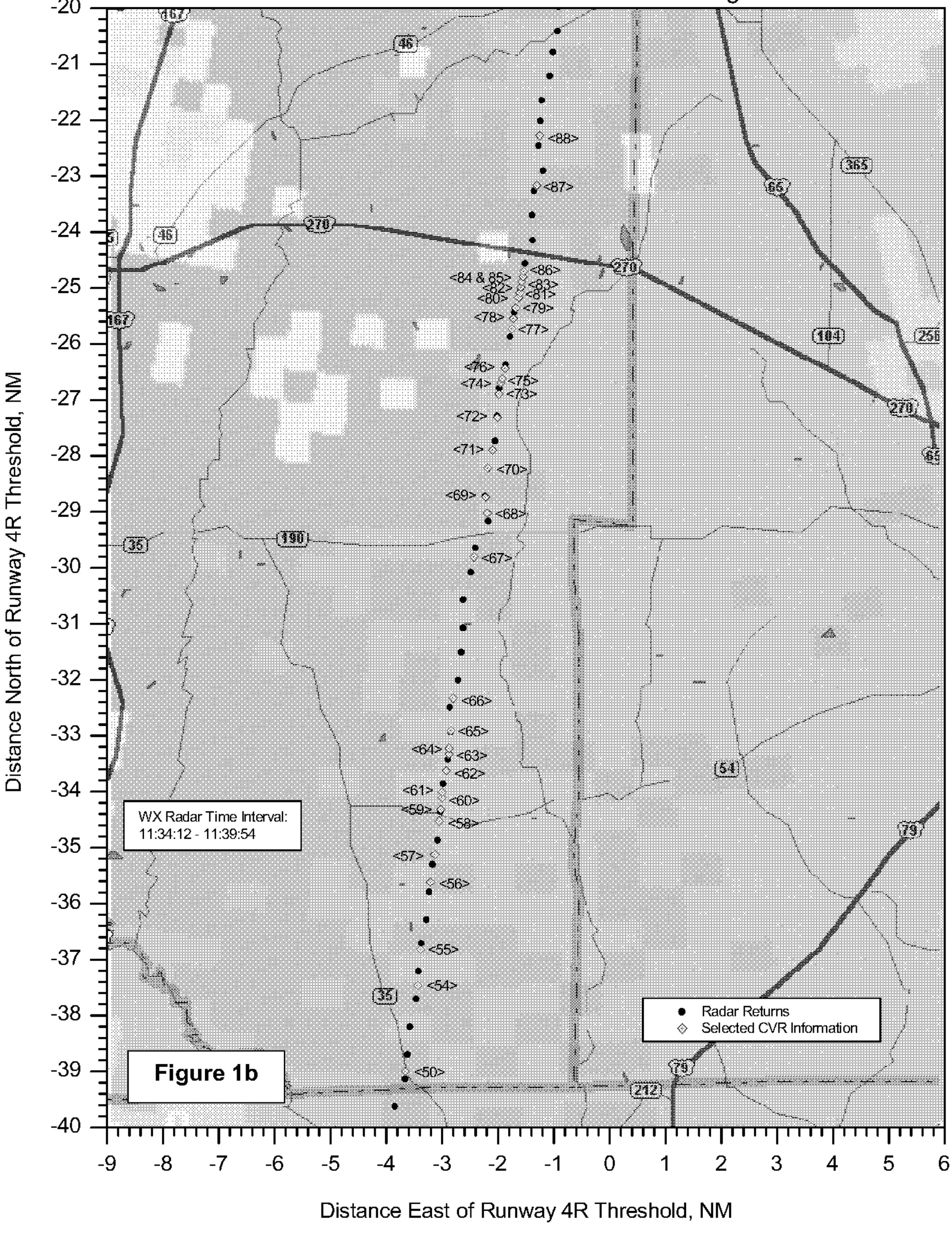

Figure 1b

American Airlines Flight 1420 - Little Rock, AR, 6/22/99
Plan View of Flight Path for Final 20 minutes of Radar Data
with Selected CVR and ATC Information - Page 2 of 5

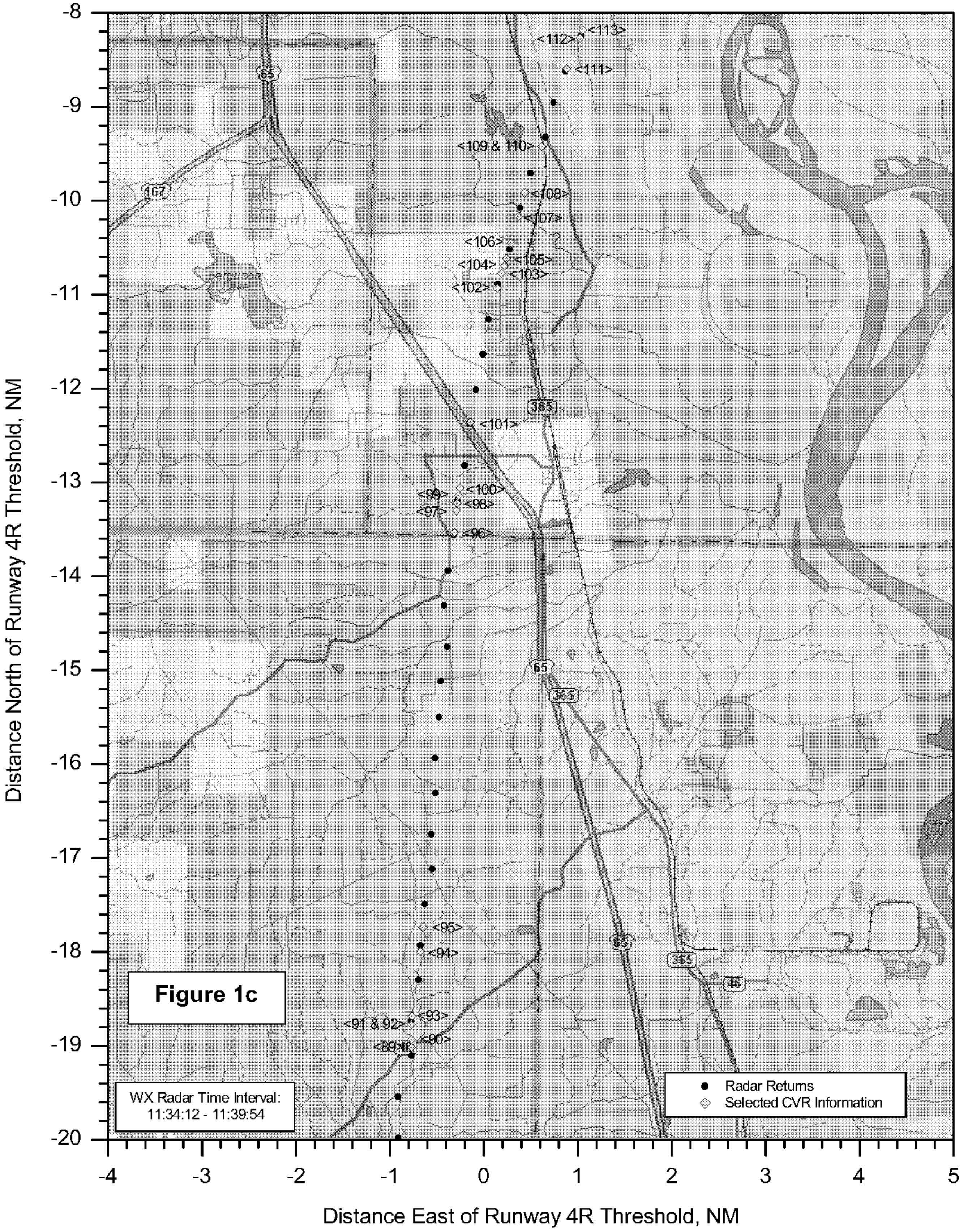

American Airlines Flight 1420 - Little Rock, AR, 6/22/99

Plan View of Flight Path for Final 20 minutes of Radar Data with Selected CVR and ATC Information - Page 3 of 5

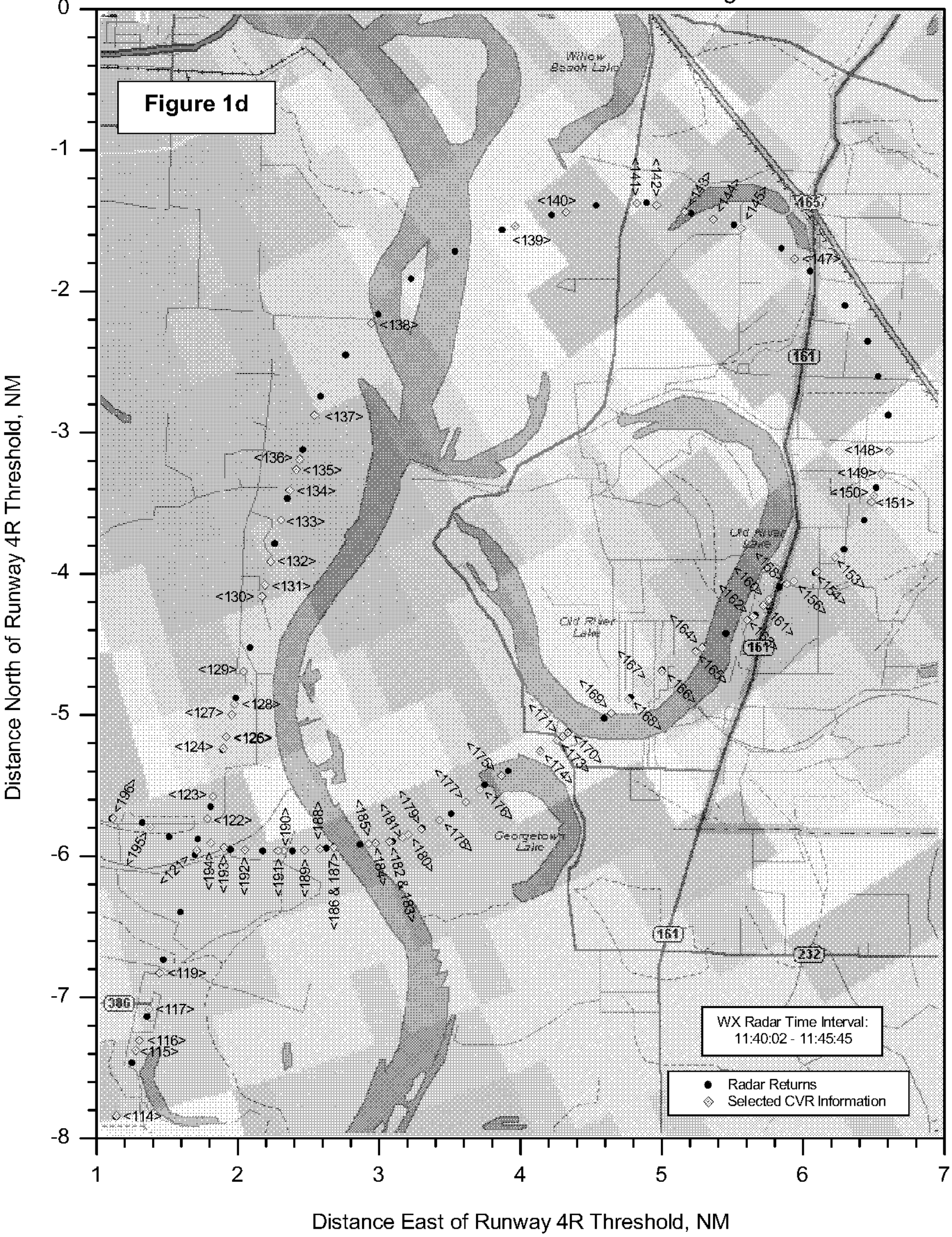

American Airlines Flight 1420 - Little Rock, AR, 6/22/99

Plan View of Flight Path for Final 20 minutes of Radar Data
with Selected CVR and ATC Information - Page 4 of 5

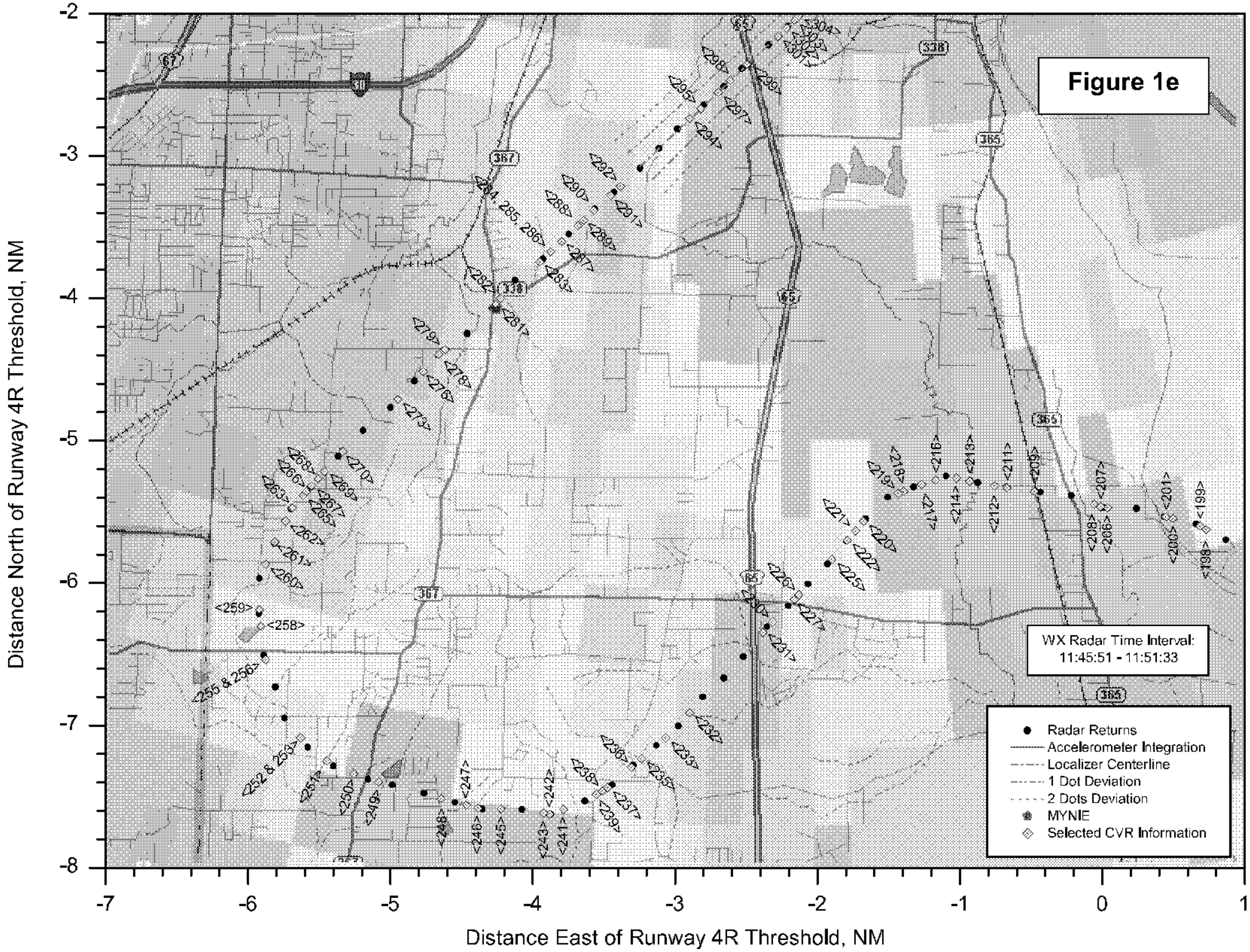

American Airlines Flight 1420 - Little Rock, AR, 6/22/99

Plan View of Flight Path for Final 20 minutes of Radar Data with Selected CVR and ATC Information - Page 5 of 5

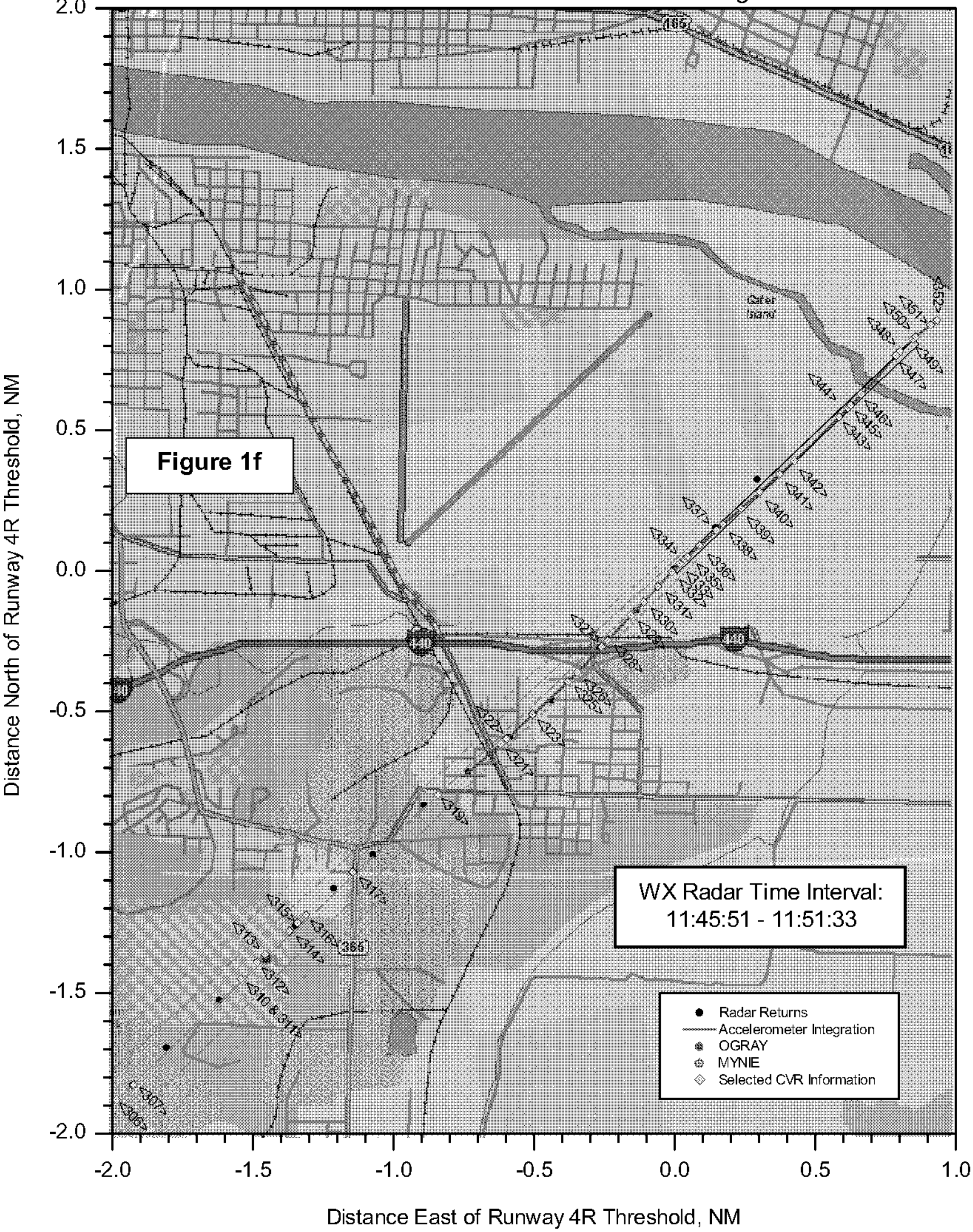

Weather Radar Information on Plan View Plots of AA1420's Flight Path

Precipitation Mode DBZ Color Codes (numbers in colored boxes indicate reflectivity in DBZ):

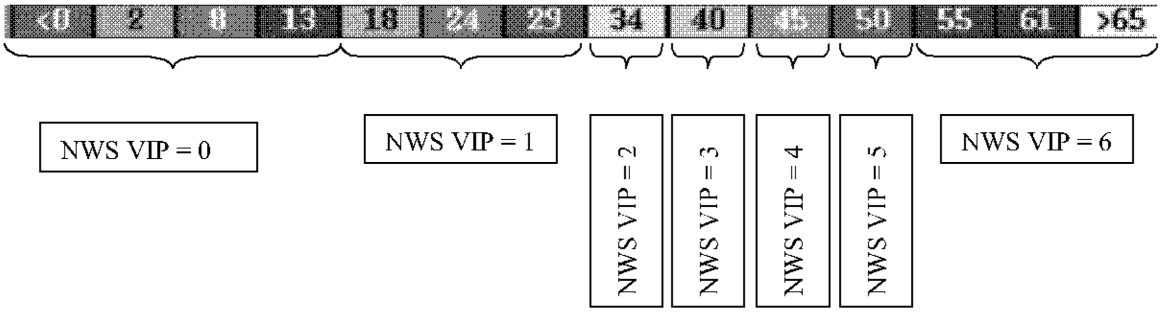

NWS VIP/DBZ CONVERSION TABLE
(Reproduced from the Weather Group Chairman's Factual Report)

NWS VIP	WSR-88D LVL	PREC MODE DBZ	RAINFALL
0	0 1 2	< 5 5 to 9 10 to 14	
1 Very Light	3 4 5	15 to 19 20 to 24 25 to 29	.01 in/hr .02 in/hr .04 in/hr
2 Light to Moderate	6 7	30 to 34 35 to 39	.09 in/hr .21 in/hr
3 Strong	8	40 to 44	.48 in/hr
4 Very Strong	9	45 to 49	1.10 in/hr
5 Intense	10	50 to 54	2.49 in/hr
6 Extreme	11 12 13 14 15	55 to 59 60 to 64 65 to 69 70 to 74 > 75	>5.67 in/hr

Figure 2.

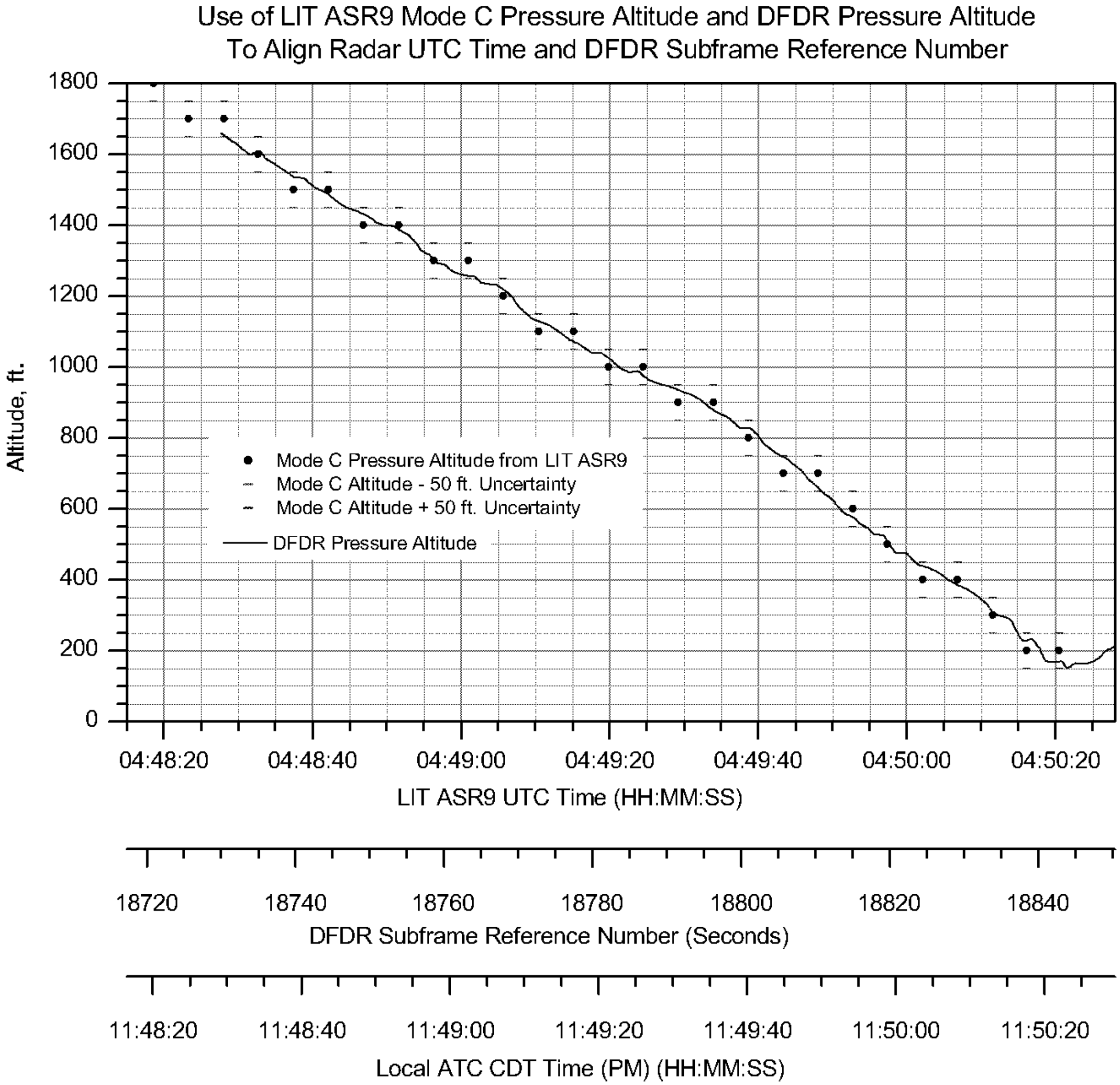
Use of LIT ASR9 Mode C Pressure Altitude and DFDR Pressure Altitude
To Align Radar UTC Time and DFDR Subframe Reference Number
Altitude, ft.
1800
1600
1400
1200
1000
800
600
400
200
0
Mode C Pressure Altitude from LIT ASR9
Mode C Altitude - 50 ft. Uncertainty
Mode C Altitude + 50 ft. Uncertainty
DFDR Pressure Altitude
04:48:20
04:48:40
04:49:00
04:49:20
04:49:40
04:50:00
04:50:20
LIT ASR9 UTC Time (HH:MM:SS)
18720
18740
18760
18780
18800
18820
18840
DFDR Subframe Reference Number (Seconds)
11:48:20
11:48:40
11:49:00
11:49:20
11:49:40
11:50:00
11:50:20
Local ATC CDT Time (PM) (HH:MM:SS)

Figure 3.

American Airlines Flight 1420 - Little Rock, AR, 6/22/99

Altitude vs. Time During Descent

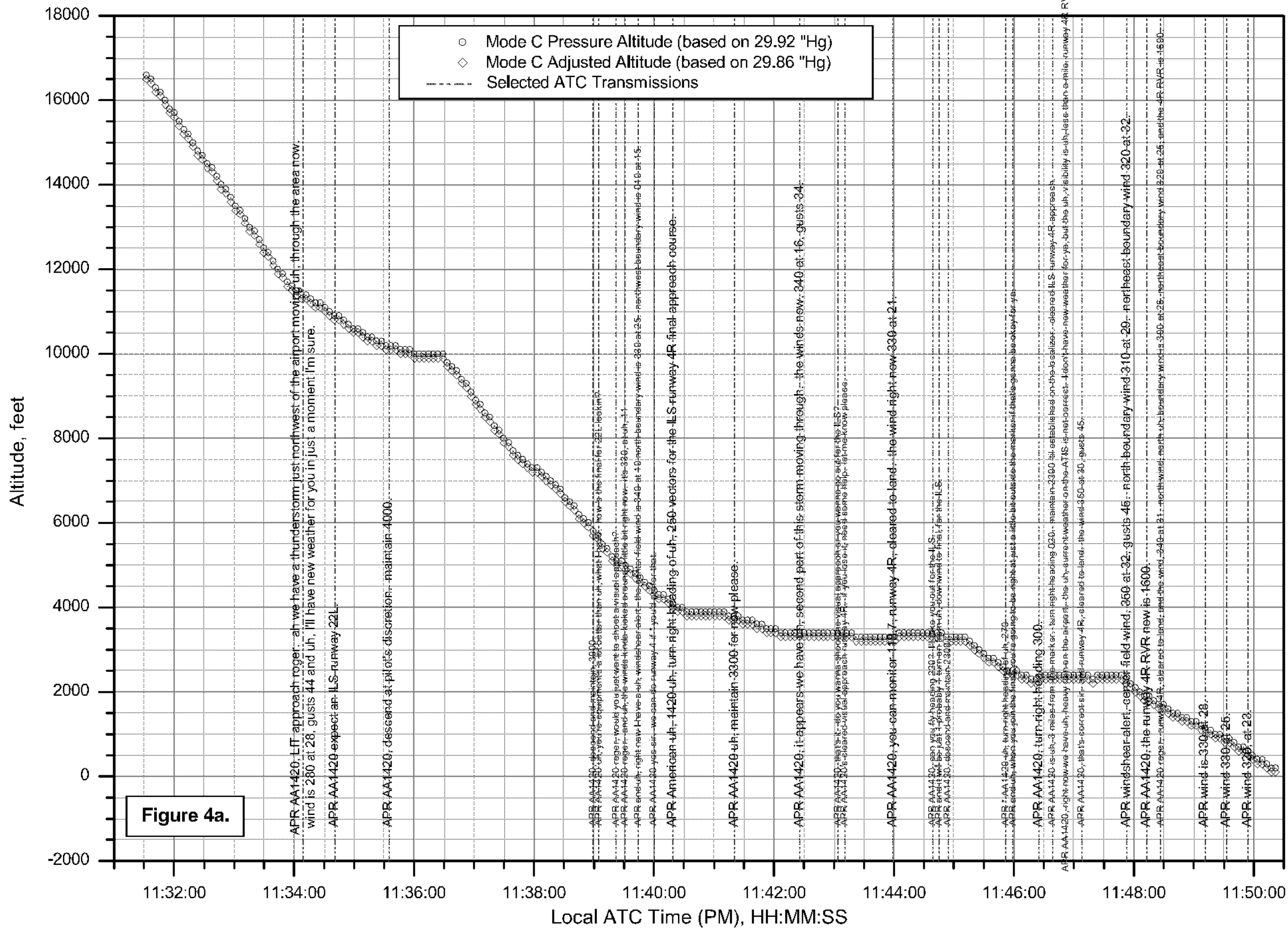

American Airlines Flight 1420 - Little Rock, AR, 6/22/99

Altitude vs. Time During Final Approach

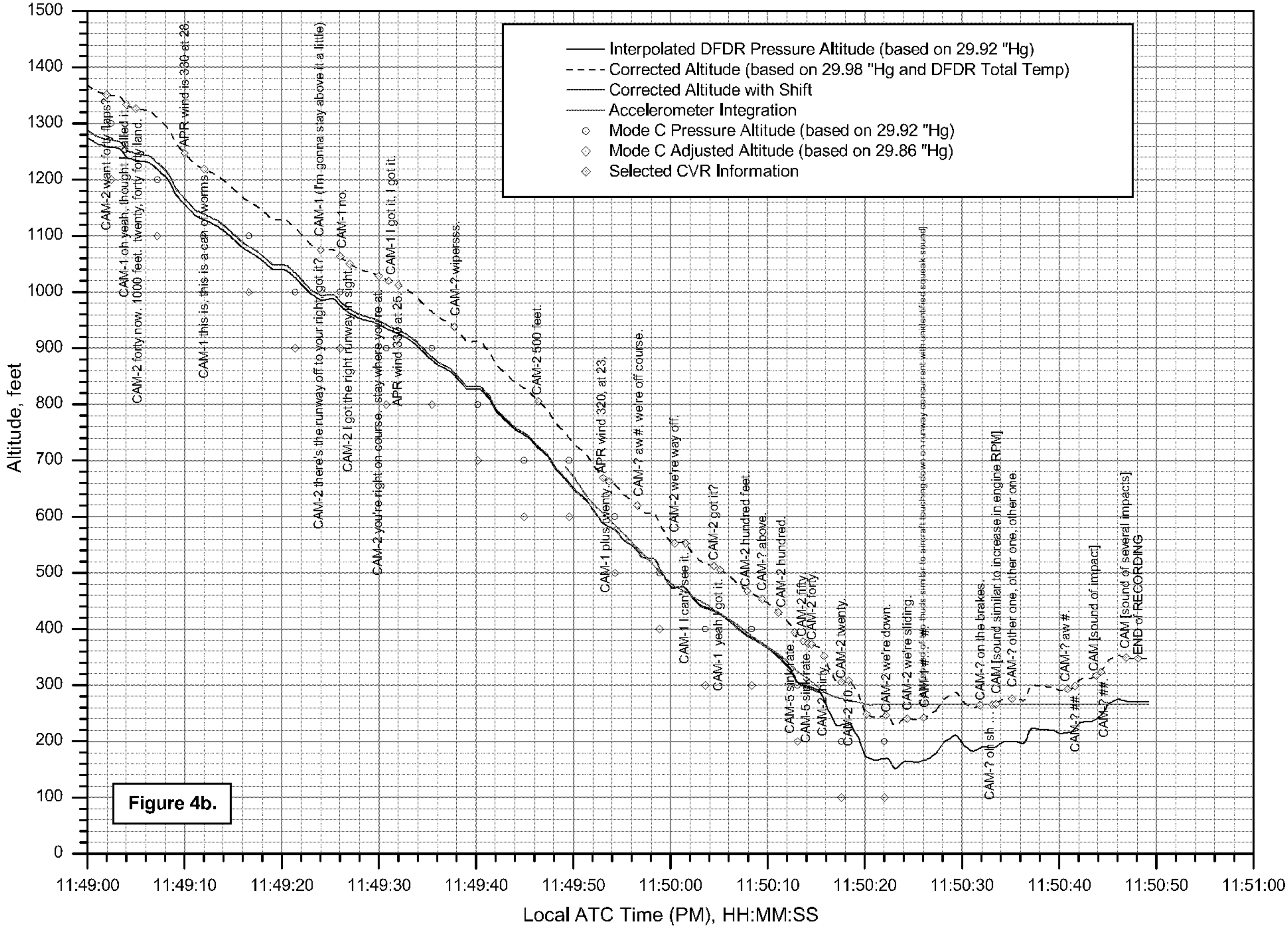

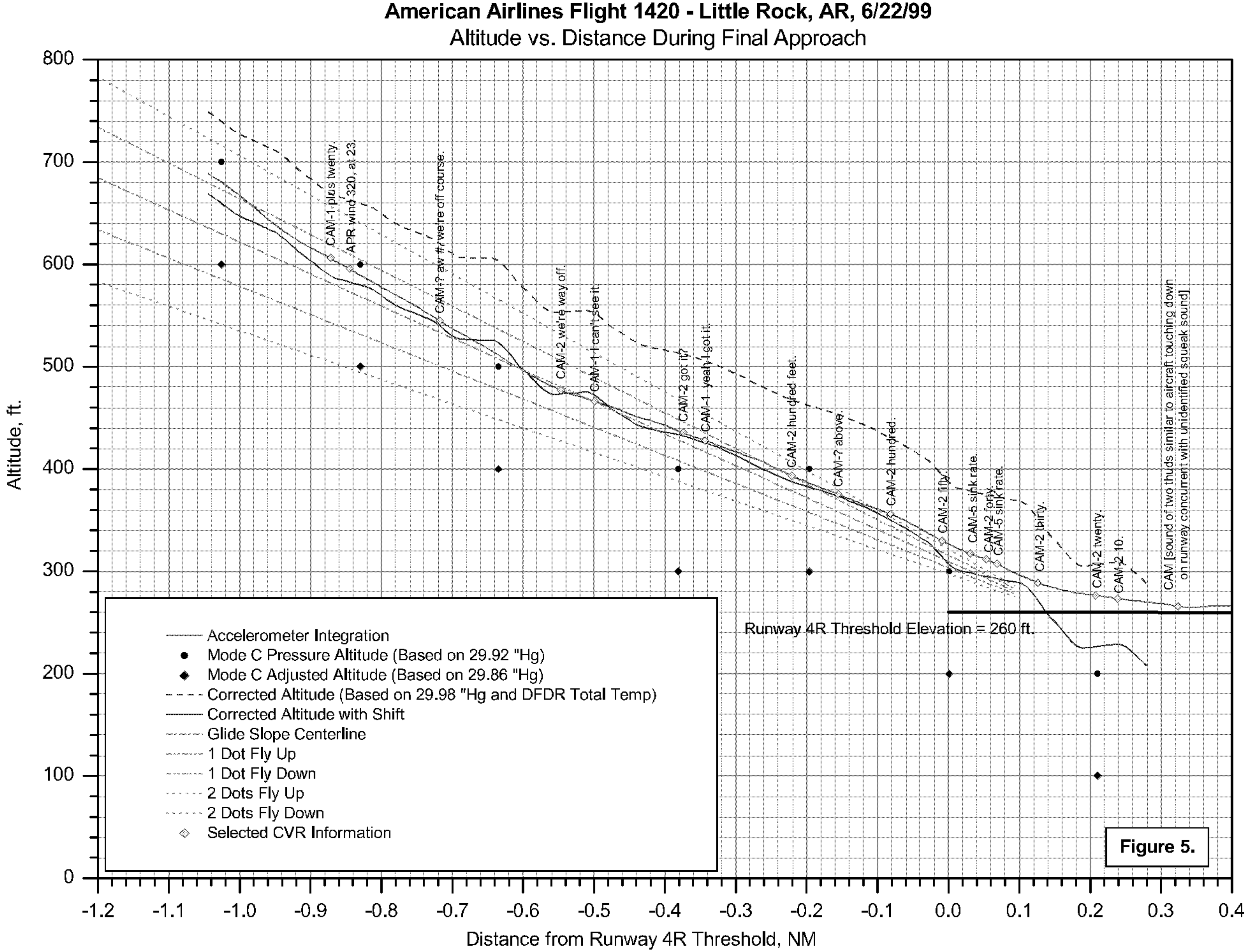
American Airlines Flight 1420 - Little Rock, AR, 6/22/99
Altitude vs. Distance During Final Approach
Altitude, ft.
Distance from Runway 4R Threshold, NM
800
700
600
500
400
300
200
100
0
-1.2
-1.1
-1.0
-0.9
-0.8
-0.7
-0.6
-0.5
-0.4
-0.3
-0.2
-0.1
0.0
0.1
0.2
0.3
0.4
CAM-1 plus twenty.
APR wind 320, at 23.
CAM-? aw #, we're off course.
CAM-2 we're way off.
CAM-1 I can't see it.
CAM-2 got it?
CAM-1 yeah, I got it.
CAM-2 hundred feet.
CAM-? above.
CAM-2 hundred.
CAM-2 fifty.
CAM-5 sink rate.
CAM-2 forty.
CAM-5 sink rate.
CAM-2 thirty.
CAM-2 twenty.
CAM-2 10.
CAM [sound of two thuds similar to aircraft touching down on runway concurrent with unidentified squeak sound]
Runway 4R Threshold Elevation = 260 ft.
Accelerometer Integration
Mode C Pressure Altitude (Based on 29.92 "Hg)
Mode C Adjusted Altitude (Based on 29.86 "Hg)
Corrected Altitude (Based on 29.98 "Hg and DFDR Total Temp)
Corrected Altitude with Shift
Glide Slope Centerline
1 Dot Fly Up
1 Dot Fly Down
2 Dots Fly Up
2 Dots Fly Down
Selected CVR Information

Figure 5.

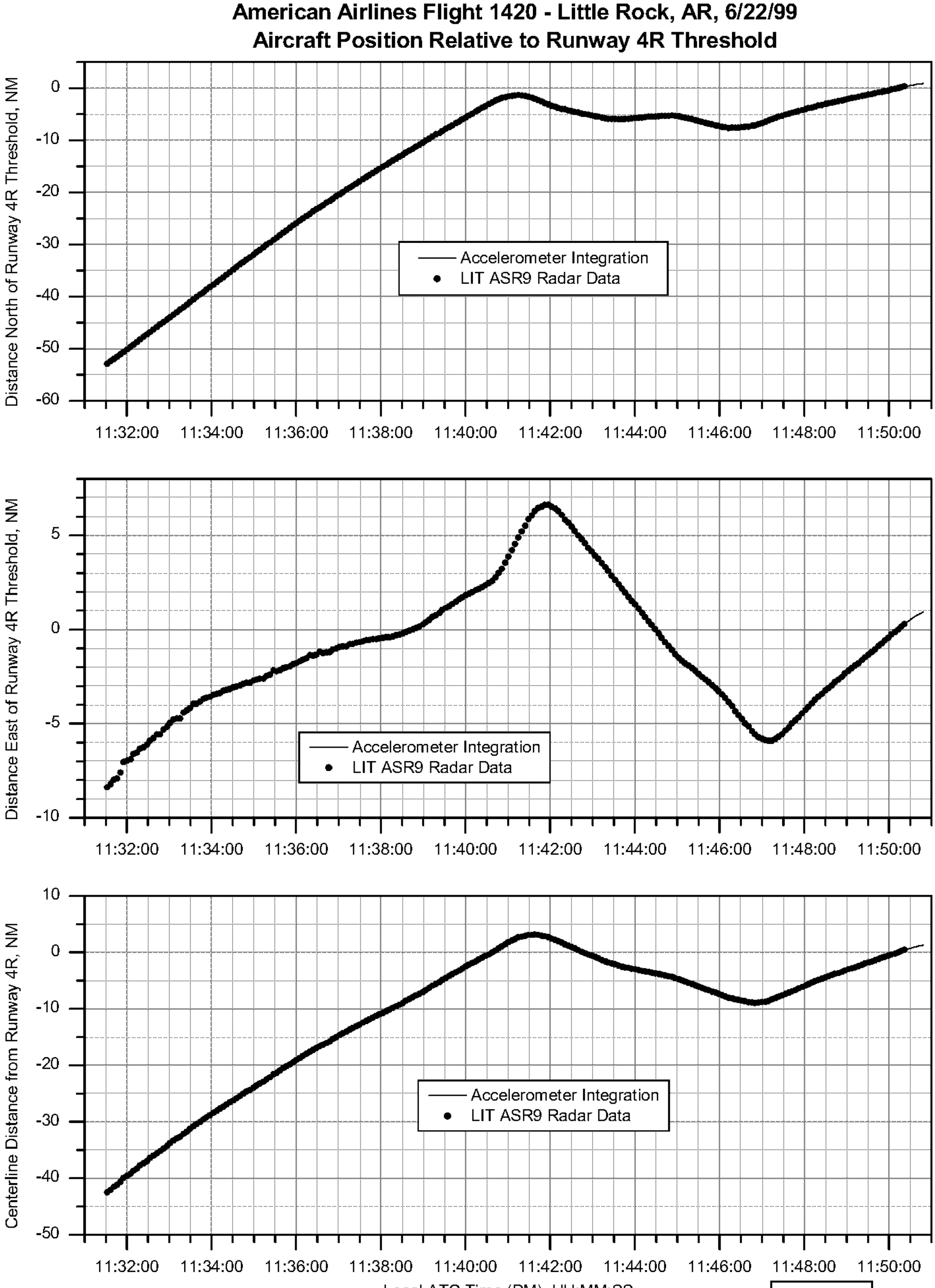
American Airlines Flight 1420 - Little Rock, AR, 6/22/99
Aircraft Position Relative to Runway 4R Threshold
Distance North of Runway 4R Threshold, NM
0
-10
-20
-30
-40
-50
-60
Accelerometer Integration
LIT ASR9 Radar Data
11:32:00
11:34:00
11:36:00
11:38:00
11:40:00
11:42:00
11:44:00
11:46:00
11:48:00
11:50:00
Distance East of Runway 4R Threshold, NM
5
0
-5
-10
Accelerometer Integration
LIT ASR9 Radar Data
Centerline Distance from Runway 4R, NM
10
0
-10
-20
-30
-40
-50
Accelerometer Integration
LIT ASR9 Radar Data
Local ATC Time (PM), HH:MM:SS

Figure 6a.

American Airlines Flight 1420 - Little Rock, AR, 6/22/99
Aircraft Position Relative to Runway 4R Threshold (Compressed Scale)

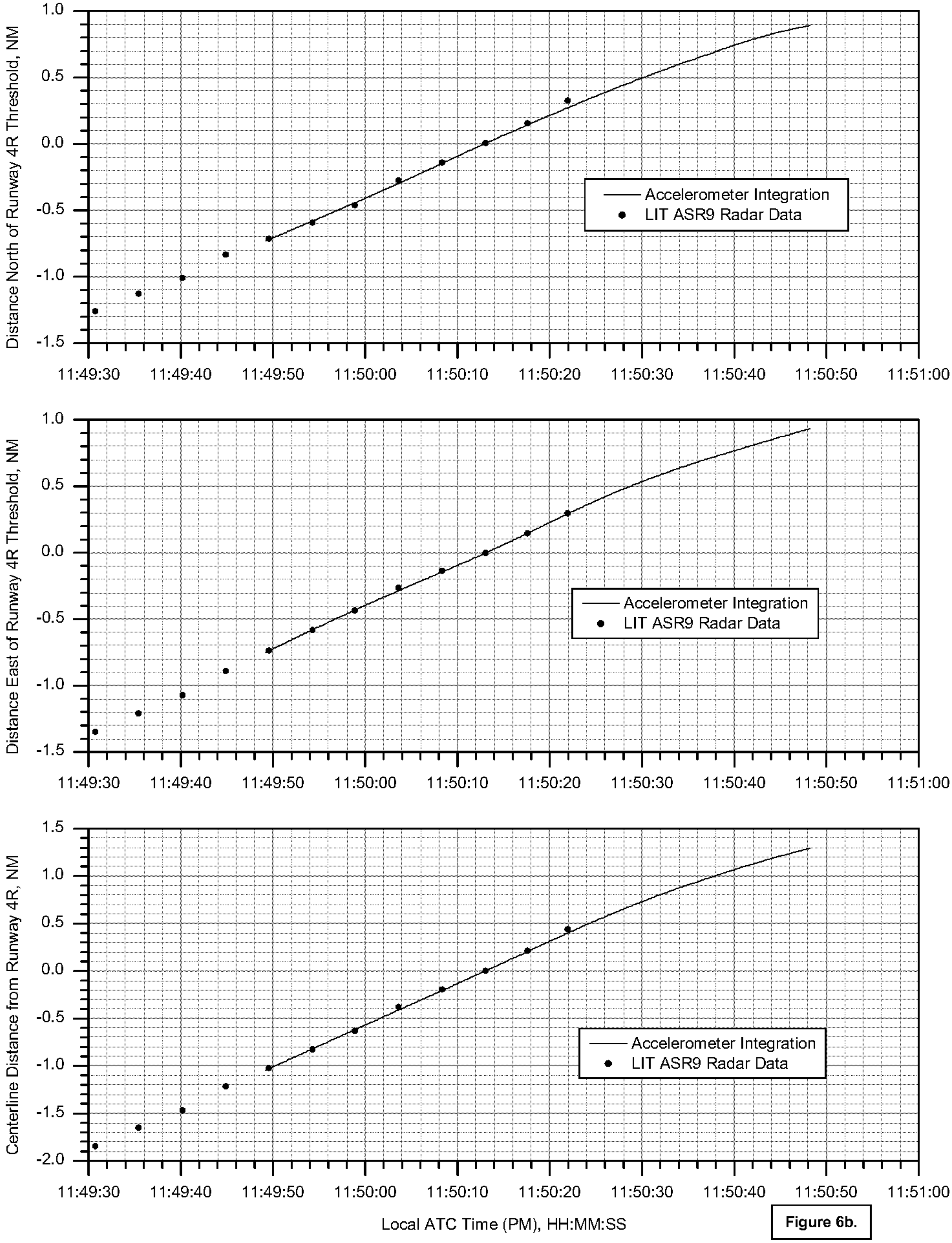

Figure 6b.

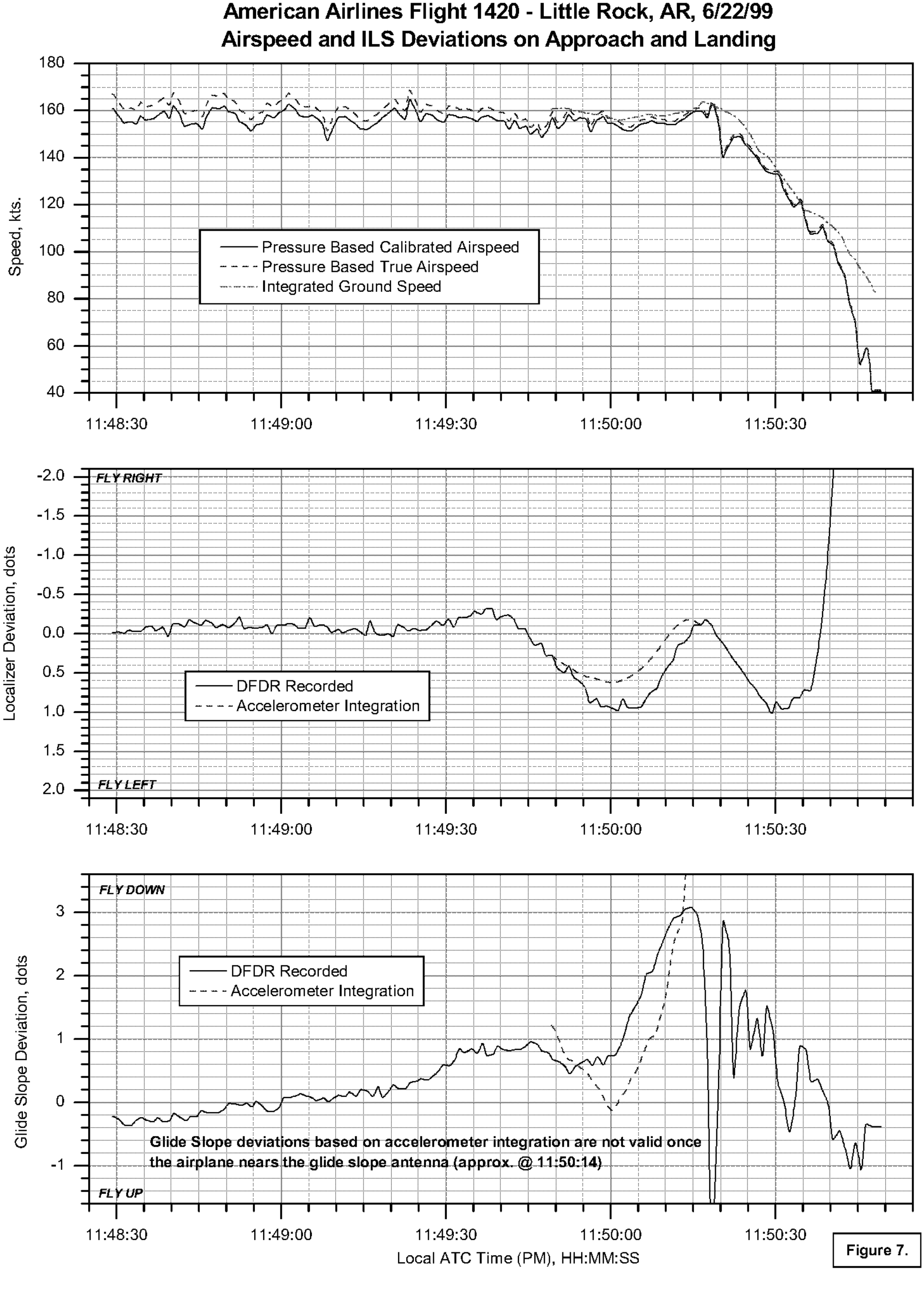
American Airlines Flight 1420 - Little Rock, AR, 6/22/99
Airspeed and ILS Deviations on Approach and Landing
Speed, kts.
180
160
140
120
100
80
60
40
Pressure Based Calibrated Airspeed
Pressure Based True Airspeed
Integrated Ground Speed
11:48:30
11:49:00
11:49:30
11:50:00
11:50:30
Localizer Deviation, dots
FLY RIGHT
FLY LEFT
-2.0
-1.5
-1.0
-0.5
0.0
0.5
1.0
1.5
2.0
DFDR Recorded
Accelerometer Integration
Glide Slope Deviation, dots
FLY DOWN
FLY UP
3
2
1
0
-1
Glide Slope deviations based on accelerometer integration are not valid once the airplane nears the glide slope antenna (approx. @ 11:50:14)
Local ATC Time (PM), HH:MM:SS

Figure 7.

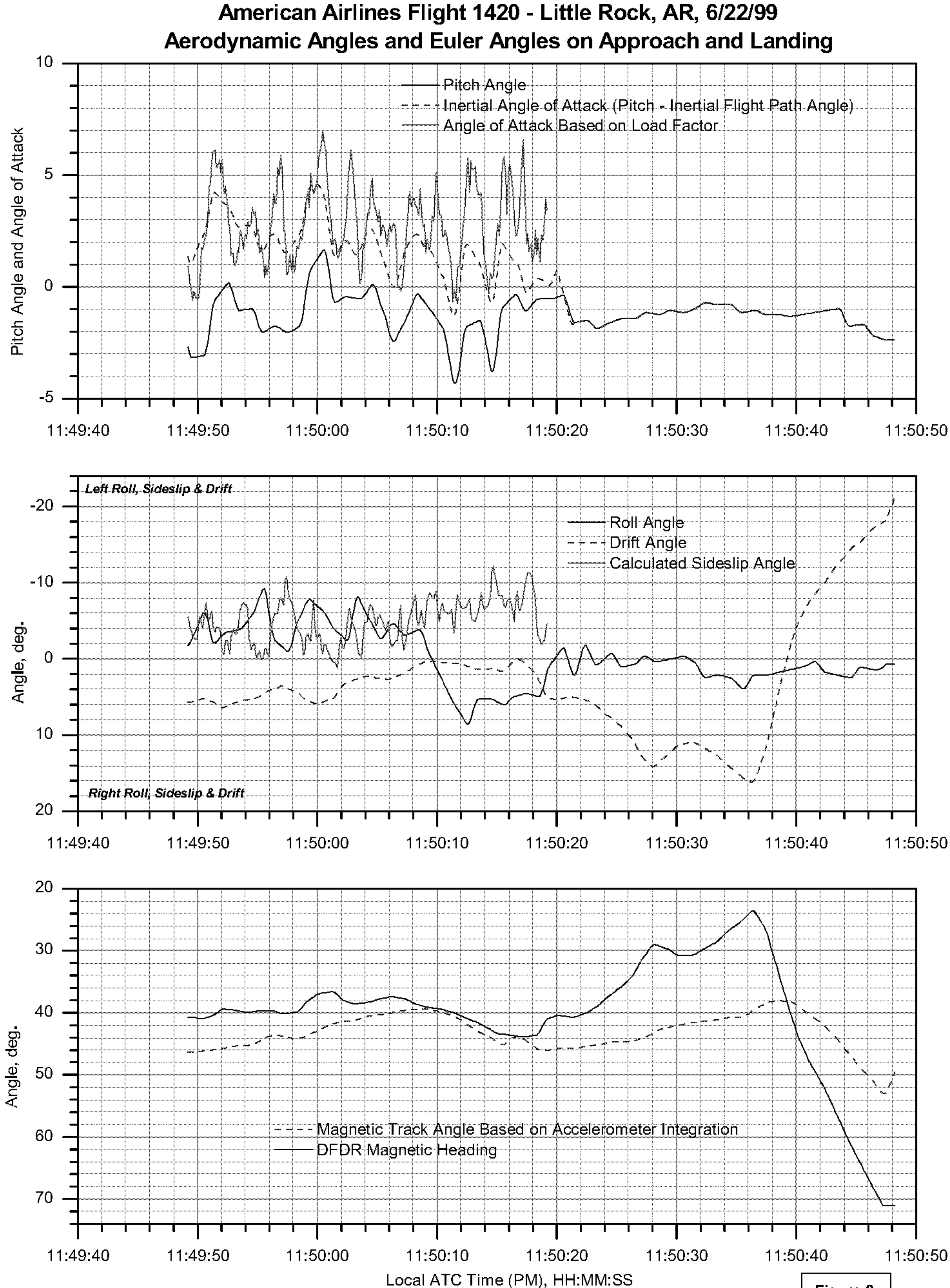
American Airlines Flight 1420 - Little Rock, AR, 6/22/99
Aerodynamic Angles and Euler Angles on Approach and Landing
Pitch Angle
Inertial Angle of Attack (Pitch - Inertial Flight Path Angle)
Angle of Attack Based on Load Factor
Pitch Angle and Angle of Attack
10
5
0
-5
11:49:40
11:49:50
11:50:00
11:50:10
11:50:20
11:50:30
11:50:40
11:50:50
Left Roll, Sideslip & Drift
Roll Angle
Drift Angle
Calculated Sideslip Angle
Angle, deg.
-20
-10
0
10
20
Right Roll, Sideslip & Drift
Magnetic Track Angle Based on Accelerometer Integration
DFDR Magnetic Heading
20
30
40
50
60
70
Local ATC Time (PM), HH:MM:SS
Figure 8.

American Airlines Flight 1420 - Little Rock, AR, 6/22/99
Altitude Above Runway and Rate of Climb on Approach and Landing

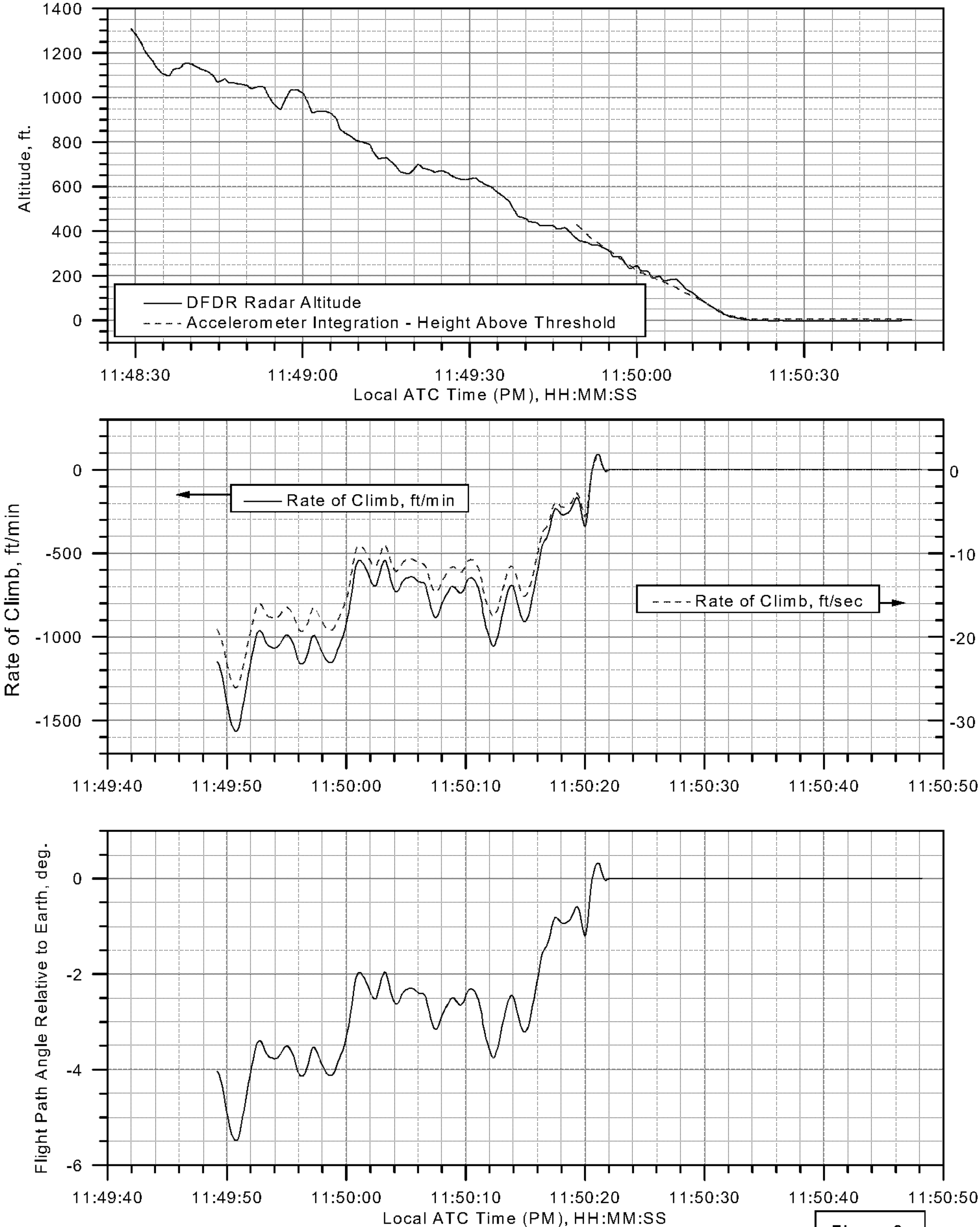

Figure 9.

American Airlines Flight 1420 - Little Rock, AR, 6/22/99
Calculated Winds on Final Approach

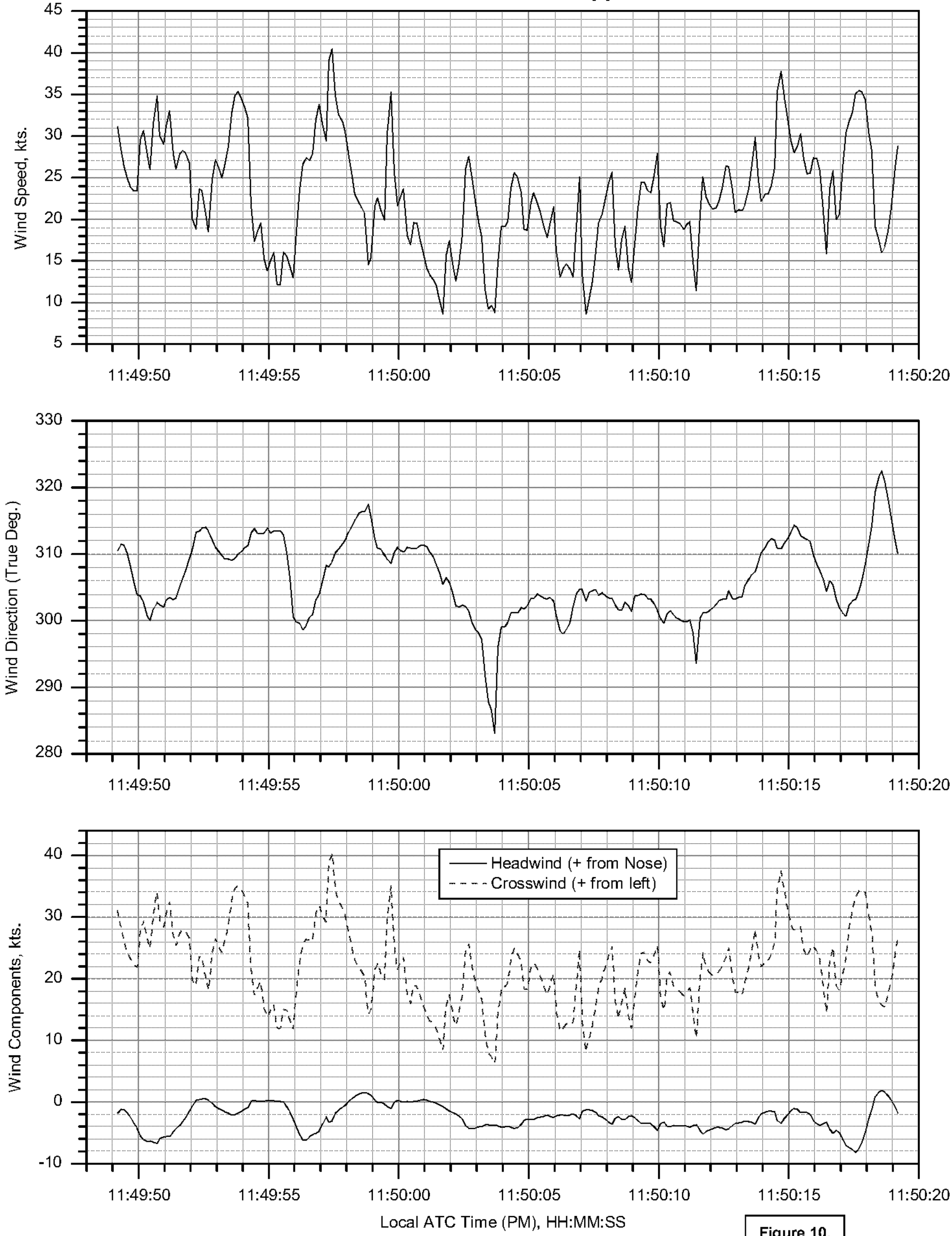

Figure 10.

American Airlines Flight 1420 - Little Rock, AR, 6/22/99
Angular Rates on Approach and Landing

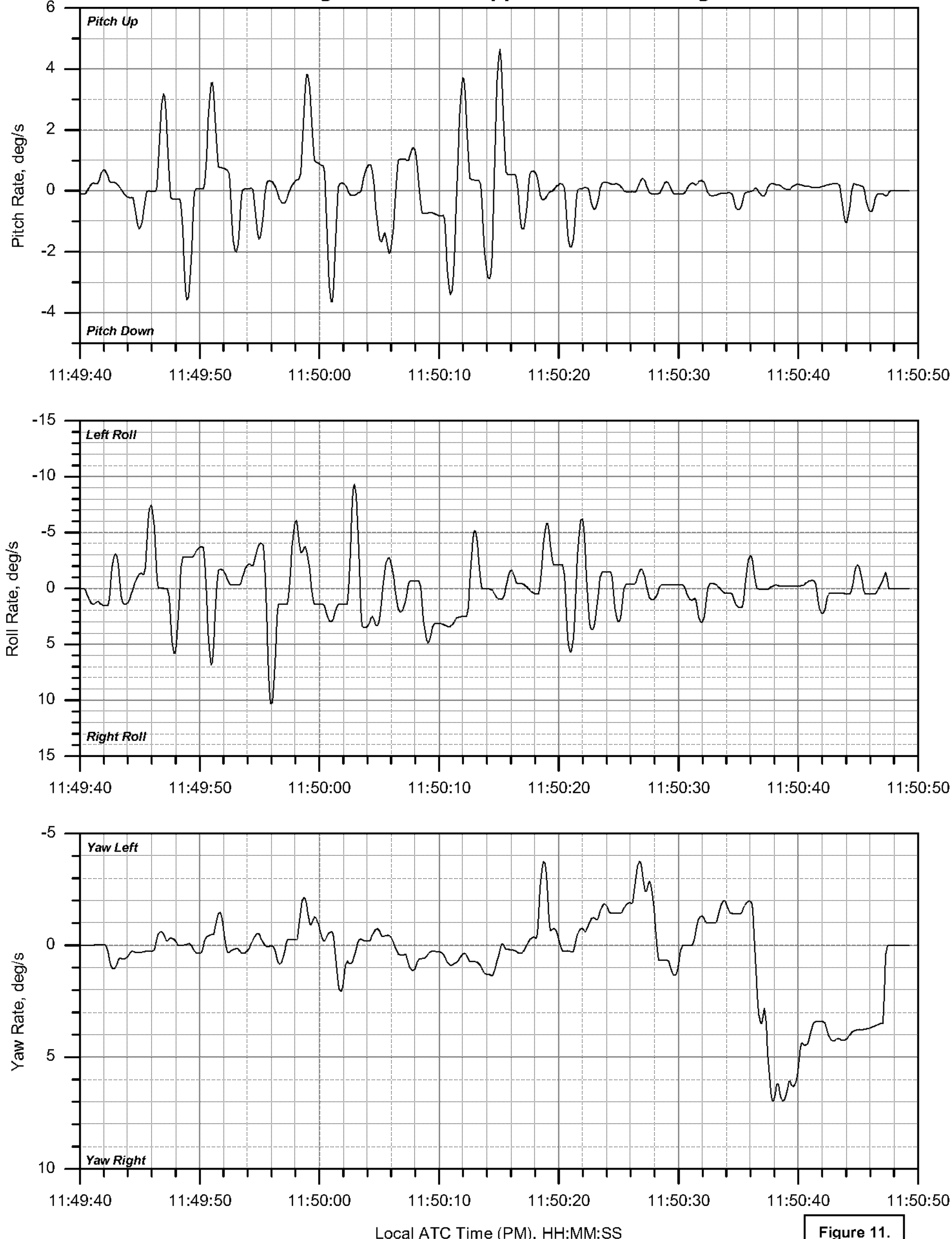

Figure 11.

American Airlines Flight 1420 - Little Rock, AR, 6/22/99
Load Factors on Approach and Landing

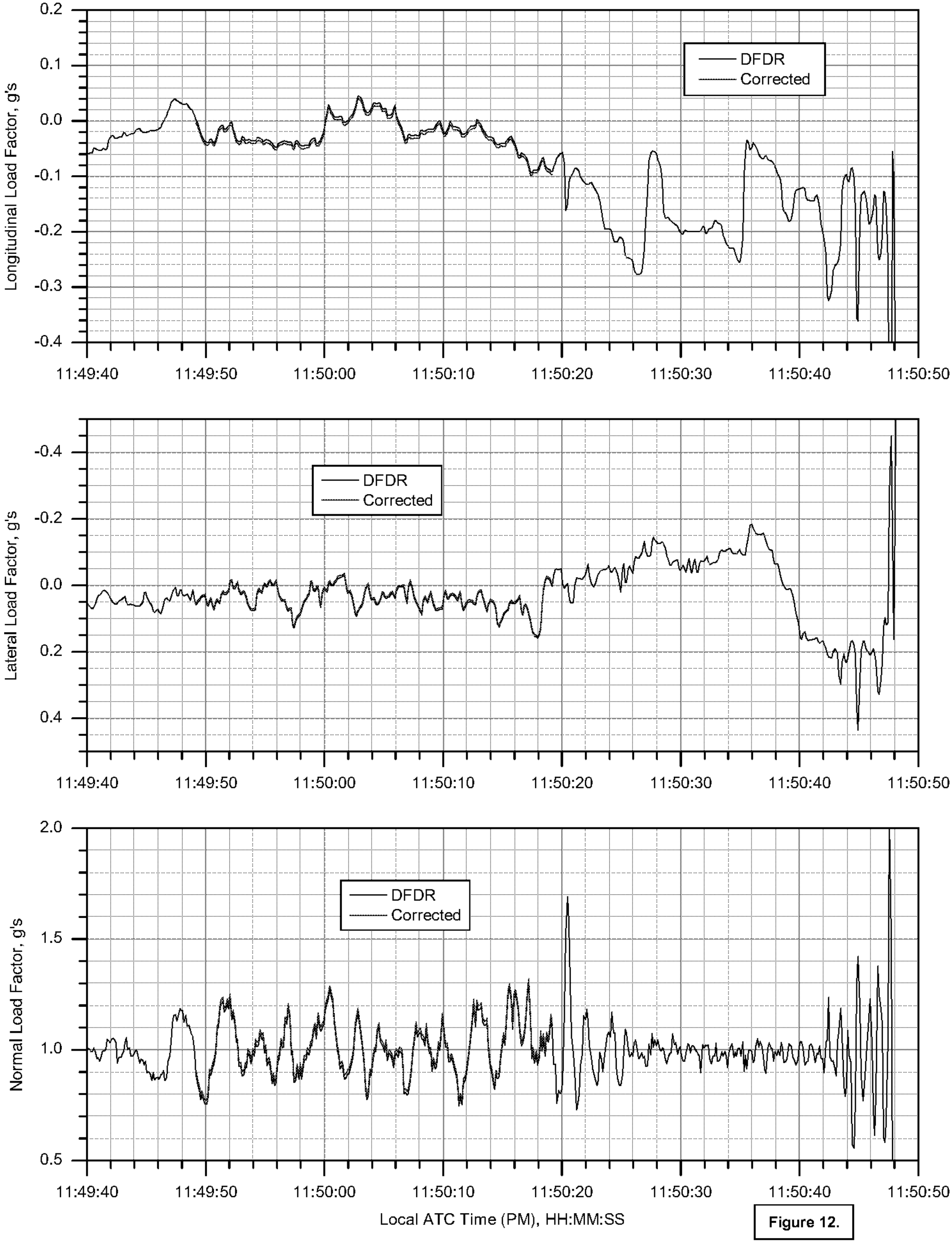

Figure 12.

American Airlines Flight 1420 - Little Rock, AR, 6/22/99
Control Surfaces and Engine EPR on Final Approach and Landing

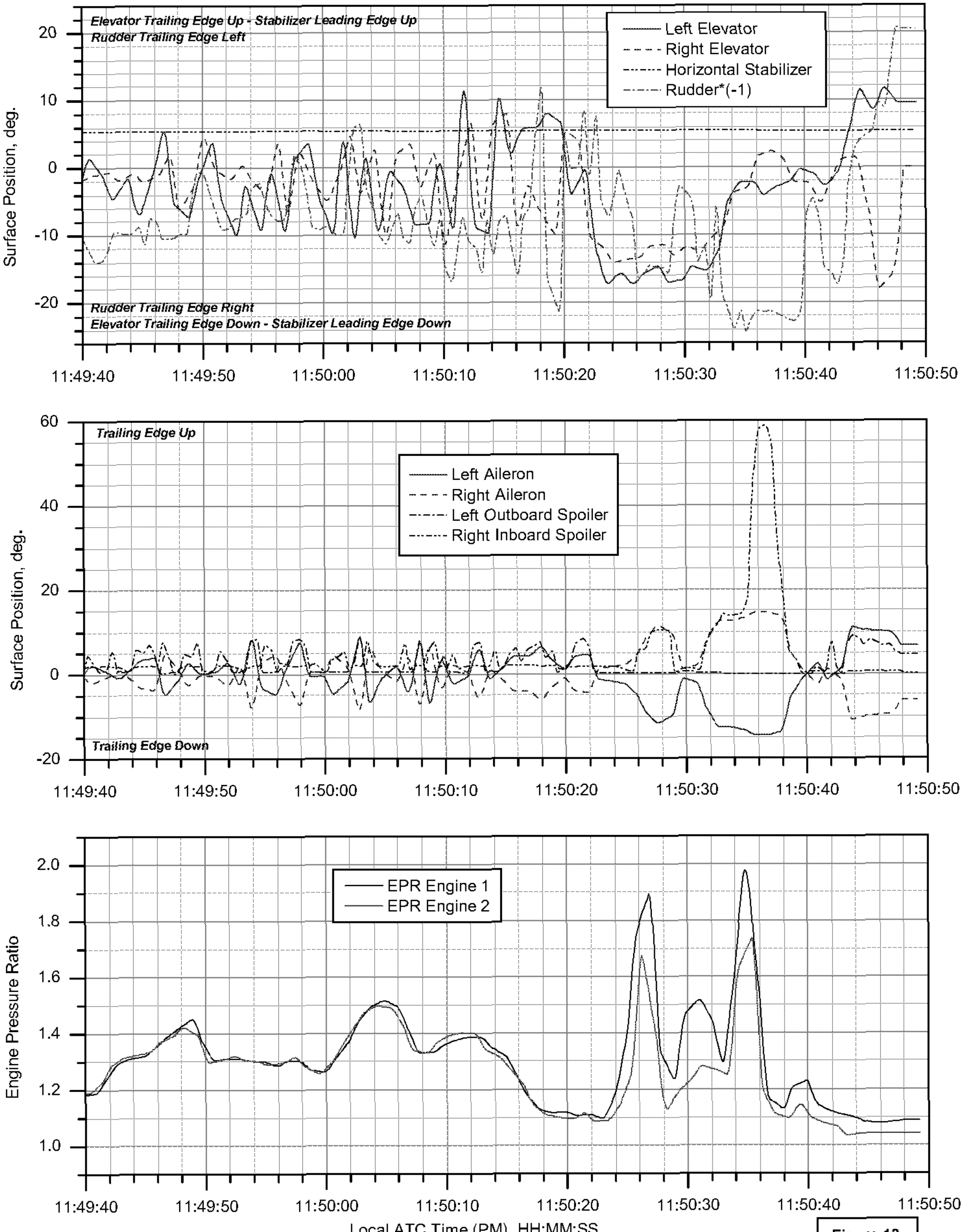

Figure 13.

American Airlines Flight 1420 - Little Rock, AR, 6/22/99

Airplane Trajectory on Runway 4R: -400 to 8000 ft. From Threshold

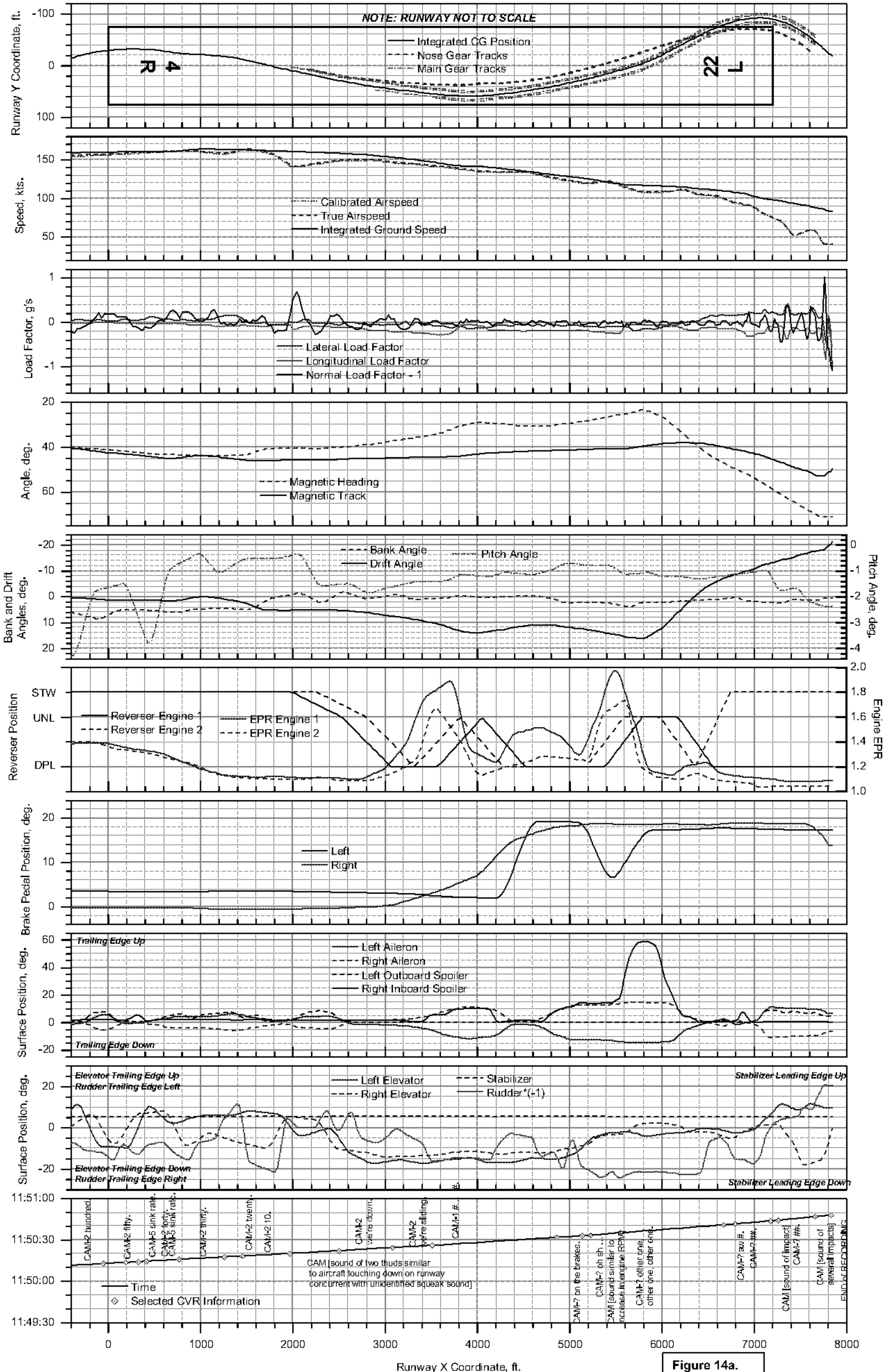

Figure 14a.

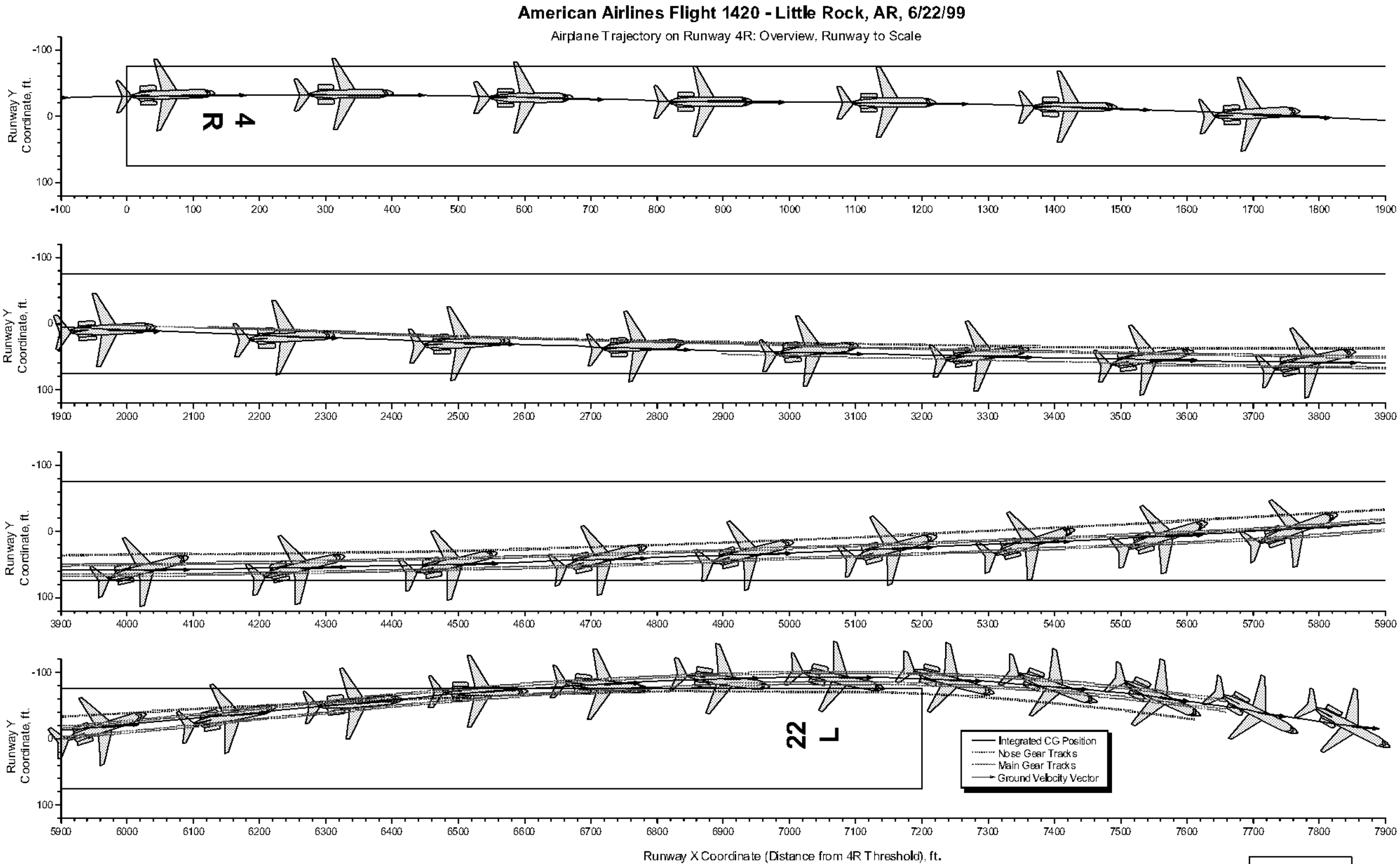
American Airlines Flight 1420 - Little Rock, AR, 6/22/99
Airplane Trajectory on Runway 4R: Overview, Runway to Scale
Runway Y Coordinate, ft.
4 R
22 L
Integrated CG Position
Nose Gear Tracks
Main Gear Tracks
Ground Velocity Vector
Runway X Coordinate (Distance from 4R Threshold), ft.

Figure 14b.

American Airlines Flight 1420 - Little Rock, AR, 6/22/99

Airplane Trajectory on Runway 4R: -500 to 1000 ft. From Threshold

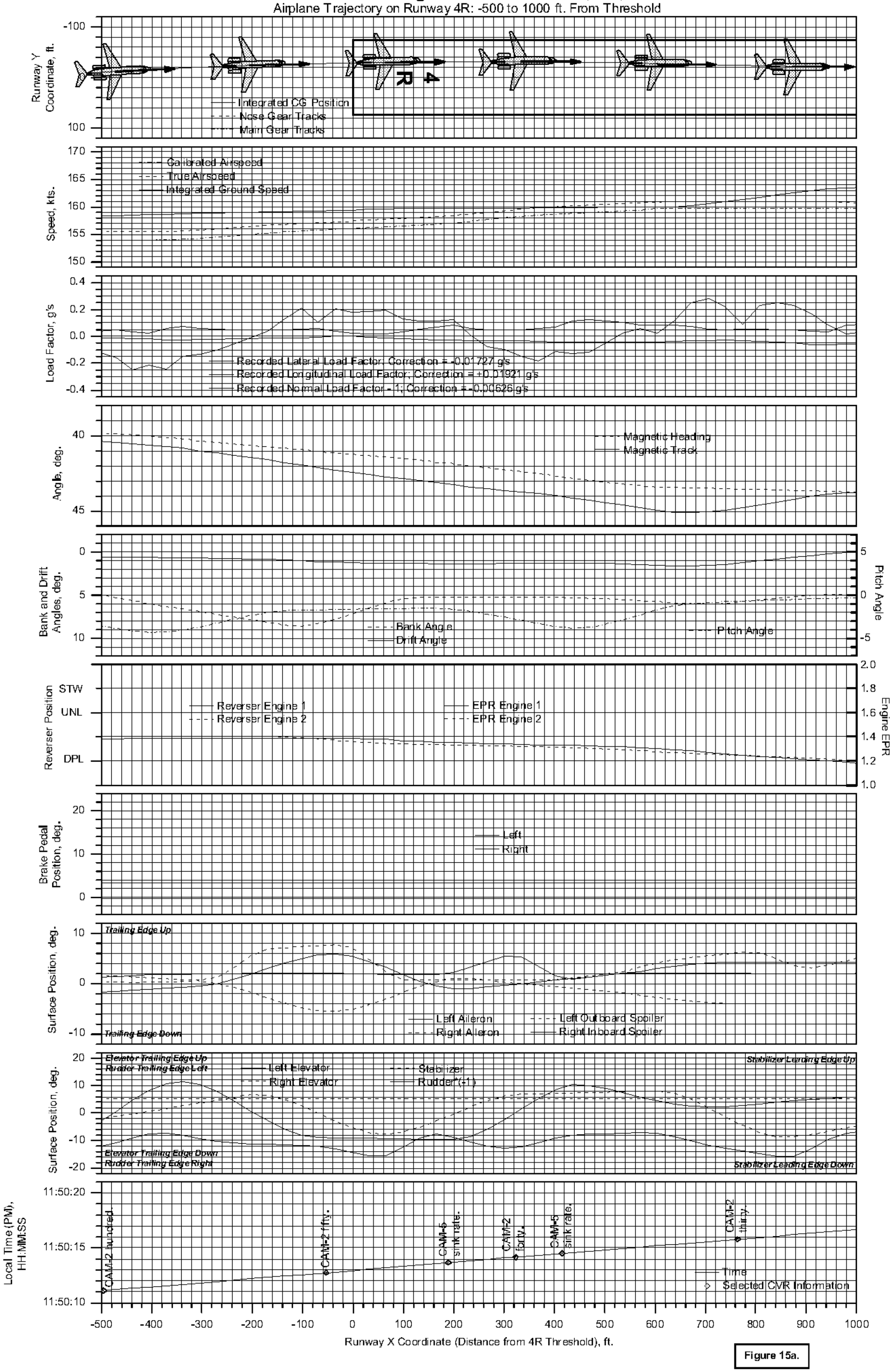

Figure 15a.

American Airlines Flight 1420 - Little Rock, AR, 6/22/99

Airplane Trajectory on Runway 4R: 1000 to 2500 ft. From Threshold

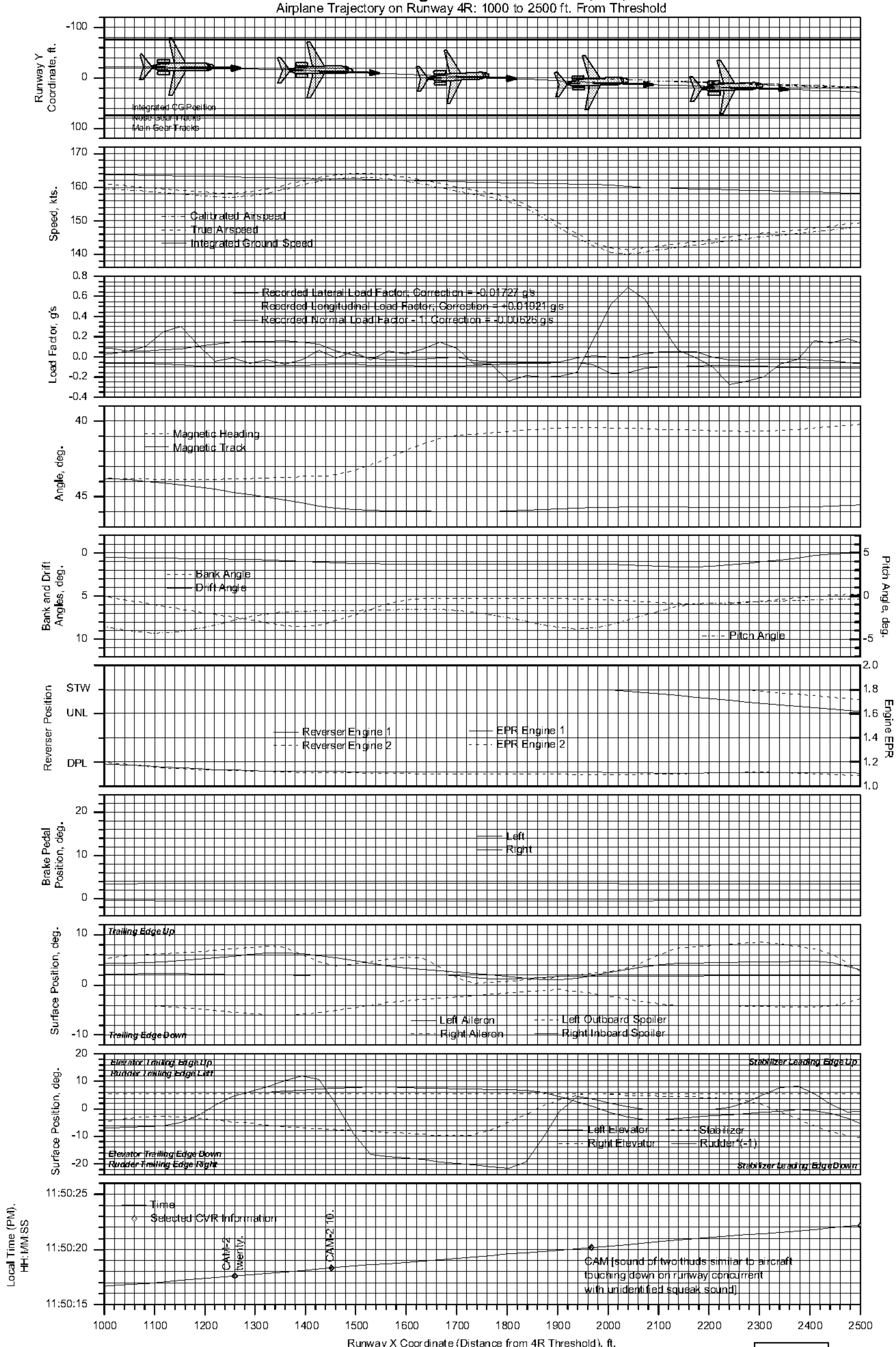

Figure 15b.

American Airlines Flight 1420 - Little Rock, AR, 6/22/99

Airplane Trajectory on Runway 4R: 2500 to 4000 ft. From Threshold

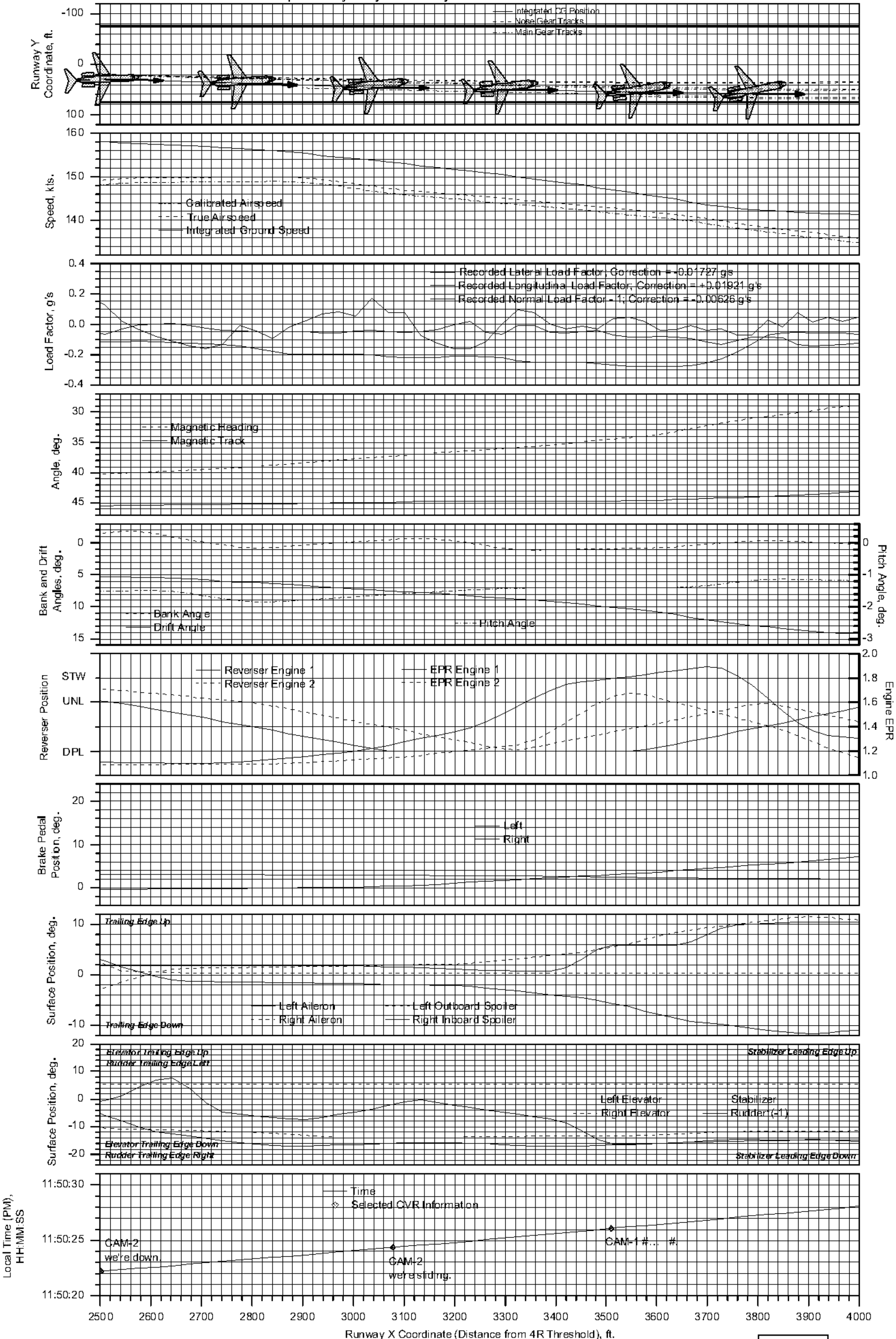

Figure 15c.

American Airlines Flight 1420 - Little Rock, AR, 6/22/99

Airplane Trajectory on Runway 4R: 4000 to 5500 ft. From Threshold

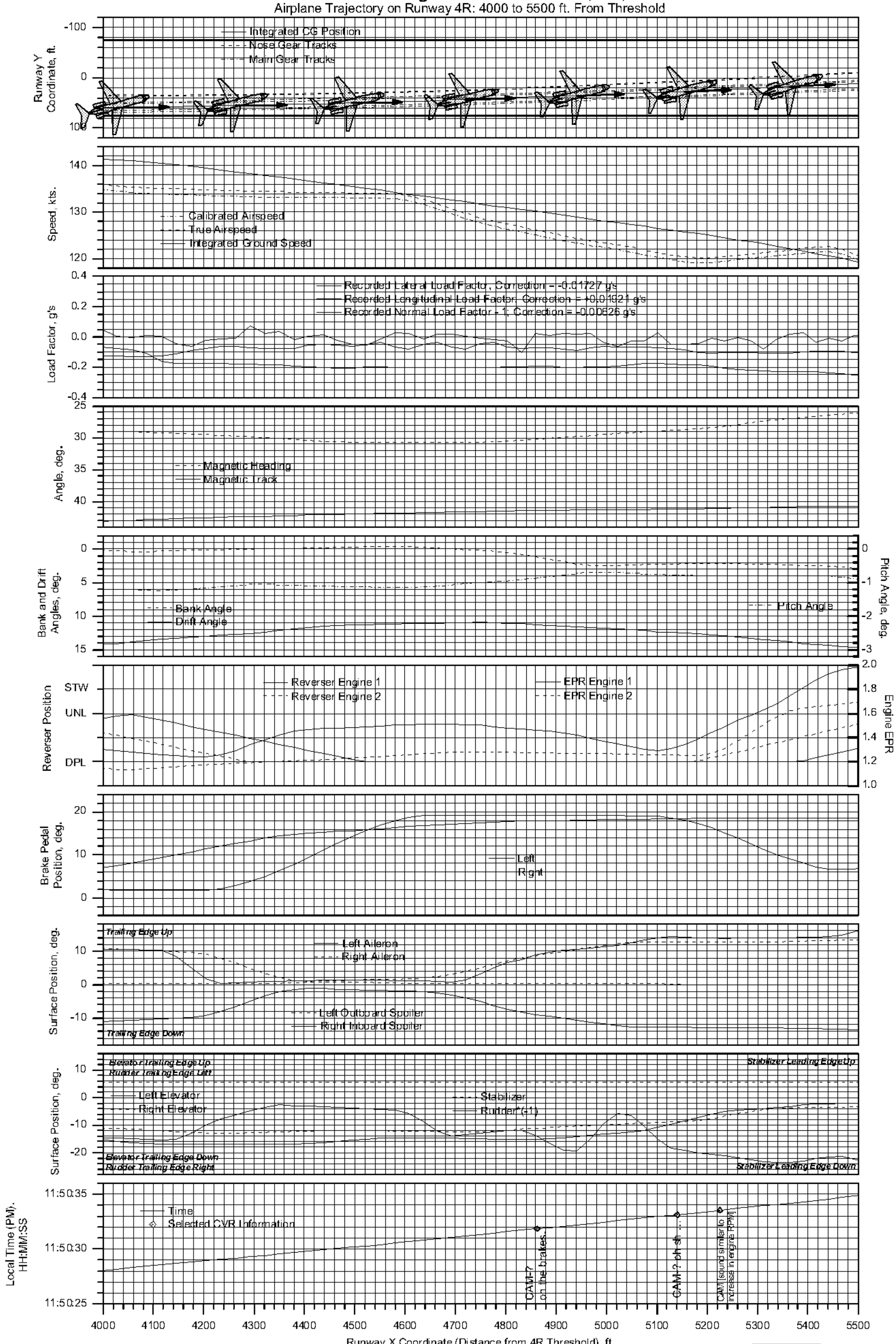

Figure 15d.

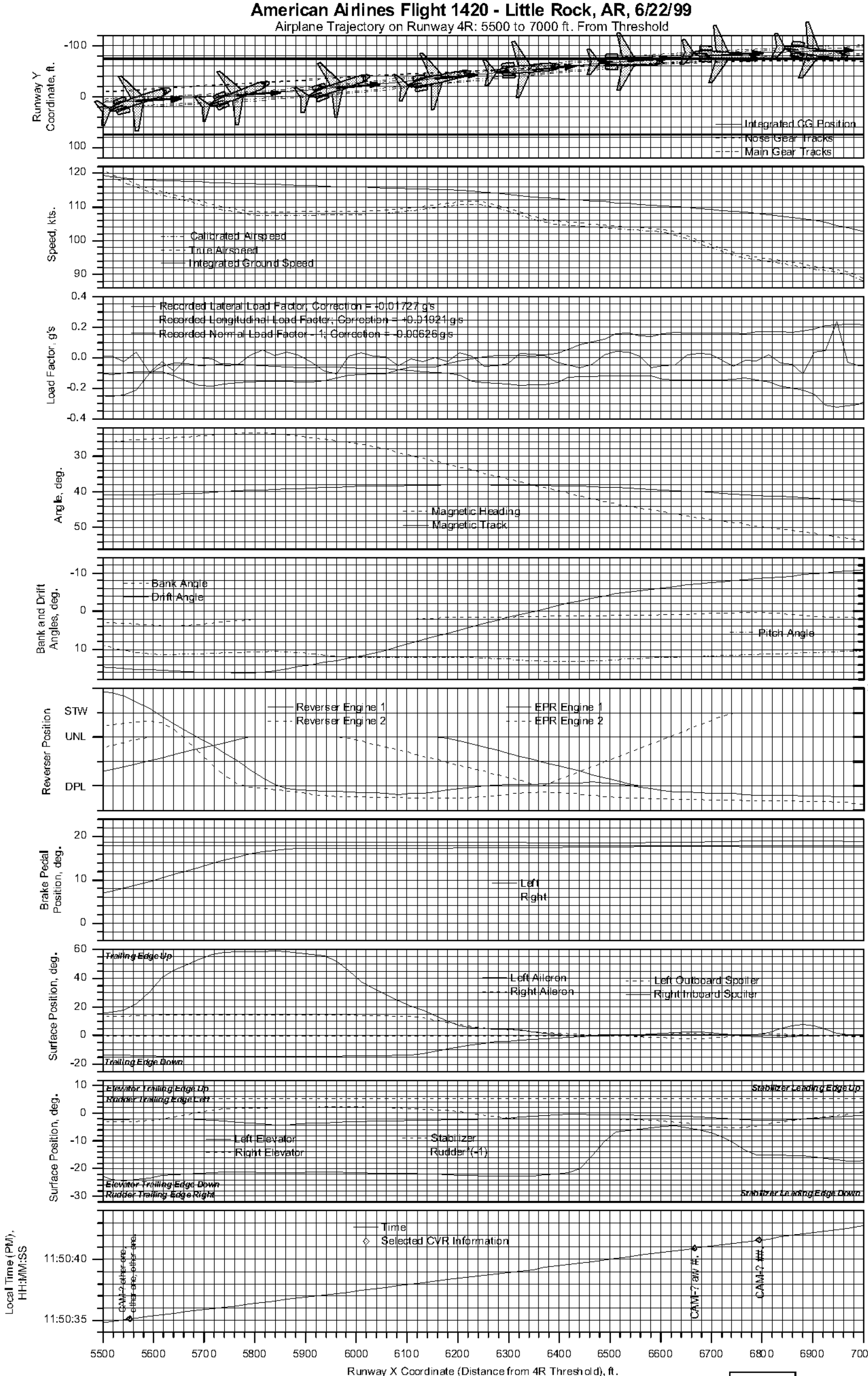
American Airlines Flight 1420 - Little Rock, AR, 6/22/99
Airplane Trajectory on Runway 4R: 5500 to 7000 ft. From Threshold
Runway Y Coordinate, ft.
Integrated CG Position
Nose Gear Tracks
Main Gear Tracks
Speed, kts.
Calibrated Airspeed
True Airspeed
Integrated Ground Speed
Load Factor, g's
Recorded Lateral Load Factor, Correction = +0.01727 g's
Recorded Longitudinal Load Factor, Correction = +0.01921 g's
Recorded Normal Load Factor - 1, Correction = -0.00626 g's
Angle, deg.
Magnetic Heading
Magnetic Track
Bank and Drift Angles, deg.
Bank Angle
Drift Angle
Pitch Angle
Pitch Angle, deg.
Reverser Position
STW
UNL
DPL
Reverser Engine 1
Reverser Engine 2
EPR Engine 1
EPR Engine 2
Engine EPR
Brake Pedal Position, deg.
Left
Right
Surface Position, deg.
Trailing Edge Up
Trailing Edge Down
Left Aileron
Right Aileron
Left Outboard Spoiler
Right Inboard Spoiler
Elevator Trailing Edge Up
Rudder Trailing Edge Left
Stabilizer Leading Edge Up
Left Elevator
Right Elevator
Stabilizer
Rudder*(-1)
Elevator Trailing Edge Down
Rudder Trailing Edge Right
Stabilizer Leading Edge Down
Local Time (PM), HH:MM:SS
Time
Selected CVR Information
CAM-? other one, other one, other one
CAM-? aw #.
CAM-? ##
Runway X Coordinate (Distance from 4R Threshold), ft.

Figure 15e.

American Airlines Flight 1420 - Little Rock, AR, 6/22/99

Airplane Trajectory on Runway 4R: 7000 to 8500 ft. From Threshold

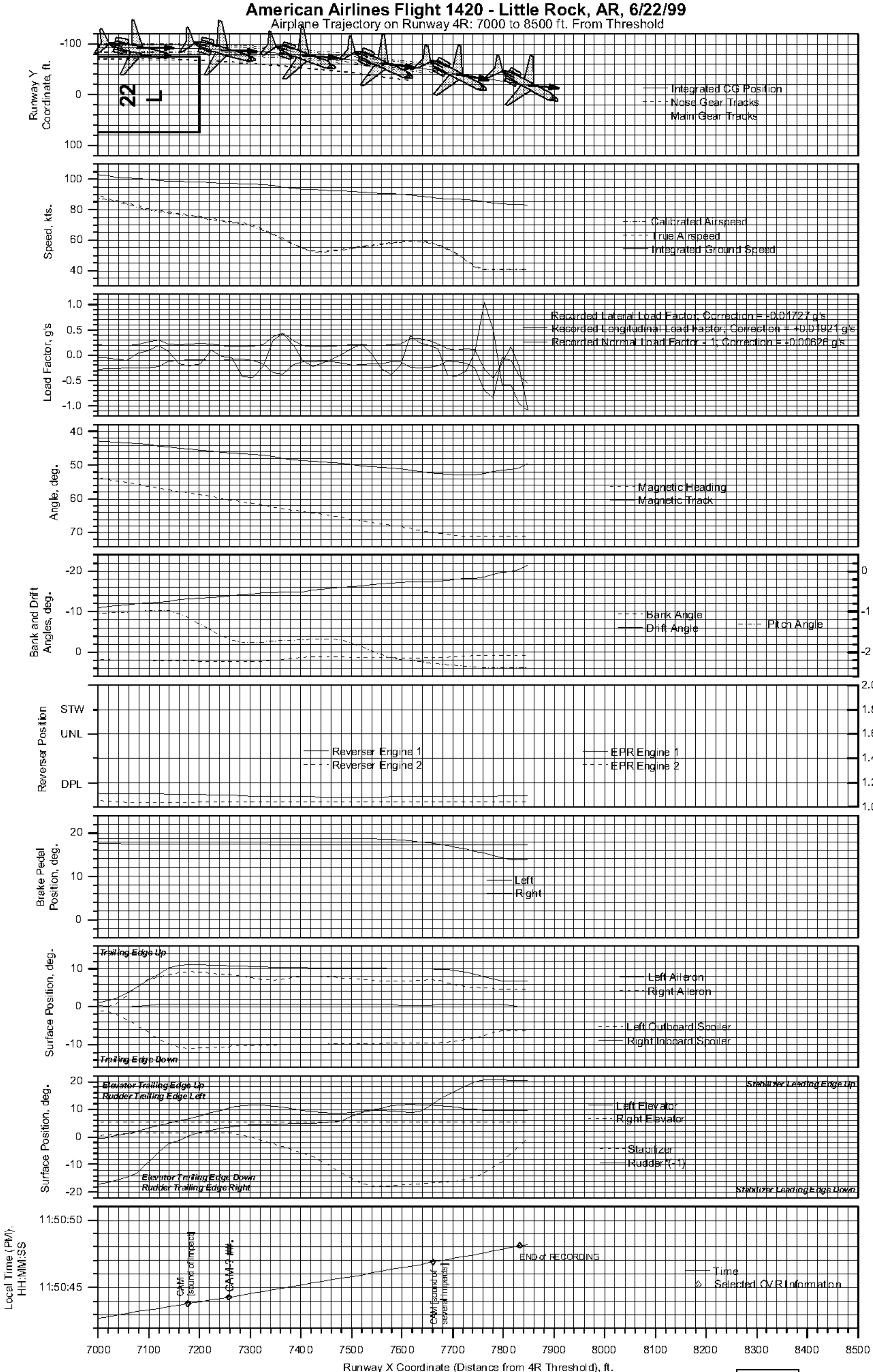

Figure 15f.

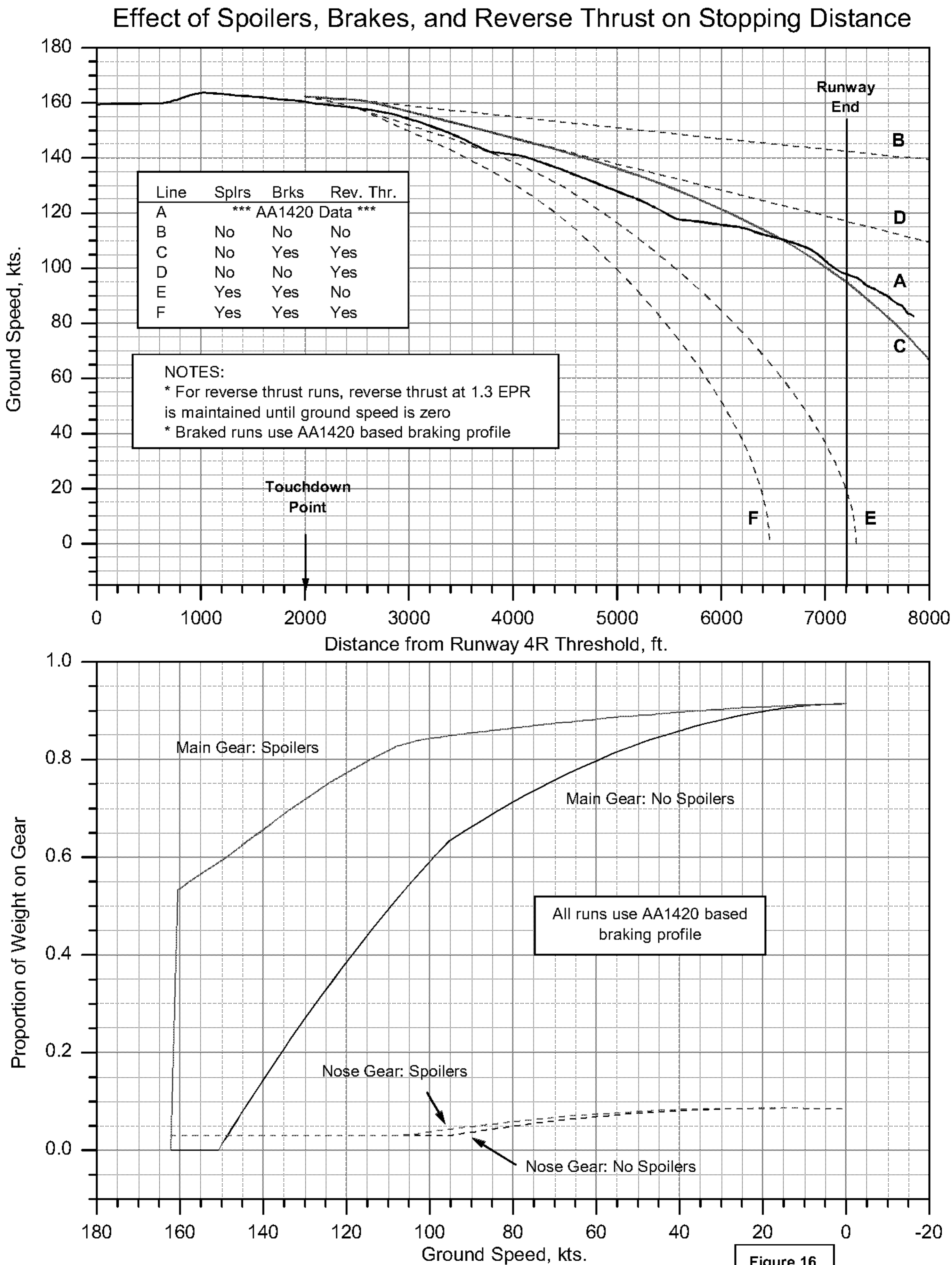
Effect of Spoilers, Brakes, and Reverse Thrust on Stopping Distance
Ground Speed, kts.
Distance from Runway 4R Threshold, ft.
Runway End
Touchdown Point
Line Splrs Brks Rev. Thr.
A *** AA1420 Data ***
B No No No
C No Yes Yes
D No No Yes
E Yes Yes No
F Yes Yes Yes
NOTES:
* For reverse thrust runs, reverse thrust at 1.3 EPR is maintained until ground speed is zero
* Braked runs use AA1420 based braking profile
A
B
C
D
E
F
Proportion of Weight on Gear
Ground Speed, kts.
Main Gear: Spoilers
Main Gear: No Spoilers
All runs use AA1420 based braking profile
Nose Gear: Spoilers
Nose Gear: No Spoilers

Figure 16.

Effective Braking Friction Coefficent Required to Make Spoiler Deployed Braking Performance Match Spoiler Stowed Braking Performance

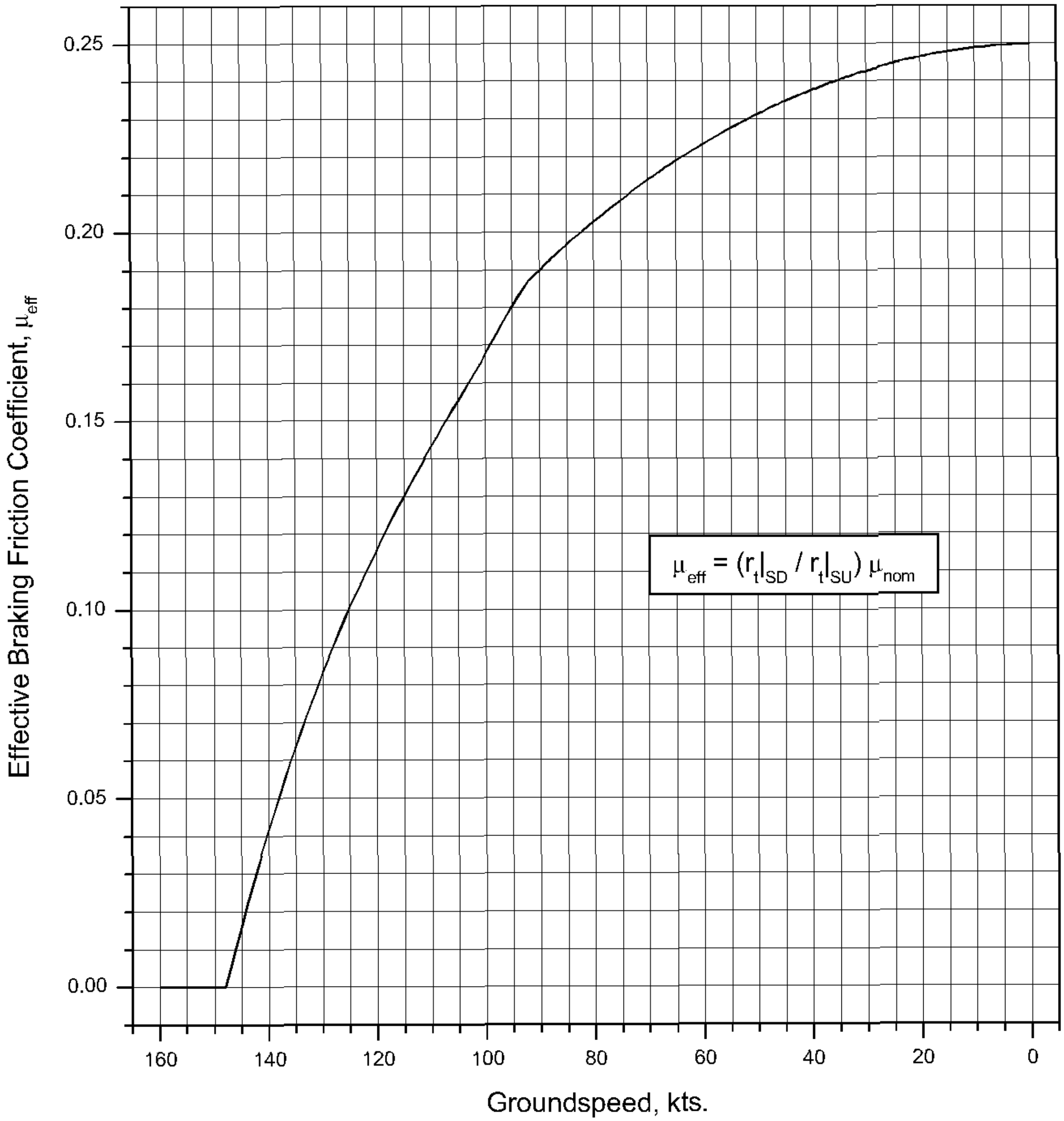

Figure 17.

Effect of Braking Technique and a 10 kt. Change in Touchdown Groundspeed on Stopping Distance

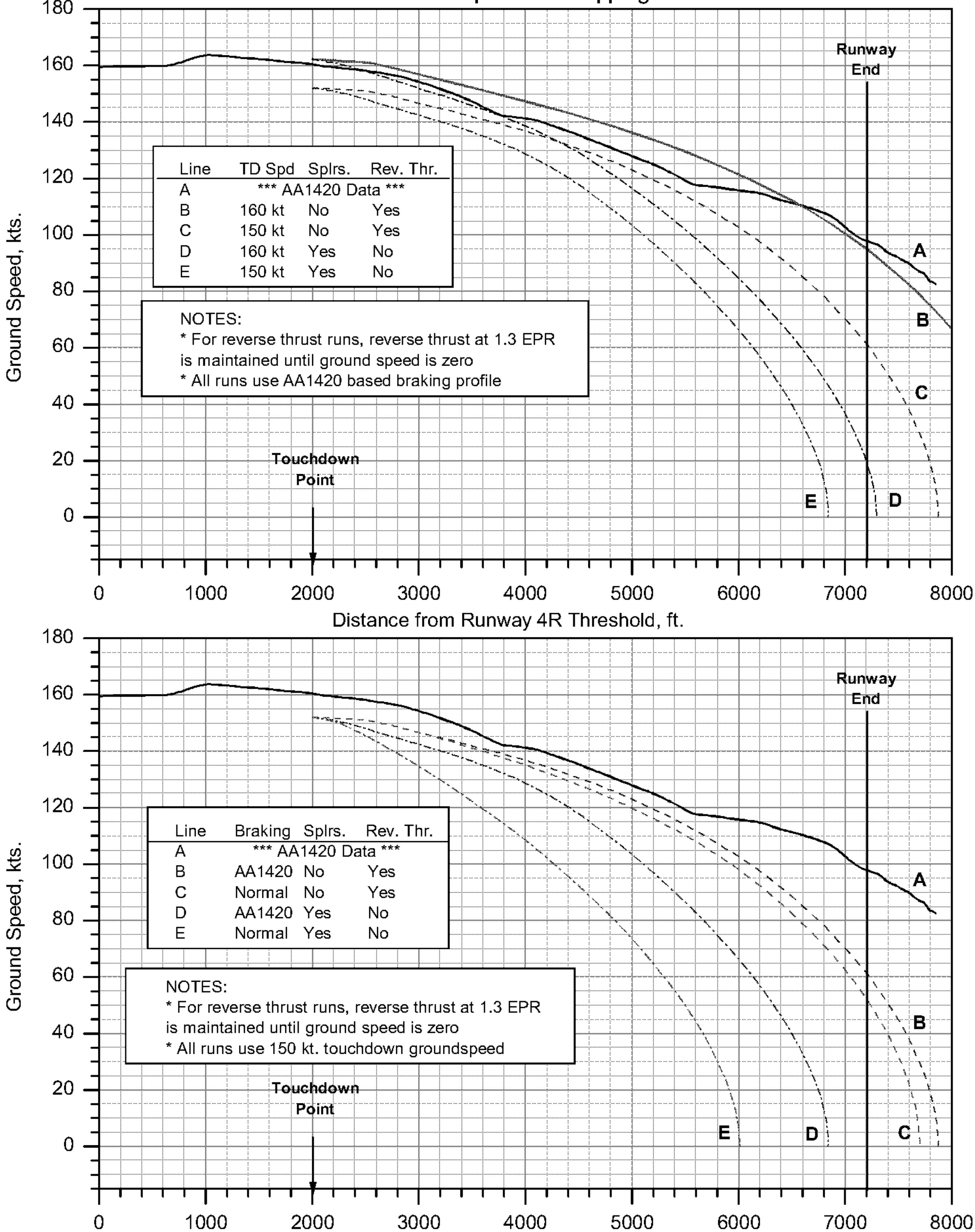

Figure 18.